

A MAP of the CANARY ISLANDS

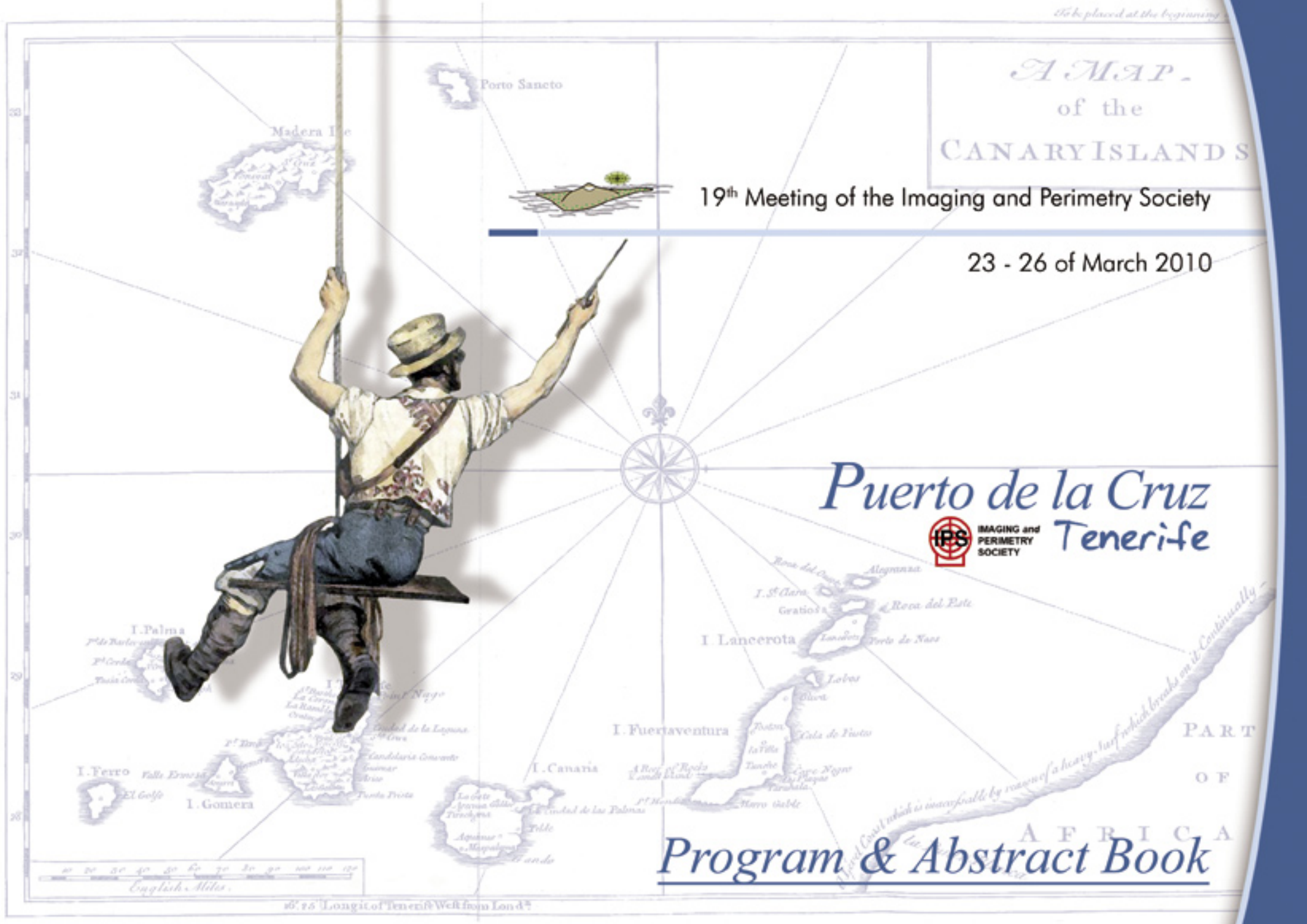
19th Meeting of the Imaging and Perimetry Society

23 - 26 of March 2010

Puerto de la Cruz Tenerife



IMAGING and
PERIMETRY
SOCIETY



Program & Abstract Book

Imaging and Perimetry Society (IPS)

formerly International Perimetric Society.

Perimetry is the quantitative evaluation of the visual field. Ocular imaging is the assessment and evaluation of the structural details of the eye. The aims of the IPS are 1) to promote the study of normal and abnormal visual function and of ocular imaging, 2) to ensure and facilitate the cooperation and friendship of scientists of different countries working and interested in these disciplines.

Previous Symposia

1974: Marseille, France
1976: Tübingen, Germany
1978: Tokyo, Japan
1980: Bristol, UK
1982: Sacramento, CA, USA
1984: Santa Margherita Ligure, Italy
1986: Amsterdam, The Netherland
1988: Vancouver, Canada
1990: Malm, Sweden
1992: Kyoto, Japan
1994: Washington D.C., USA
1996: Wurzburg, Germany
1998: Gardone Riviera, Italy
2000: Halifax, Nova Scotia, Canada
2002: Stratford upon Avon, UK
2004: Barcelona, Spain
2006: Portland, OR, USA
2008: Nara, Japan

Table of contents

| | |
|--|----|
| Welcome to Tenerife | 3 |
| Committees and Honorary Members | 4 |
| Meeting Information | 5 |
| Floor Plan Hotel Semiramis | 6 |
| Social Events | 7 |
| General Information | 8 |
| Map of Puerto de la Cruz (Hotel Semiramis area) | 10 |
| Program at a Glance | 11 |
| IPS Lecture | 12 |
| Aulhorn Lecture | 13 |
| Grantecan presentation | 14 |
| Scientific Program | 15 |
| Sponsors | 19 |
| Abstracts | 20 |



Dear Colleagues & Friends:

I would like to give you a warm welcome to our island in the name of the Local Committee.

We would like to thank the Board of Directors and all the members of the Imaging and Perimetry Society for having entrusted us with the organization of the 19th Annual Meeting (IPS 2010), in Puerto de la Cruz, Tenerife, Canary Islands, Spain.

The Canary Islands are a much-visited tourist region of Europe, situated off the coast of Africa but strongly linked to Latin America, with deep historical and cultural ties. The region's two great attractions are its temperate all-year climate and its most beautiful and diverse landscapes, included here on the island of Tenerife. As a venue for the symposium we have chosen a northern city, somewhat cooler than the south, with richer vegetation and beautiful scenery, at some distance from the tourist crowds and beaches.

The congress will be held at the Hotel Semiramis in Puerto de la Cruz, near to the old Botanical Garden, created in 1,788 by King Charles III to acclimatize exotic plants from the Philippines and America to cooler conditions.

If you arrive to our island with time enough, you may visit the Loro Parque (Parrot Park) the 23rd of March. The Loro Park is an excellent attraction with orchids, dolphins, killer whales, penguins etc and the greatest collection in the world of parrots, cockatoos, macaws etc. In the evening we will be offering a private cocktail party to welcome you all at the Lago Martiánez, an area with great swimming pools, next to the sea, which was designed by the artist Cesar Manrique.

We cordially invite you to share with us a few days in which we will endeavour to combine the science that inspires us with the pleasure of visiting unique countryside, including the Teide National Park (Parque Nacional de las Cañadas del Teide), an UNESCO World Heritage natural site; enjoy our gastronomical specialties and promote our friendship.

Welcome to Tenerife IPS-2010!



Manuel Gonzalez de la Rosa
Department of Ophthalmology
Universidad de La Laguna
Local Committee President



Committees and Honorary Members

IPS Board Members

President:

Michael Wall, MD, Iowa City, IA, USA

Vice President:

Chota Matsumoto, MD, Osaka-Sayama City, JAPAN

Vice President:

Chris Johnson, PhD, Iowa, IA, USA

Secretary:

David Henson, PhD, Manchester, England, UK

Treasurer:

Ulrich Schiefer, MD, Tübingen, GERMANY

Program Committee

David Henson, PhD, Manchester, England, UK

Chris Johnson, PhD, Iowa City, IA, USA

Manuel Gonzalez de la Rosa, PhD, Tenerife, SPAIN

Marta Gonzalez-Hernandez, PhD, Tenerife, SPAIN

Members at Large

Paolo Brusini, MD, Udine, ITALY

Ron Harwerth, PhD, Houston, TX, USA

Linda Zangwill, PhD, La Jolla, CA, USA

Yoshio Yamazaki, MD, Nihon University, JAPAN

Paul Artes, PhD, Manchester, England, UK

Other Board Members

Richard Mills, MD, Seattle, WA, USA

Fritz Dannheim, MD, Rosengarten, GERMANY

Mario Zulauf, MD, Shur, SWITZERLAND

Aiko Iwase, MD, Gifu, JAPAN (Public Relations)

Shaban Demirel, PhD, Portland, OR, USA

Group Chairs

Education:

Perimetry: Francisco Goñi, Barcelona, SPAIN

Imaging: Ted Garway-Heath, MD, London, UK

Standards: Pamela Sample, San Diego, CA, USA

Imaging Standards: Linda Zangwill, PhD, La Jolla, CA, USA

Honorary Members of the IPS

Prof. Stephen Drance

Prof. Jay Enoch

Prof. Franz Fankhauser

Prof. Erik Greve

Prof. Yoshi Kitazawa

In Memoriam Honorary Members of the IPS

Prof. Elfriede Aulhorn

Prof. Alan Friedmann

Prof. Hans Goldmann

Prof. Heinrich Harms

Prof. Haratuke Matsuo

Prof. Mario Zingirian

Local Organizing Committee

Host: Manuel Gonzalez de la Rosa, MD

Local Executive Committee:

Marta Gonzalez-Hernandez PhD

Manuel Sanchez Mendez MD

Jose Aguilar Estevez MD

Tinguaro Diaz Aleman MD

Javier Rodriguez Martin MD

Jose Alberto Muiños Gomez-Camacho MD



Meeting Information

Venue

Hotel Semiramis
C/ Leopoldo Cologan Zulueta, 12
38400 Puerto de la Cruz (Tenerife), Spain
Phone: +34 922 373 200
Fax: +34 922 373 193
Web page: <http://www.hotasa.es>

Official Language

English

Registration

| | |
|---------------------------------|-------|
| On-Site Fees are | |
| IPS Members | 495 € |
| Non Members | 560 € |
| Residents* /Fellows* /Others... | 360 € |

*Residents/Fellows must submit an official university certificate or letter, in conjunction with their registration, which confirm their status. Documentation must come from a supervisor, or department head.

Registration Entitlement

For IPS Members, Non Members, Residents/Fellows

- Congress Kit
- All Scientific Programs/Exhibition
- Welcome Party at the "Lago Martianez" on March 23rd
- Luncheon-Tour "Monasterio" on March 25th
- "Las Cañadas del Teide" tour on March 25th
- Closing Banquet on March 26th
- Morning/Luncheon Seminars
- Coffee Breaks

For Other Persons

- Welcome Party at the "Lago Martianez" on March 23rd
- Luncheon-Tour "Monasterio" on March 25th
- "Las Cañadas del Teide" tour on March 25th
- Closing Banquet on March 26th
- Coffee Breaks

Registration and General Information Desk

The Registration and General Information Desk for the meeting is located in the 17th floor of the Hotel Semiramis. (NOTE: The hotel is located at a cliff, and 16th floor is the entrance).

Registration Desk opening hours are:

| | |
|--------------------------|---------------|
| March 23 rd : | 10.00 - 18.00 |
| March 24 th : | 07.45 - 18.00 |
| March 25 th : | 07.45 - 13.00 |
| March 26 th : | 08.45 - 18.00 |

Name Badge

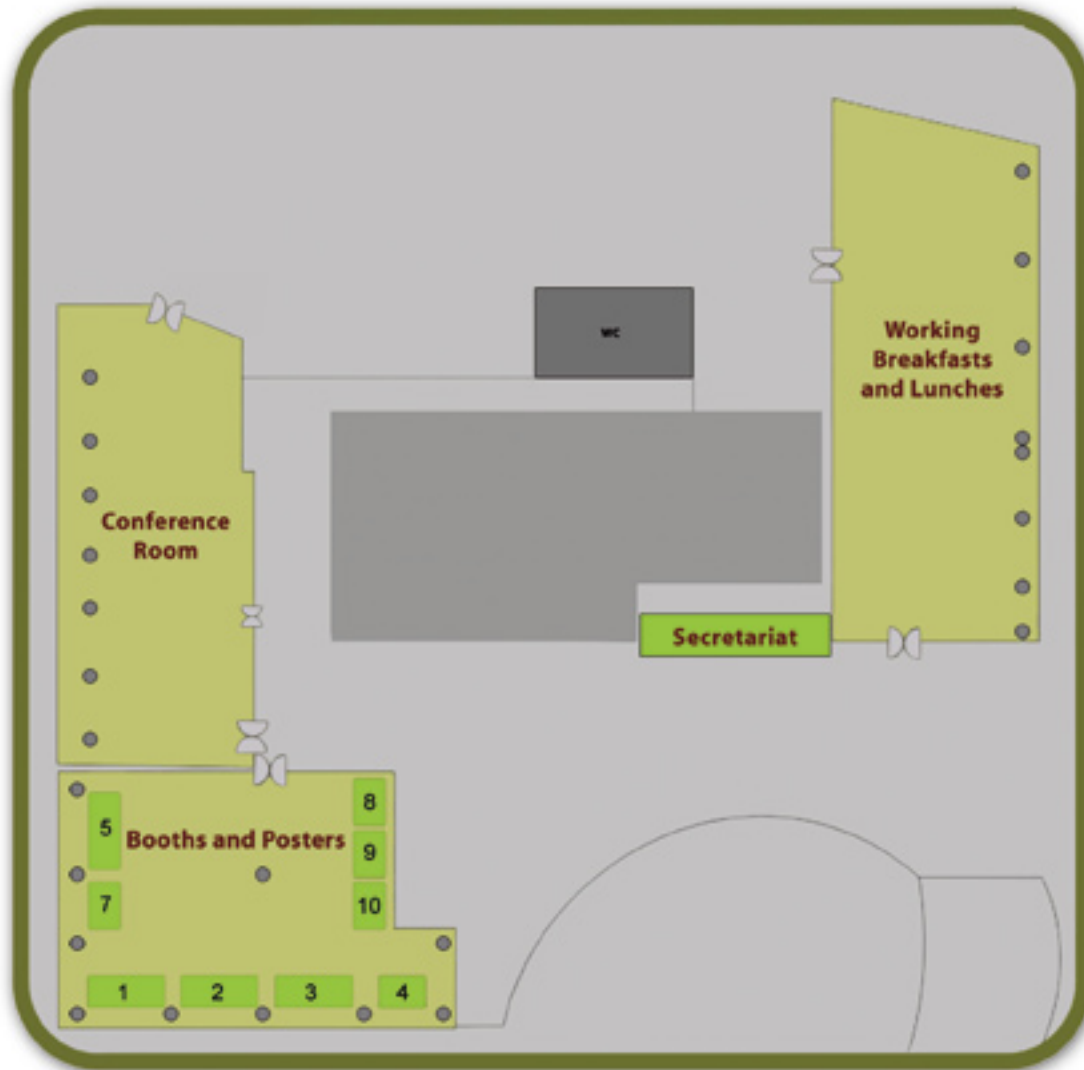
All registered attendees will receive a name badge. Please wear the badge for all meeting activities.

Secretariat

Magna Congressos, the Meeting Official Agency, will be available right next to the Registration and General Information Desk for any information about hotels, tours or transport, etc.



Floor Plan Hotel Semiramis



17th floor plan Hotel Semiramis

STAND NUMBER EXHIBITOR

- 1 
- 2 
- 3 
- 4 
- 5 
- 7 
- 8 **IPS 2012**
- 9 
- 10 

Social Events

Tuesday, March 23rd

Loro Parque visit

Location: Puerto de la Cruz

Transport: Not included

Dress: Casual

The "Loro Parque" (Parrot Park) is an excellent attraction with orchids, dolphins, killer whales, penguins etc and the greatest collection in the world of parrots, cockatoos, macaws etc. If you can arrive early enough, the congress inscription fee includes an entrance ticket to this park for the whole day of the 23rd March. Park opening time: 10:00 am. Closing time : 18:00 h

Welcome Party

Time: 19:30-21:00

Location: Lago Martiane

Bus: Shuttle at 19:00 leaving Hotel Semiramis

Fee: Included

Dress: Casual

Wednesday, March 24th

Optional dinner at Colonial Scenery in "Abaco"

Time: 20:30

Location: Shuttle bus leaving Hotel Semiramis at 18:30

Fee: 85€

Dress: Casual

After a short tour visiting La Orotava colonial city, we will attend dinner and a concert of local musicians.

Thursday, March 25th

Luncheon at El Monasterio, tour to Las Cañadas del Teide and visit to the IAC Astrophysical Observatory

Location: Los Realejos

Time: 13:00

Bus: Shuttle bus leaving Hotel Semiramis at 12:45

Fee: Included

Dress: Casual. Take warm clothes for the evening at the mountain

After lunch at a popular restaurant, we will go up 2,000 meters to El Teide National Park (Parque Nacional de las Cañadas del Teide), an UNESCO World Heritage natural site. We will enjoy a moonlike landscape, the highest mountain in Spain and the Astrophysical Observatory.

Friday, March 26th

Closing Banquet

Location: Casino de Tenerife (Private Club)

Time: 21:00

Bus: Shuttle bus leaving Hotel Semiramis at 19:00

Fee: Included

Dress: Smart Casual

The Casino is centrally located at the capital of the island (Santa Cruz). It is not a gambling casino, but a social club located at an "art deco" building. Following the meal, we will enjoy the traditional national singing.





About Tenerife

Situation

Tenerife is one of the seven Canary Islands, which are Spanish territory in the Atlantic Ocean. Together with the islands of Azores, Madeira and Cape Verde, they constitute a group of archipelagos called "Macaronesia".

Because of its privileged climate, the Canary Islands were known in the past as "Fortunatae Insulae" or the Fortunate Isles. Not even during the Ice Age did the cold become too intense. For this reason there is still vegetation, called "Laurisilva" or laurel forest, dating from the Tertiary Period.

History

Some of the islands were colonized by the Norman Jean de Bethencourt (1,360-1,422) by order of the King of Spain, but when Christopher Columbus passed by in 1,492 heading for America, and stopped at one of the islands called Gomera, Tenerife had still not been conquered.

The native people, called "Guanches" were white. It is thought that they were closely related to the native Berbers who lived in the north of Africa before the Romans or the Arabians. The Guanches were conquered by the Spanish in 1,496 after a century of resistance. Due to intermingling and the proximity

General Information

of the two races, two centuries later they were indistinguishable from the Spanish colonizers. That is why you will not find remains of an "aboriginal" race today.

The Canary Islands were crucial places for the sea routes between Europe and America, Africa and Asia. As long as sailing boats were in use and until the construction of the Suez Canal, the population was enriched by commercial relations and immigrants from all over Europe. This explains why the Spanish language spoken in the Canary Islands today is tinged with numerous Portuguese, English and French words.

At the same time, for more than five centuries, many Canary islanders emigrated to America. They founded cities such as San Antonio de Texas in USA or Montevideo in Uruguay, and they played a very important role in the colonization of many other places, like New Orleans, Cuba, Venezuela etc.

Society

The islands basically depended on agriculture until tourism began to develop as from 1,960. Because of the climate, one of the most stable and temperate in the world, and because of their location at the southernmost point of the European Union, the Canary Islands have become one of the most common tourist destinations. Although the population is currently two million people, the Canary Islands receive more than ten million tourists a year.

Despite their location, the Canary Islands have few cultural or population relations with Africa. The society is purely European. Only in the last ten years have the

Canary islanders had to remember their geographic situation, having received immigrants from Africa who arrive in little wooden boats, seeking a better life and fleeing from the poverty that engulfs that continent. These immigrants are redistributed among the islands and the rest of Spain.

Geography and climate

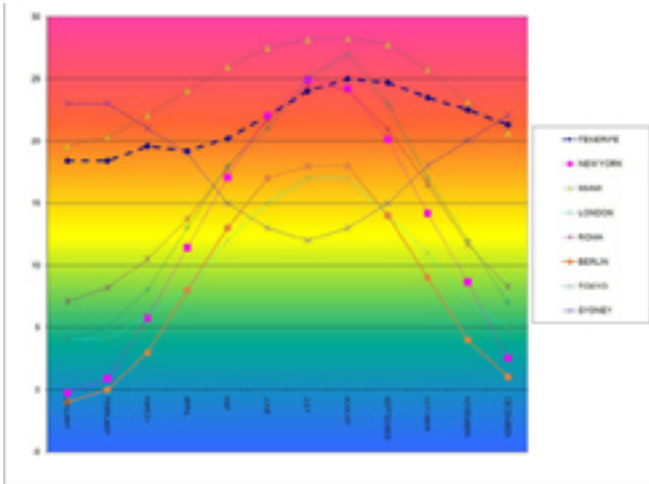
With a territory of 19,103 km², Tenerife is one of the larger islands and without doubt the most varied of the Canaries. A great part of this variety is due to the altitude of El Teide, the volcano located in the middle of the island, which reaches 3,718 metres (12,198 feet) and which has been declared an UNESCO World Heritage natural site. The whole island is very mountainous, so from the coast you can climb to an altitude of 2,000 metres (6,562 feet) in less than 50 kilometres (31 miles) by road. The differences in altitude create continuous changes of climate, giving rise to an enormous variety of vegetation and landscape. In addition, the Trade Winds from the north-east influence humidity levels, which are higher in the north than in the south, creating a wide range of micro-climates to the point that Tenerife is said to resemble a mini-continent.

Whilst visiting Tenerife, you must be prepared for changes of temperature during a single day. In March you may be swimming in the hotel pool at a temperature ambience of 20-25°C (55-60° F), but if you decide to visit one of the interior villages, you will find a cooler, fresher climate of 15-20° C (49-55° F), and if you choose to join us on the congress trip to the high central part of the island, you should not forget to take warm clothing with you. Although the atmosphere is dry up here, the remains of the last snowfall may



still be on the ground and the temperature could be around 5-10° C (38-43° F).

The only problem with Tenerife is a relatively high population density: the reason is that everybody wants to live here.



Airport

The Local Committee recommends to use the Tenerife North-Los Rodeos airport (TFN) whenever possible, both for arrival and departure.

Tenerife has two airports. Tenerife North - Los Rodeos (TFN) and Tenerife South - Reina Sofia (TFS). We recommend that your flight should be programmed to the Tenerife-North airport, because it is placed to 25km (15.5 miles) of the hotel. The Tenerife - South airport is placed to 100km (57.8 miles) and the transport will turn out to be much more expensive.

Taxi cost from Tenerife South airport: around 100€ (one hour). Public Bus cost 12€ (two hours, because it is necessary to change busses at Santa Cruz, the main city of the island).

Taxi cost from Los Rodeos: around 30€ (twenty minutes). Public Bus cost: 4€ (thirty minutes, using the stop at Hotel Botanico).



Banks

Banks are open from Monday to Friday, 9:00-14:00. Automatic teller machines are available for withdrawing by credit card everyday at almost all major banks. Most hotels offer Money exchange.

Climate

The temperature in Puerto de la Cruz in March can vary between 18-22 degrees centigrade during the day. Night temperature is around 16 degrees.

Credit Cards

Visa, MasterCard, American Express, and Diners Club cards are widely accepted at hotels, department stores, shops, and restaurants.

Currency

Like in the rest of the European Union, the official currency is the Euro (€). The most common credit cards are accepted in most of the businesses and hotels.

Electricity

220-240 volts alternating current at a frequency of 50 Hz is used in Spain. Outlets in Spain generally accept only plugs with two round pins.

Insurance

The Organizing Committee will assume no liability whatsoever for injury or damage to persons or property during the Congress. The European health card covers all European Union citizens for the Servicio Canario de Salud (Canary Health Care System). Please make your own arrangements for health insurance and any other necessary insurance.

Passport and Visa requirements

If you are coming from a EU country, Switzerland, Norway, Iceland or Liechtenstein, you can enter the country with a valid passport or identity card. From other countries, a valid passport is required and in many cases also a visa. Please consult your nearest Spanish embassy. If you need an individual invitation letter to IPS2010, please contact IPS2010 secretariat office at secretariat@ips2010.es

Postal Service

Hotels often provide simple postage services. Post offices are open from Monday to Saturday, 9:00 to 14:00.

Time

Canary Island Standard Time is 00:00:00 UTC (Coordinated Universal Time).

Tipping and Consumption Tax

Tipping is not a must. All establishments include the service in the price. However, tipping is very usual and the amount depends on the generosity of the client: 10% in restaurants, 1 euro per bag.

Map of Puerto de la Cruz (Hotel Semiramis area)

Symposium Venue

Hotel Semiramis - Puerto de la Cruz - Tenerife

Bus Services

All hotels proposed by the Organizing Committee are located at around five minutes walk from Hotel Semiramis. There will be a shuttle bus leaving from Hotel Semiramis to attend the social events.



Program at a Glance

| IPS2016 | Tuesday, March 23 | Wednesday, March 24 | Thursday, March 25 | Friday, March 26 |
|---------|--|--|---|--|
| 8:30 | | BREAKFAST | BREAKFAST | |
| | | BREAKFAST SEMINAR PFIZER - Dr. David Garway-Heath Imaging and Perimetry: Optimizing Test Intervals for Clinical Trials | BREAKFAST SEMINAR ZEISS Dr. David Garway-Heath, Dr. Francisco Góth Clinical Management using Quantitative Progression Tools | |
| 9:00 | | OPENING REMARKS | SESSION 5 Morphology, NBI | SESSION 6 Cornea, retina, alternatives |
| 10:00 | | SESSION 1 Structure function relationships | COFFEE, POSTERS & EXHIBITS | COFFEE, POSTERS & EXHIBITS |
| | | COFFEE, POSTERS & EXHIBITS | AULHORN LECTURE Dr. J. L. González-Bora Seeing through the ears: visual field perception using auditory substitution | SESSION 7 Quantification of visual field data |
| 11:00 | | SESSION 2 Structure function relationships | Dr. Pedro Alvarez - The Great Telescope CANARIAS: a Universe to discover | |
| 12:00 | | IPS LECTURE Prof. Dr. Richard Penev Mills State of the art in glaucoma screening | | BUSINESS MEETING |
| 13:00 | | LUNCH | LUNCH | LUNCH |
| 14:00 | | LUNCHEON SEMINAR - HAAG-STREIT Prof. Fritz Dannheim Practical application of linear and non-linear trend analysis in visual field series | | LUNCHEON SEMINAR ALLERGAN |
| 15:00 | Registration (Hotel Semiramis) | SESSION 3 Visual field and optic disc progression | Visit to the OBSERVATORY of the INSTITUTO DE ASTROFISICA DE CANARIAS at LAS CAÑADAS DEL TEIDE | SESSION 8 Quantification of visual field data |
| 16:00 | | COFFEE, POSTERS & EXHIBITS | | COFFEE, POSTERS & EXHIBITS |
| 17:00 | | SESSION 4 Kinetic, pupil | | SESSION 9 Quantification of visual field data |
| 18:00 | | | | CLOSING REMARKS |
| 19:00 | | | | |
| 20:00 | Welcome Reception at "LAGO MARTIANEZ" | | | |
| 21:00 | | OPTIONAL DINNER "ABACO" | | |
| 22:00 | | | | CLOSING BANQUET |
| 23:00 | | | | |



IPS lecture Richard Pence Mills



Ophthalmology, Chairman of the Department of Ophthalmology at the University of Kentucky, and Director of the American Board of Ophthalmology.

He has participated in 11 funded research projects, has published 5 books, 27 books' chapters and more than 100 papers. He is an outstanding and entertaining lecturer and has been invited for more than 300 lectures.

Prof. Mills has been one of the most active members of the International Perimetric Society, belonging to its board since 1,986, where he has been editor of Perimetry Update and has held the posts of Secretary and Treasurer.

Few have the knowledge and perspective of Professor Mills to address "State of the art in glaucoma screening"

"State of the art in glaucoma screening"

Richard Pence Mills Chairperson: Michael Wall

Department of Ophthalmology, University of Washington

Since the abandonment of tonometry as a glaucoma screening test, many functional and structural tests and combinations thereof have been proposed for use in screening. Whenever screening is to be done, the first question to ask is "Who is to be screened?" Once that is determined, a sensible screening strategy can be developed. The concepts of pre-test and post-test probability are important constructs to guide thinking about glaucoma screening.



Richard Pence Mills, MD, MPH Wednesday, March 24. 12:15-13:15

Professor Mills obtained his MD at Yale and his MPH at U. Washington. He completed Neuro-Ophthalmology fellowships at the University of Utah and University of California, San Francisco. He completed a Glaucoma fellowship with Stephen Drance at the University of British Columbia.

He has been Director at Large of the American Glaucoma Society, Director of the Foundation of the American Academy of Ophthalmology, President of the Washington Academy of Eye Physicians and Surgeons, President of the American Academy of

Aulhorn Lecture

Jose Luis Gonzalez Mora



Jose Luis Gonzalez Mora, MD, PhD
Thursday, March 25. 10:30-11:15

J. L. Gonzalez-Mora has been Senior Professor in the Department of Physiology, University of La Laguna (ULL), and is the head of the Neurochemical and Neuroimaging Laboratory. His group has been working on “in vivo” voltammetry since 1,988. His laboratory at ULL focuses on the use of electrochemical microelectrode techniques. This has led to commercially interesting technological

developments and 3 patents. He is the author or co-author of more than 80 international publications in the field of neurobiology and neurochemistry, and has given over 50 scientific conference presentations in these fields. Since 1,990 he has been the organiser of various international activities about neuroscientific methods, as well as collaboration projects with international scientific groups. He is currently involved, as the scientist in charge, in several European Projects, Dr. Gonzalez-Mora’s recent honours include the Canary Award for Research into Accessibility, 2,004.

“Seeing through the ears: visual field perception using auditory substitution”

Jose Luis Gonzalez Mora Chairperson: David Henson

Our main goal is to work with technology oriented to sensory substitution, especially in blindness. Sensory substitution can be defined as a technical-scientific discipline which aims to provide sensory disabled people with information they cannot acquire from the disabled sense through their intact senses. We present here an overview of our team’s work in this R+D line for providing blind and severe visually impaired people with real time spatial and text environmental information through sounds.

The ability to “perceive” the local, immediate and even global environment for daily living activities is needed by all people. People with visual impairments (or even cognitive impairments) require technology that identifies obstacles in their immediate path both inside and outside of buildings and assists in navigational tasks.

We have developed a series of prototypes for blind people’s orientation, mobility and environmental perception, which provide the user with two types of real time information: information on the spatial volume occupied by the objects and surfaces located in front of him, and information on the written text present in the frontal scene (i.e., shop signs, advertisings, etc). The volume information is translated into a special sound code which is delivered through headphones in order to generate an auditory spatial representation coherent with the environment. The text information is presented as verbal spatial sound, as if a reading voice was coming from the area where the text is located. This research is complemented with the study of the disabled people’s neurological substrate of the sensory substitution experience, through brain function registering techniques such as functional Magnetic Resonance Imaging (fMRI) and Event Related Potentials (ERP).





Gran Telescopio CANARIAS presentation

Pedro Alvarez

Pedro Alvarez PhD
Thursday, March 25. 11:15-12:00

Pedro Alvarez is Doctor in Physical Sciences and director of the company GRANTECAN which has designed the "Gran Telescopio CANARIAS". 28 years ago he collaborated with Prof. Gonzalez de la Rosa designing the software of the Hipocampus, an automatic perimeter which used a photometrical monitor controlled as a test screen.

"The Great Telescope CANARIAS: a Universe to discover"

Pedro Alvarez Chairperson: Manuel Gonzalez de la Rosa

In 2,009 the "Gran Telescopio CANARIAS" (GTC) has been inaugurated in the island of La Palma, the major astronomic observation's instrument of the north hemisphere, with a segmented mirror of 10.4 meters of diameter, which readjusts its focus in a continuous way with procedures of active optics. We will comment the principal aspects of the design and how it allows us to begin to observe the universe through one of its two first scientific instruments.

Completed its set up, it begins now to study the cosmos in visible light an soon, it will also do it in infrared light.

Thanks to its singular capacities it allows to realize newly observation's programs with which we can verify the present theories that try to explain the heavenly objects. We all hope that the GTC will show aspects not observed till now with other instruments.

Scientific Program

Wednesday, March 24

8:00-8:30 Breakfast at Room La Palma

8:30-9:15 Morning Seminar Room La Palma

Pfizer

Optimizing Test Intervals for Clinical Trials

David Garway-Heath

9:15-9:45 Opening Remarks Room Islas Canarias

9:45-10:45 Session 1 Room Islas Canarias

Structure Function Relationships

Moderators: Linda Zangwill, Paul Artes

9:45 _____ 1-01

Evaluating the Strength of the Topographic Structure Function Relationship in Glaucoma

Jonathan Dennis

9:57 _____ 1-02

Relationship between Retinal Structure and Function Measurements over Time

Madhusudhanan Balasubramanian

10:09 _____ 1-03

Relationship between Structural and Functional Measures in the Perifovea of Patients with Glaucoma

Mitchell Dul

10:21 _____ 1-04

Comparison of Polar Graph Retinal Nerve Fiber Layer Model with Patient's Layer Images taken by Scanning Laser Ophthalmoscope

Fumi Tanabe

10:33 _____ 1-05

A Mathematical Description of Nerve Fiber Trajectories and their Variability in the Human Retina

Nomdo Jansonius

10:45-11:15 Coffee, Posters & Exhibits

11:15-12:15 Session 2 Room Islas Canarias

Structure function relationships

Moderators: Mario Zulauf, Manuel Gonzalez de la Rosa

11:15 _____ 2-01

Visual Function Specific Perimetric Tests and Structural Changes using SD-OCT in Early and Preperimetric Glaucoma

Chota Matsumoto

11:27 _____ 2-02

Optic Nerve Head, Visual Field and Global Indices

Jara Hornova

11:39 _____ 2-03

Relationship between Metamorphopsia Score and Structural Changes using SD-OCT in Patients with ERM

Eiko Arimura

11:51 _____ 2-04

Imaging of Retinal Nerve Fiber Layers in Retinitis Pigmentosa Patients with Concentric Visual Field Loss

Leva Sliesoraityte

12:03 _____ 2-05

The Rate of Glaucomatous Structural Change in the Ocular Hypertensive Treatment Study (OHTS), Diagnostic Innovations in Glaucoma Study (DIGS) and African Descent and Glaucoma Evaluation Study (ADAGES)

Linda Zangwill

12:15-13:15 IPS Lecture Room Islas Canarias

Chairman: Michael Wall

State of the Art in Glaucoma Screening

Richard Pence Mills

13:15-14:00 Lunch at Room La Palma

14:00-14:45 Luncheon Seminar Room La Palma

Haag Streit

Practical Application of Linear and Non-Linear Trend Analysis in Visual Field Series

Fritz Dannheim

14:45-15:15 Break

15:15-16:30 Session 3 Room Islas Canarias

Visual Field and Optic Disc Progression

Moderators: Ronald Harwerth, Marta Gonzalez Hernandez

15:15 Poster _____ 3-01

The Optimum Distribution of Visual Field Test Points to Maximize Structure-Function Correlation

Ryo Asaka

15:20 Poster _____ 3-02

Structure-Function Relationship in Glaucoma: Optical Coherence Tomography versus Frequency-Doubling Perimetry

Maria Isabel Fuertes Lazaro

15:25 _____ 3-03

Progression of Patterns (POP): Machine Classifier Identifies Glaucoma Progression

Pamela Sample

15:37 _____ 3-04

Differentiated Trend Analysis of the Visual Field in Glaucoma

Fritz Dannheim

Scientific Program

15:49 Poster _____ **3-05**
Perimetric Progression in Open Angle Glaucoma and the Visual Field Index (VFI)

Mohammed Sohaib Mustafa

15:54 _____ **3-06**
Probability of Visual Field Progression in Multiple Point Trend Analysis

Manuel Gonzalez de la Rosa

16:06 _____ **3-07**
Comparison of the Threshold Noiseless Trend Programs Versions 1 and 2 (TNT1 Vs TNT2)

Julian Garcia-Feijoo

16:18 _____ **3-08**
Effect on HRT Topographic Change Analysis Parameter Estimates when Combining HRT-I and HRT-II Examinations in Longitudinal Series

Christopher Bowd

16:30-17:00 Coffee, Posters & Exhibits

17:00-18:01 Session 4 Room Islas Canarias
Kinetic, Pupil

Moderators: Fritz Dannheim, Shaban Demirel

17:00 Poster _____ **4-01**
Utility of Fully Automated Kinetic Perimetry (Program K) in Detecting and Evaluating Visual Fields with Superior Segmental Optic Hypoplasia (SSOH)

Tomoyasu Kayazawa

17:05 _____ **4-02**
Effects of False-Positive and False-Negative Responses and FOS Curve on Fully Automated Kinetic Perimetry (Program K) in Virtual Patients

Shigeki Hashimoto

17:17 Poster _____ **4-03**
The Intrasubject Intrasession Variability of Isopter's Position and the Fatigue Effect during Semi-Automated Kinetic Perimetry in Patients With Advanced Visual Field Loss

Katarzyna Nowomiejska

17:22 Poster _____ **4-04**
Reproducibility of Semi-Automated Kinetic Visual Field Examinations (SKP)

Elke Krapp

17:27 Poster _____ **4-05**
Evaluating Pupil Light Reflexes with Three Color Stimuli of Different of Sizes and Intensities under the Same Energy at each Eccentricity of the Visual Field

Keiichi Tanzawa

17:32 _____ **4-06**
Identifying the State of Vigilance during Perimetry with Pupil Dynamics

Yanfang Wang

17:44 _____ **4-07**
Luminance-Balanced Multifocal Objective Perimetry

Ted Maddess

17:56 Poster _____ **4-08**
Multifocal Pupillographic Objective Perimetry in Glaucoma using Blue Stimuli

Corinne Carle

20:30-22:30 Optional Dinner at "Abaco"



Thursday, March 25

8:00-8:30 Breakfast at Room La Palma

8:30-9:15 Morning Seminar Room La Palma

Carl Zeiss

Clinical Management using Quantitative Progression Tools

David Garway-Heath, Francisco Goñi

9:15-10:06 Session 5 Room Islas Canarias

Morphology. fMRI

Moderators: Chris Johnson, David Henson

9:15 Poster _____ **5-01**

Correlation between SLP with and without ECC and HD-OCT in Normal and Glaucomatous Eyes

Javier Benítez del Castillo

9:20 _____ **5-02**

SD OCT Measurements of Cross-Section Area of the RNFL for the Assessment of Optic Neuropathy

Ron Harwerth

9:32 Poster _____ **5-03**

Reproducibility of Topcon 3D OCT-1000 Measurements of Retinal Nerve Fiber Layer in Healthy Subjects

Alexander Shpak

9:37 Poster _____ **5-04**

Gdx Staging System: A New Method for Retinal Nerve Fiber Layer Damage Classification

Paolo Brusini, Mark Zeppieri

9:42 _____ **5-05**

Extracting More Information from Optic Disc Topography Using Shape Analysis

Haogang Zhu

9:54 _____ **5-06**

Comparing Fmri-Based Visual Field Representation with Perimetry: Can Fmri Provide Objective Measures of Visual Field Enlargement?

Ronald Schuchard

10:06-10:30 Coffee, Posters & Exhibits

10:30-11:15 Aulhorn Lecture Room Islas Canarias

Chairman: David Henson

Seeing through the Ears

Jose Luis Gonzalez Mora

11:15-12:00 Grantecan Room Islas Canarias

Chairman: Manuel Gonzalez de la Rosa

The Great Telescope Canarias (GRANTECAN):

a Universe to Discover

Pedro Alvarez

12:45 Lunch and Visit to the Observatory of the Instituto de Astrofísica de Canarias at Las Cañadas del Teide



Scientific Program

Friday, March 26

9:15-10:13 Session 6 Room Islas Canarias

Cornea, Retina, Alternatives

Moderators: Ulrich Schiefer, Chota Matsumoto

9:15 Poster _____ 6-01
Corneal Structure and Function Measures as Markers of Diabetic Peripheral Neuropathy
Geoff Sampson

9:20 _____ 6-02
The Extent of Presenting Visual Field Loss in Patients with Glaucoma
David Henson

9:32 _____ 6-03
Progression Rate of Central 10 Degree Mean Deviation in Eyes with Retinitis Pigmentosa
Hiroyuki Iijima

9:44 Poster _____ 6-04
Logistic Regression Analysis for Glaucoma Diagnosis using Frequency-Doubling Perimetry
Maria Isabel Fuertes Lazaro

9:49 _____ 6-05
Within-Individual Between-Visit Performance with the Pulsar Perimeter
Mario Zulauf

10:01 _____ 6-06
Threshold Responses in Glaucomatous Eyes in Areas of Visual Field judged Normal with Rarebit Perimetry
Andrew Anderson

10:15-10:45 Coffee, Posters & Exhibits

10:45-12:10 Session 7 Room Islas Canarias

Quantification of Visual Field Data

Moderators: Richard Mills, Michael Wall

10:45 Poster _____ 7-01
A Comparison of Detection Rates using Total Deviation Probability Plots for SAP Sizes III and V, Motion Perimetry and Matrix
Carrie Doyle

10:50 _____ 7-02
Demonstrating a Rapid Testing Strategy for the Moorfields Motion Displacement Test for Glaucoma Case Detection
Ciara Bergin

11:02 Poster _____ 7-03
The Effects of Optical Correction on Motion Displacement Thresholds in Glaucoma
Reza Moosavi

11:07 _____ 7-04
Defect Curve Fluctuation in Standard and Pulsar Perimetries
Manuel Gonzalez de la Rosa

11:19 Poster _____ 7-05
The Variability of the SITA Standard, SITA Fast and SITA SWAP Algorithm
Christoph Castelberg

11:24 _____ 7-06
Comparison of the Visual Field Testing Results Of FDT, Flicker Perimetry and SWAP between Patients with NTG and POAG
Hiroki Nomoto

11:36 _____ 7-07
The Comparative Performance of Standard Automated Perimetry and Critical Flicker Frequency Perimetry in Individuals with Cataract
Knut Luraas

11:48 Poster _____ 7-08
Intermittent Visual Loss during Eye Movements
Anna Regina Bruckmann

11:53 _____ 7-09
Quantification of Perimetric Results - A Volumetric Approach
Ulrich Schiefer

12:05 Poster _____ 7-10
Reduction of Learning Effects in Studies of Multiple Perimetric Tests in Glaucoma Patients
Kathryn Sherman

12:15-13:15 Business Meeting

13:15-14:00 Lunch at Room La Palma

14:00-14:45 Luncheon Seminar Room La Palma
Allergan
Rates of Visual Field Progression in Clinical Practice
Dr. Francisco Javier Goñi and Dr. David Garway-Heath

14:45-15:15 Break

15:15-16:13 Session 8 Room Islas Canarias

Quantification of Visual Field Data

Moderators: Pamela Sample, Andrew Anderson

15:15 _____ 8-01
Automatically Identified Patterns of Glaucomatous Visual Field Loss in SITA Fields from Independent Component Analysis
Michael Goldbaum

15:27 Poster _____ 8-02
Comparison of Local Differential Luminance Sensitivity (LDS) between Oculus Easyfield Perimeter and Humphrey Field Analyzer 740 (HFA II) in Normal Subjects of Varying Ages
Zoltan Gagy-Palfy



15:32 _____ **8-03**
Exploratory Eye Movements – A Compensatory Option for Patients with Homonymous Visual Field Defects?
Eleni Papageorgiou

15:44 Poster _____ **8-04**
Visual Acuity Loss of Unknown Origin in a Patient with Suspected Low Tension Glaucoma
Christian Heine

15:49 _____ **8-05**
Predictability of Future Perimetric Change in Glaucoma Using a Linear-Scaled Global Index
Stuart Gardiner

16:01 _____ **8-06**
Properties of the Statpac Visual Field Index (VFI)
Paul Artes

16:15-16:45 Coffee, Posters & Exhibits

16:45-17:36 Session 9 Room Islas Canarias
Quantification of Visual Field Data
Moderators: David Garway-Heath, Julian García Feijoo

16:45 Poster _____ **9-01**
Grey Scale Map of Perimetric Progression Using Multiple Defect Curves
Marta Gonzalez Hernandez

16:50 _____ **9-02**
A Continuous Probability Scale for Size III, Size V, Motion and Matrix Perimetry
Chris Johnson

17:02 Poster _____ **9-03**
AutoSCOPE - An Algorithm for Automated Regional Condensation of Stimulus Density for Polar and Rectangular Perimetric Grids
Janko Dietzsch

17:07 _____ **9-04**
Modeling the Hill of Vision in Health and Disease
Richard Weleber

17:19 _____ **9-05**
The Effect of Stimulus Size on Repeatability in Glaucoma Using Goldmann Sizes III, V, and VI
Michael Wall

17:31 Poster _____ **9-06**
Introduction of a Portable Campimeter, Based on a Laptop/Tablet PC
Enkelejda Tafaj

17:36-17:45 Closing Remarks Room Islas Canarias

20:00 Closing Banquet at “Casino de Tenerife”



Abstracts



1-01 Evaluating the Strength of the Topographic Structure-Function Relationship in Glaucoma

J Dennis¹, DB Henson¹, I Schiessl¹

¹ University of Manchester, Manchester, UK

Purpose: To evaluate the strength of the topographic structure-function relationship in glaucoma both with an existing structure-based map (SBM)¹ and through computer-generation of random maps.

Methods: Sample: SITA 24-2 visual field (VF) and HRTII sectoral Moorfields Regression Analysis (sMRA) optic nerve head (ONH) data from 257 eyes of 257 patients (age 35-96 years, median 70) with clinically diagnosed glaucoma, glaucomatous VF loss and prior VF test experience were taken from previous studies in Manchester, UK (n=152) and Halifax, Canada (n=105).

Analysis: VF test points were divided into 6 groups, either as in the SBM or randomly to generate 10,000 random maps. VF Total Deviation values were split into 3 grades, and the mode grade of all points within a group taken to represent the extent of loss within the group. An error measure was devised whereby a VF group whose grade was not equal to the corresponding sMRA grade for a particular map was marked an error. The proportion of errors in all 6 corresponding VF/ONH areas across all patients was calculated for each map (0=perfect relationship, 1=no relationship). Error was compared for all random maps and all possible permutations of the SBM.

Results: The SBM error was 0.3872 which was less than all other permutations of itself (n=720, t-test, p<0.01). Lowest error from the 10,000 randomly generated maps was 0.3729. This map appears to have no anatomical/structural foundation, with points from each group being scattered throughout the VF. 33.5% of randomly generated maps had one or more permutation with error less than or equal to the SBM.

Conclusions: A weak topographic structure-function relationship was found using the SBM. If a strong relationship existed within the data, the best performing randomly generated map should approximate to it, yet no such plausible relationship was found. Variation in both depth and location of damage in current measures may partially account for the lack of a strong relationship, but variation in disease process between patients cannot be ruled out.

Acknowledgement/support: We thank Dr Paul H Artes and Dr Balwantray C Chauhan, Dalhousie University, Canada for use of their dataset, and the College of Optometrists, UK for funding.

Reference:

1. DF Garway-Heath et al (2000) Ophthalmology 107:1809-1815

1-02 Relationship between Retinal Structure and Function Measurements over Time

M Balasubramanian, L Racette, C Bowd, PA Sample, RN Weinreb, LM Zangwill

Hamilton Glaucoma Center, Ophthalmology, University of California San Diego, La Jolla, CA, USA

Purpose: To investigate longitudinal relationship between rim area and visual function threshold sensitivity in non-progressing and progressing glaucoma eyes and compare with their cross-sectional relationships.

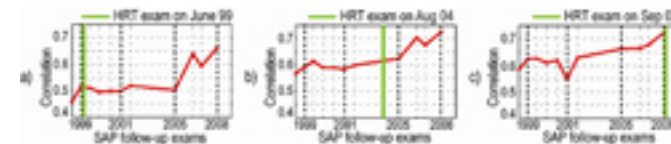
Methods: 30 progressing eyes (by stereophotograph and/or visual field GPA) and 187 non-progressing eyes with ≥4 Heidelberg Retina Tomograph (HRT)-II exams and ≥5 Standard Automated Perimetry (SAP) exams from the UCSD Diagnostic Innovations in Glaucoma Study (DIGS) were included. For the longitudinal analysis, an HRT and a SAP exam-pair was chosen among all available HRT-SAP pairs that maximized the correlation among 6 regional HRT rim areas and mean threshold sensitivities. For the cross-sectional analysis, the SAP exam within 3 months of the HRT exam was selected from each eye. Quadratic fit was used to assess the strengths of cross-sectional and longitudinal structure-function relationships (R²) in study eyes.

Results: Correlation results (R²) are presented in Table 1. Case 1 depicts the variation in the association among HRT and SAP exams over time in one progressing eye. In the longitudinal analysis of progressors, the strongest correlations were found when SAP measures led HRT by a mean of 2.3 years in 5 eyes (17%), lagged HRT by a mean of 3.6 years in 10 eyes (33%), and were within 3 months of HRT in 15 eyes (50%). Similar results were found in the non-progressing eyes (SAP led in 23%, lagged in 18%, and within 3 months of HRT in 59% of eyes).

Conclusions: The longitudinal analysis of structure-function relationship provides specific quantitative information on the variation in the strength of the temporal (time) relationship between structure and function measurements. In 41% of non-progressing eyes, the strongest HRT-SAP relationships are not within 3 months suggesting that their structure and/or function are changing over time but not enough to be classified as progressing by stereophoto or visual field GPA.

Table 1: The longitudinal analysis significantly improved the strength of the structure-function relationship in the temporal and infero-nasal sectors in progressors

| | HRT-SAP Relationship | Mean Time Difference Between HRT and SAP | R ² Values for Retinal Sectors | | | | | |
|-----------------------------|----------------------|--|---|------|------|------|------|------|
| | | | T | ST | IT | N | SN | IN |
| Progressors (n=30 eyes) | Cross-sectional | -0.02 years | 0.06 | 0.09 | 0.38 | 0 | 0.06 | 0.09 |
| | Longitudinal | 0.79 years | 0.20 | 0.10 | 0.41 | 0 | 0.06 | 0.18 |
| Nonprogressors (n=187 eyes) | Cross-sectional | -0.01 years | 0.05 | 0.18 | 0.27 | 0.08 | 0.01 | 0.13 |
| | Longitudinal | -0.15 years | 0.03 | 0.21 | 0.26 | 0.17 | 0.05 | 0.17 |



Case 1—Progressing eye: a) For an HRT exam on June 99, correlation with the closest SAP exam on April 1999 was lower (0.51) than the correlation with the SAP exam on August 2008 (0.66); b) for an HRT exam on August 2004, correlation with the closest SAP exam on September 2005 (0.62) was lower than the correlation with the SAP exam on August 2008 (0.73); and c) for an HRT exam on September 2008, the closest SAP exam on August 2008 had the highest correlation (0.73).

Support: NIH/NEI grants EY11008 (LMZ) and EY08208 (PAS)



1-03 Relationship between Structural and Functional Measures in the Perifovea of Patients with Glaucoma

MW Dul, WH Swanson, A Veerappan

State University of NY, State College of Optometry
Indiana University School of Optometry

Purpose: To study the relationship between perifoveal FD-OCT Ganglion Cell Complex (GCC) thickness and, differential light sensitivity (DLS) in patients with glaucoma involving the central ten degrees of visual field. We hypothesized that perimetric defects and structural defects would on average be similar when both were expressed as percent defect relative to mean normal.

Methods: One eye each was tested for 17 patients with open angle glaucoma involving the central ten degrees of visual field, and 14 age-similar controls (range 48-84 years, average 66.6 ± 10.4). GCC thicknesses of the superior and inferior perifoveal regions were measured using the Optovue FD-OCT macular EMM5 program. DLS was measured using stimulus size III white-on-white (HFAii-i, Carl Zeiss Meditek), 10-2 SITA Standard algorithm. DLS values were converted into linear units and averaged across locations corresponding to the perifoveal sectors, accounting for displacement of the Henle fibers. The GCC and DLS measures were then expressed as a percent of mean normal, using a linear model of effects of age..

Results: For all patients, the DLS defects were deeper than the GCC defects: superior DLS (mean \pm SD: $-0.59\% \pm .32\%$) v. inferior GCC ($-0.14\% \pm 0.18\%$), $t = -7.07$, $p < 0.0001$), inferior DLS ($-0.41\% \pm 0.25\%$) v. superior GCC ($-0.08\% \pm 0.09\%$) $t = -6.89$ $p < 0.0001$). Each sector with DLS within the 95% confidence limit for normal also had GCC within the 95% confidence limit, while in 9 cases DLS was below this limit while GCC was not.

Conclusions: We reject the hypothesis that perimetric defects and structural defects would on average be similar in this population of patients. DLS indices were abnormal more often than GCC indices, and DLS defects were significantly deeper than GCC defects.

1-04 Comparison of Polar Graph Retinal Nerve Fiber Layer Model with Patients' Layer Images taken by Scanning Laser Ophthalmoscope

F Tanabe¹, C Matsumoto¹, S Okuyama¹, S Takada¹, E Arimura², S Hashimoto¹, H Nomoto¹, Y Shimomura¹

¹ Department of Ophthalmology, Kinki University School of Medicine, Osaka-Sayama, Japan

² Department of Ophthalmology, Kinki University School of Medicine, Sakai Hospital, Sakai, Japan

Purpose: Octopus EyeSuite polar graph is a new visual field representation that rearranges the test locations round the optic disc based on a retinal nerve fiber layer (RNFL) bundle model. Here we investigated the difference between the polar graph RNFL bundle model and patients' bundle images taken by scanning laser ophthalmoscope (SLO)

Subjects and Methods: Subjects were 5eyes of 5glaucoma patients and 7eyes of 7normal subjects (corrected visual acuity > 0.8 , spherical: $-3.0D$ - $+3.0D$,) with clear fundus images by SLO (F-10, NIDEK) with a 490-nm diode laser and a confocal aperture. All the SLO images were averaged using the software tracking method with Registax V4.0, and high-quality 30-degree RNFL bundle images were constructed. Under the conditions of target size I, a background luminance of 31.4 asb, and a stimulus duration of 100 msec, we also detected the shape of the blind spot in each subject using the Octopus 900 custom test with one-degree intervals. Based on the blind spot area and fixation point, all the 30-degree visual field test locations were overlapped on the SLO images. The RNFL bundle angle at the optic disc for each test location was evaluated.

Results: The difference in the RNFL bundle angle at the optic disc between the polar graph model and the SLO images ranged from -16.7 to 31.3 degrees (mean, 7.4 degrees; SD, 12.3 degrees) in all the subjects. Furthermore, the angle difference did not vary regularly with the test locations.

Conclusion: The polar graph is a useful tool to evaluate the agreement between the functional and structural findings in glaucoma. However, a maximum difference of 30 degree between the polar graph RNFL model and patient's RNFL pattern should be taken into consideration for clinical evaluation.



1-05 A Mathematical Description of Nerve Fiber Trajectories and their Variability in the Human Retina

NM Jansonius¹, J Nevalainen², B Selig³, LM Zangwill⁴, PA Sample⁴, WM Budde⁵, JB Jonas⁶, WA Lagrèze⁷, PJ Airaksinen², R Vonthein⁸, LA Levin⁹, J Paetzold³, U Schiefer³

1 Department of Ophthalmology, University of Groningen, The Netherlands

2 University Eye Hospital Oulu, Finland

3 Centre for Ophthalmology, University of Tübingen, Germany

4 Hamilton Glaucoma Center, University of California, San Diego, USA

5 Private Practice, Essen-Steele, Germany

6 University Eye Hospital Mannheim, Germany

7 University Eye Hospital Freiburg, Germany

8 Department of Medical Biometry, University of Tübingen, Germany

9 Department of Ophthalmology and Visual Sciences, University of Wisconsin, Madison, USA;

Department of Ophthalmology, University of Montreal, Canada

Purpose: To develop a mathematical model for describing retinal nerve fiber bundle (RNFB) trajectories and to make an estimate with regard to the overall inter-subject variability of these trajectories.

Methods: Fundus images from 55 eyes of 55 human subjects were assessed. All visible RNFBs were electronically traced. Twenty seven of 55 fundus images were used to fit the RNFB trajectories by a mathematical model; the remaining 28 images were reserved as a test sample for an independent check of the model.

Results: A total of 1660 RNFB trajectories could be traced (mean 30 RNFBs per eye, range 3–118), with a mean of 10 sampling points per RNFB (range 3–48). Depending on the location of the visual field test point, the standard deviation of the calculated corresponding angular location at the optic nerve head circumference ranged from less than 1 to 18, with an average of 8.8. The model resembled the typical retinal nerve fiber layer course within 20° eccentricity.

Conclusions: This study confirms the presence of considerable variability of the RNFB trajectories in the human retina, yields a detailed location-specific estimate of the magnitude of this variability and provides a useful mathematical tool for further analyzing it.

2-01 Visual Function Specific Perimetric Tests and Structural Changes using SD-OCT in Early and Preperimetric Glaucoma

C Matsumoto¹, H Nomoto¹, S Takada¹, S Okuyama¹, E Arimura², S Hashimoto¹, F Tanabe¹, Y Shimomura¹

¹ Department of Ophthalmology, Kinki University School of Medicine, Osaka-Sayama, Japan
² Department of Ophthalmology, Kinki University School of Medicine, Sakai Hospital, Sakai, Japan

Purpose: To investigate the relationship between the retinal nerve fibre layer thickness (RNFLT) obtained from the spectral-domain OCT (SD-OCT) and the visual function specific perimetric tests in early and preperimetric glaucoma

Subjects and Methods: Subjects were 25 eyes of 25 preperimetric glaucoma and 30 eyes of 30 early glaucoma patients. All subjects underwent functional tests, HFA 24-2 full threshold (SAP), Matrix (24-2-5,1), flicker perimetry (4-zone 38S), SITA-SWAP (24-2). Their RNFLT were examined using SD-OCT (Cirrus HDOCT). The relationship between the visual field abnormality at each test point, sectors and their NFLT at each area obtained by SD-OCT were investigated.

Results: In early and preperimetric glaucoma patients, there were significant relationships between the abnormal test locations obtained by SAP, Matrix, Flicker, SITA-SWAP and anatomically-corresponded RNFLT by SD-OCT. Matrix, flicker perimetry and SWAP showed more abnormal test points than SAP on the 5% abnormality area (yellow zone) by the SD-OCT depending on the thickness of the NFLT.

Conclusion: Early functional changes detected by Matrix, flicker perimetry and SWAP relate to the anatomically corresponded structural changes obtained by SD-OCT in early and preperimetric glaucoma.

2-02 Optic Nerve Head, Visual Field and Global Indices

J Hornova^{1,2,3}

¹ Dept. of Ophthalmology, Third Faculty of Medicine, Charles University, Prague, Czech Republic
² Vinohrady Teaching Hospital, Prague, Czech Republic
³ Institute for Postgraduate Medical Education, Prague, Czech Republic

Purpose: To monitor changes of the global indices (GI) in correlation with optic nerve head (ONH) and visual field (VF) in our glaucoma patients.

Methods: Sixty five eyes (57 eyes with POAG and 8 controls) were evaluated using Humphrey Field Analyzer (HFA) perimeter. The VF was examined by Full Threshold test (30-2) and evaluated by Aulhorn's scale of 0 to 6, and by GI: Mean deviation (MD), Pattern standard deviation (PSD), Correlated pattern standard deviation (CPSD), Sort fluctuation (SF). GI were correlated with Optic nerve head (ONH) using Disc Damage Likelihood Scale (DDLS) from 1 to 9.

Results: in all correlations MD coefficient worsens very slowly, especially in the early glaucoma, changes are from VF 3 and from DDLS 4. Due to other glaucoma progression MD index accelerates. The apparent evolution of PSD index is from VF 2 and DDLS 4, values of PSD are lower when irregularities in the VF are mild (shallow scotomata), and increase as there is additional depression in the VF. Maximal level of PSD is due VF 4-5 and DDLS 7, later is PSD index decreased. CPSD curve is authentic image of PSD with lower values due to correlations. SF parameter slowly increases with crescentic changes in the VF and on the ONH by DDLS classification.

Conclusions: GI correlate with evolution of glaucoma changes, but every index has its own specific trend. PSD index is sensitive for initial-mild glaucoma changes on the ONH and in the VF. MD index worsens very quickly between moderate-late glaucoma changes. All GI have to be compared with probability plots and greyscale of the VF and together with the objective examination of the ONH.



2-03 Relationship between Metamorphopsia Score and Structural Changes using SD-OCT in Patients with ERM

E Arimura¹, C Matsumoto², H Nomoto², F Tanabe², S Hashimoto², S Takada², S Okuyama², Y Shimomura²

¹ Department of Ophthalmology, Kinki University School of Medicine, Sakai Hospital, Sakai, Japan

² Department of Ophthalmology, Kinki University School of Medicine, Osaka-Sayama, Japan

Purpose: We previously reported the significant relationship between the degree of retinal contraction and the change in metamorphopsia score measured by M-CHARTS in patients with idiopathic epiretinal membrane (ERM). In this study, we investigated the relationship between the structural changes of ERM using Spectral domain OCT (SD-OCT) and metamorphopsia score.

Methods: Subjects were 36 eyes of 36 patients with idiopathic ERM. For functional analysis, the corrected visual acuity and the central 10° differential light sensitivity using the Octopus 101 program M2 were also assessed in addition to M-CHARTS score which was obtained using 19 dotted lines with dot intervals between 0.2° to 2.0° visual angles. For the structural changes of ERM, retinal thickness and the irregularity of the IS/OS line were evaluated using SD-OCT (Cirrus).

Results: Retinal thickness significantly correlated to visual acuity but not to the mean defect of program M2 or metamorphopsia score. In addition, the irregularity of the IS/OS line also did not correlate to any of the three functional tests in ERM.

Conclusions: Metamorphopsia in patients with ERM is mainly influenced by the retinal displacement caused by membrane contraction and/or traction rather than by the local morphological retinal structural changes including retinal thickness and the irregularity of the IS/OS line.

2-04 Imaging of Retinal Nerve Fiber Layers in Retinitis Pigmentosa Patients with Concentric Visual Field Loss

I Sliesoraityte¹, A Kurtenbach¹, E Troeger¹, U Schiefer¹, E Zrenner¹

¹ Centre for Ophthalmology, Institute for Ophthalmic Research, University of Tuebingen, Germany

Purpose: Retinitis pigmentosa (RP) is a group of heterogeneous diseases and the most common cause of inherited blindness worldwide. Imaging of retinal nerve fiber layer thickness (RNFLT), as a measure of the integrity of retinal ganglion cells, could provide new insights regarding the inner retina morphology in advanced RP cases. The purpose of this paper is to evaluate the relation between structure and function of the inner retina in advanced retinitis pigmentosa cases.

Methods: Prospective observational cross-sectional study comprised 18 RP affected eyes with concentric visual field loss ($\leq 10^\circ$). All patients (mean age 48 ± 18 years) underwent comprehensive ophthalmologic examination, including visual field testing, retinal nerve fiber layer thickness imaging and full-field electroretinography. RNFLT was assessed using scanning laser polarimetry with enhanced corneal compensation (GDx-ECC). RNFLT parameters, i.e. temporal-superior-nasal-inferior-temporal (TSNIT), superior, and inferior were used for the analysis. Additionally, RNFLT were compared with 18 age-matched healthy eyes. Visual field was tested using semi-automatic kinetic Octopus 900 perimeter (Haag-Streit Inc., Koeniz, Switzerland). The preserved visual field area for III4e target was measured by electronic planimetry in square degrees.

Results: The mean TSNIT was $61.3 \pm 2.9 \mu\text{m}$, the mean superior was $72.3 \pm 4.3 \mu\text{m}$, and the mean inferior was $69.9 \pm 3.9 \mu\text{m}$ in RP; and $48.3 \pm 1.2 \mu\text{m}$, $58.8 \pm 1.9 \mu\text{m}$, $62.8 \pm 1.8 \mu\text{m}$ in healthy, respectively ($p < 0.05$). The mean preserved visual field area was $223.1 \pm 54.4 \text{deg}^2$ in RP (normal values for healthy were $13307.7 \pm 212.9 \text{deg}^2$). In multivariate logistic regression models adjusted for age, gender, and RP duration, retinal nerve fiber layer thickness was negatively ($r = -0.507$) associated with the preserved visual field area ($p = 0.02$).

Conclusions: Data suggest that, although retinitis pigmentosa with concentric visual field loss is associated with subtle morphological changes of the inner retina, the integrity of the retinal ganglion cells might be preserved even in advanced RP cases. Combination of advanced imaging technologies with visual field testing modalities could highlight new insights in understanding the relation between structure and function of the inner retina in blindness associated diseases e.g. as a inclusion criterion for treatment trials.



2-05 The Rate of Glaucomatous Structural Change in the Ocular Hypertensive Treatment Study (OHTS), Diagnostic Innovations in Glaucoma Study (DIGS) and African Descent and Glaucoma Evaluation Study (ADAGES)

LM Zangwill¹, L Alencar¹, S Jain¹, PA Sample¹, C Bowd¹, J Liebmann², CA Girkin³, RN Weinreb¹, MO Gordon⁴, MA Kass⁴, FA Medeiros¹

1 University of California, San Diego, La Jolla, CA, USA

2 New York Eye and Ear Infirmary, New York, NY, USA

3 University of Alabama, Birmingham, AL, USA

4 Washington University, St. Louis, MO, USA

Purpose: Estimating the rate of glaucomatous change is a challenging yet important aspect of the clinical management of glaucoma. The objective of this study is to compare rates of structural change in progressing and non-progressing eyes from 3 different study cohorts, and to evaluate factors that influence the rate of change.

Methods: Progressing eyes were identified based on fields and/or stereo-photograph-based change. The rate of change of HRT optic disc parameters and/or GDx RNFL thickness were measured in the 3 cohorts: 1) OHTS Confocal Scanning Laser Ophthalmoscopy Ancillary Study, (median follow-up: 10 years, 50 of 438 participants develop primary open angle glaucoma (POAG)), 2) DIGS (median follow-up: 3.9 years, with 34 of 335 participants progressing), and 3) ADAGES (median follow-up: 3.5 years, with 46 of 629 participants progressing).. Multivariable mixed effects models were used to compare slopes in progressing and nonprogressing eyes.

Results: In OHTS, the rate of HRT rim area change (95% CI) was significantly faster in eyes developing POAG than in eyes that did not (-0.0136 (-0.0178, -0.0093) mm²/yr and -0.0024 (-0.0155, -0.0067) mm²/yr, respectively). In the ADAGES and DIGS cohorts, the rate of RNFL thinning was significantly faster in the progressing eyes, compared to the non-progressing eyes (ADAGES and DIGS GDx VCC: -0.72 mm/yr and -0.09 mm/yr, respectively and DIGS1 GDx ECC -0.95 and -0.17 mm/yr, respectively). In these 3 cohorts, the slope of change in both the non-progressing and progressing eyes was significantly different from zero. In addition, the rate of structural change in the inferior and superior regions was significantly faster than in other regions, and faster in eyes with worse visual field pattern standard deviation at baseline.

Conclusions: In OHTS, DIGS and ADAGES, the rate of structural change in progressing eyes was between 5 and 8 times faster than in non-progressing eyes, with change occurring in the expected regions. Additional follow-up is needed to determine whether the significant change in the “non-progressing eyes” represents normal aging or change not detected by conventional methods.

Support: NIH/NEI grants: EY11008 (LZ), EY11158 (RNW), EY08208, EY14267 (PAS), (EY09341, EY09307 (MOG, MAK), EY13959 (CAG), Eyesight Foundation (CAG), Grants for participants' glaucoma medications from Alcon, Allergan, Pfizer, and Santen

References:

1. Medeiros FA, et al. Ophthalmol 2009;116:1125-33.

3-01 The Optimum Distribution of Visual Field Test Points to maximize Structure-Function Correlation

R Asaka^{1,2,3}, R Richard¹, DF Garway-Heath^{1,2,3}

¹ NIHR Biomedical Research Centre for Ophthalmology, Moorfields Eye Hospital NHS Foundation Trust and UCL Institute of Ophthalmology, London, UK

² Department of Optometry and Visual Science, City University London, UK

³ GB Bietti Foundation for Research in Ophthalmology - IRCCS, Rome, Italy

Purpose: To infer the optimum distribution of test points on the visual field (VF) that maximizes structurefunction correlation with optical coherence tomography-derived retinal nerve fiber layer thickness (RNFLT) measurements.

Methods: 50 eyes with ocular hypertension or open angle glaucoma were enrolled (MD: average -9.4dB, range +1.6 to -25.6dB). Patients' VFs were measured using the Humphrey 24-2 full-threshold (see Figure 1, triangle symbols) and using a novel disc-centred VF (DCF) (full-threshold) that was created from the custom mode of the Humphrey Field Analyzer (see Figure 1, circle symbols). Test points from the DCF were combined with those from the 24-2 VF. Sensitivity values were converted to ganglion cell density using the 'hockey-stick' model (Swanson, IOVS 1994). The VF was then divided into 12 sectors according to Garway-Heath's map (Ophthalmology, 2000). Pearson's R correlation coefficient was calculated between sectorial RNFLT measurements and the corresponding sectorial average of ganglion cell density. The number of test points in each sector was reduced to maintain >90% of original R value. Bootstrap analysis was carried out to calculate a 95% confidence interval.

Results: The optimum combination of test points (totaling 52) are illustrated in Figure 1 (filled symbols). R values for each sector are depicted in Table 1. Bootstrap analysis suggests there is a significant structure - function relationship in every sector.

Conclusions: Novel distribution of test points showed much stronger structure-function relationship than 24-2.

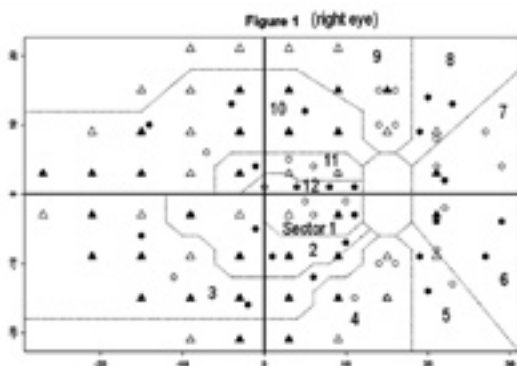


Table 1

| Sector | R (R with 242 only) | Sector | R (R with 242 only) |
|-------------|---------------------|-------------|---------------------|
| 1 | 0.29 (0.27) | 7 | 0.46 (0.44) |
| 2 | 0.27 (0.07) | 8 | 0.51 (0.25) |
| 3 | 0.50 (0.33) | 9 | 0.60 (0.57) |
| 4 | 0.63 (0.60) | 10 | 0.86 (0.69) |
| 5 | 0.48 (0.36) | 11 | 0.53 (0.46) |
| 6 | 0.40 (0.49) | 12 | 0.24 (n/a) |
| Whole field | | 0.59 (0.50) | |

3-02 Structure-Function Relationship in Glaucoma: Optical Coherence Tomography versus Frequency-Doubling Perimetry

MI Fuertes¹, A Ferreras¹, JM Larrosa¹, V Polo¹, LE Pablo¹

¹ Department of Ophthalmology, Miguel Servet University Hospital, Instituto Aragonés de Ciencias de la Salud, Zaragoza, Spain

Purpose: To evaluate the structure-function relationship between peripapillary retinal nerve fiber layer (RNFL) thickness measured with time-domain optical coherence tomography (OCT) and threshold values obtained with frequency-doubling perimetry (FDT) in glaucoma patients.

Methods: Seventy two glaucomatous eyes of 72 subjects were prospective and consecutively selected. All of them underwent a comprehensive ophthalmic examination, at least 2 reliable standard automated perimetry (SAP) tests, a full threshold FDT test (Welch Allyn/Humphrey Zeiss, Dublin, Ca, USA) and imaging with the Stratus OCT (Carl Zeiss Meditec, Dublin, Ca, USA). All glaucomatous eyes had intraocular pressure higher than 21 mmHg and abnormal SAP results. Left eyes were converted to a right eye format. After checking for a normal distribution of the variables, Pearson correlations were calculated between the threshold values at 17 tested-points of FDT (C-20-5 strategy), converted to a linear scale, and the RNFL thickness at 12 clock-hours positions and at 4 quadrants.

Results: Both techniques presented abnormal results in most patients. Nevertheless, mild to moderate correlations were found between a few FDT points and the RNFL thickness in the vertical axis. The strongest correlation was observed between the point 5 of FDT and the RNFL thickness at 7 clock-hour position (0.434, $p < 0.001$).

Conclusions: Both FDT and OCT detected changes in glaucoma patients with visual field losses in SAP. The poor agreement found between FDT parameters and RNFL thickness measured with OCT suggest that both instruments evaluated glaucoma damage independently.

3-03 Progression of Patterns (POP): Machine Classifier identifies Glaucoma Progression

PA Sample¹, G Jang¹, M Balasubramanian¹, DR Anderson², MJ Fredette^{2,3}, C Girkin⁴, J Liebmann⁵, C Bowd¹, TP Jung¹, LM Zangwill¹, RN Weinreb¹, M Goldbaum¹

1 University of California, San Diego, La Jolla, CA, USA
 2 University of Miami Miller School of Medicine, FL, USA
 3 Laval University, CEVQ, CHA-CUO, Québec, Canada
 4 University of Alabama, Birmingham, AL, USA
 5 New York Eye and Ear Infirmary, New York, NY, USA

Purpose: To determine if 1) the improved Progression of Patterns (POP) using an ICA-derived, data-driven, selflearning algorithm, VIM,1 identifies and quantifies areas of progression in serial visual fields (VFs) obtained with SITA and 2) POP improves the progression/noise ratio compared to other methods.

Methods: POP looks at progression of specific defect patterns using two datasets independent from the VIM dataset, 1) 55 stable eyes with 5 VFs collected within 4 weeks and 2) 628 eyes (4,186 VFs) from the DIGS and ADAGES studies with a mean + std of 6.67+1.66 VFs followed for change for 4.01+1.40 years. Each field was placed in reduced multidimensional space along the VIM glaucoma axes to reduce noise by concentrating on the most changed pattern of VF defect relative to the other patterns with less or no presence in that same VF. Applying linear regression (lr) to eyes followed for change, the percentage (%) progressing and the (rate) of change/year outside of the stable group's 95% confidence limits are shown below, grouped by risk for field progression (including progressing glaucomatous optic neuropathy (PGON)). POP is compared to the Humphrey Visual Field Index (VFI) and AGIS scores, all at 95% specificity defined by the stable group.

Results:

| Method | Suspects (n=362) | | VF only (n=71) | | VF+GON (n=119) | | PGON (n=76) | |
|---------|------------------|--------|----------------|--------|----------------|--------|-------------|--------|
| VFI-lr | 0.8% | (1.38) | 1.4% | (1.28) | 8.4% | (1.55) | 21.1% | (1.68) |
| AGIS-lr | 0.6% | (1.37) | 2.8% | (1.57) | 5.0% | (1.68) | 17.1% | (2.01) |
| POP-lr | 1.7% | (1.82) | 5.6% | (1.85) | 10.9% | (2.41) | 28.9% | (2.80) |

Conclusions: By looking at specific defect patterns, POP 1) is more sensitive to change than global indices, 2) identifies a higher percentage and faster rates of progression, 3) and gives probability of progression.

Support: NIH/NEI grants: EY08208, EY11008, EY14267, EY13959, Eyesight Foundation, Pfizer, David and Marilyn Dunn Fund, Grants for participants' glaucoma medications from Alcon, Allergan, Pfizer, and Santen

3-04 Differentiated Trend Analysis of the Visual Field in Glaucoma

F Dannheim¹, M Monhart²

1 Dept. of Ophthalmology, General Hospital Hamburg-Harburg, Germany
 2 Haag-Streit, Koeniz-Berne, Switzerland

Purpose: Conventional trend analysis is performed by calculation of the linear regression of the "Mean Defect" in the central visual field. We tried a new non-linear regression analysis both for the whole field and for regions typically affected by glaucomatous nerve fibre defects ("clusters") for a more individual estimation of the patients' actual risk.

Methods: Non-linear trends using a 2-segments approximation and the linear regression analysis were calculated on visual field series comprising 10 consecutive examinations over a period of 5-8 years. The indices used for the calculation were mean defect ("MD") and square root of loss variance ("sLV" resembling "PSD"). Two new indices were added which describe separate components of the defect curve: Diffuse defect ("DD") reflects the diffuse depression of sensitivity, local defect ("LD") is calculated of the 75% worse deviations (the right part of the defect curve). The calculations were performed for the whole 30° field and for 10 zones containing typical clusters of affected positions due to glaucomatous nerve fibre defects. This method was applied to the white on white serial visual fields of 50 patients with chronic glaucoma, obtained with the Octopus 1-2-3 perimeter, the G program and the TOP strategy. The results were compared with available clinical data, e.g. trend analysis of the optic disc (HRT 3).

Results: Of the 100 eyes of 50 patients, about 1/4 were considered unstable. Of this subgroup, more than half did show a 2-segment non-linear trend with significantly less fluctuation from the trend line compared to the conventional linear regression analysis. The non-linearity could either be more pronounced in the global indices or in the clusters. The index LD most often showed significant non-linearity. The individual patterns corresponded in the majority of cases to morphometric trend analysis or other clinical data. The 2 new indices facilitate the follow-up of the diffuse and the localized component of alterations of glaucomatous visual fields.

Conclusions: The 2-segment approximation gives more differentiated insights in the course of the disease, which may lead to a more realistic estimation of the functional prognosis.



3-05 Perimetric Progression in Open Angle Glaucoma and the Visual Field Index (VFI)

MS Mustafa¹, GS Ang¹, N Scott², VT Diaz Aleman³, A Azuara Blanco¹

¹ Department of Ophthalmology, NHS Grampian, Aberdeen Royal Infirmary, United Kingdom

² Department of Public Health, University of Aberdeen, United Kingdom

³ Hospital Universitario de Canarias, La Laguna, Spain

Purpose: To evaluate the changes in the Visual Field Index (VFI) in eyes with perimetric glaucomatous progression, and to compare these against stable glaucoma patients

Methods: Consecutive patients with open angle glaucoma with a minimum of six reliable visual fields and two years of follow-up were identified. Perimetric progression was assessed by four masked glaucoma experts from different units, and classified into three categories: "definite progression", "suspected progression", or "no progression". This was compared with the Glaucoma Progression Analysis (GPA) II and VFI linear regression analysis, where progression was defined as a negative slope with significance of <5%.

Results: 397 visual fields from 51 eyes of 39 patients were assessed. The mean number of visual fields was 7.8 (SD 1.1) per eye, and the mean follow-up duration was 63.7 (SD 13.4) months. The mean VFI linear regression slope showed an overall statistically significant difference ($p < 0.001$, ANOVA) for each category of progression. Using expert consensus opinion as the gold standard, both VFI analysis and GPA II had high specificity (0.93 and 0.90 respectively) but relatively low sensitivity (0.45 and 0.41 respectively).

Conclusions: The mean VFI regression slope in our cohort of eyes without perimetric progression showed a statistically significant difference compared to those with suspected and definite progression. VFI analysis and GPA II both had similarly high specificity but low sensitivity when compared to expert consensus opinion.

3-06 Probability of Visual Field Progression in Multiple Point Trend Analysis

M Gonzalez de la Rosa, M Gonzalez Hernandez

Hospital Universitario de Canarias. University of La Laguna. Canary Islands. Spain

Purpose: To establish the limits of random or false progression in glaucomatous visual field (VF).

Methods: Due to chance, certain points in stable fields often show false progression. We calculated the probability of progression (p) of each point in 1,318 series of VF (8.9 VF per series, $sd=3.7$). The series were stable for the TNT (Vers. 1) program but, in addition, each was randomized by disordering the dates of VF measurement, before performing a second analysis with the same program. For each series, the values of " p " obtained were plotted from lowest to highest to create "Curves of Chance Probability" (CCP). The 1.5% and 0.3% percentiles of all the CCPs allow us to define certain limits of Random Progression; values exceeding these limits confirm real progression (Fig 1).

Results: The number of points exceeding the CCPs allow calculating the probability that progression in any series of VF is real or due to chance (Table 1). Fig. 1 shows the 1.5% and 0.3% CCPs and an example with significant progression (Example). In Example, 18 points exceed the 1.5% percentile and 7 points exceed the 0.3% percentile. As shown in Table 1, the probability that the progression observed is due to chance is less than 0.5% ($p < 0.005$).

Conclusions: It is possible to obtain a value of the global probability of real progression after establishing the limits of probability due to chance. This idea was applied to the second version of the Threshold Noiseless Trend program (TNT2).

| Nº POINTS | CCP 1.5% | CCP 0.3% |
|-----------|----------|----------|
| | p< | p< |
| 1 | 0.05 | 0.01 |
| 2 | 0.04 | 0.008 |
| 5 | 0.03 | 0.005 |
| 25 | 0.02 | 0.004 |
| 50 | 0.01 | 0.002 |

Table 1

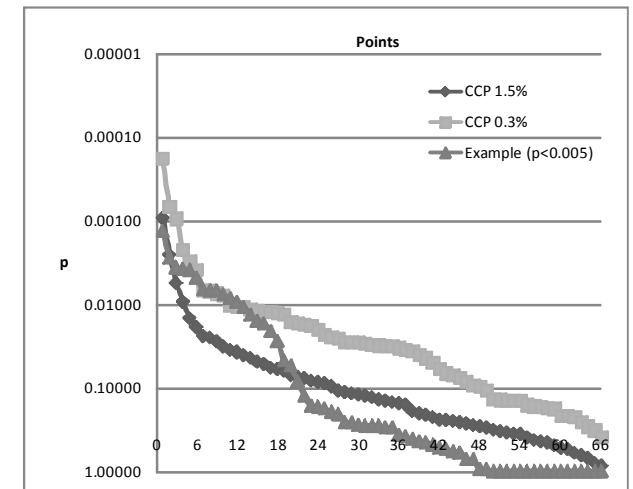


Fig. 1

References

1. Gonzalez de la Rosa M et al. Europ J Ophthalmol 2009;19:416-424



3-07 Comparison of the Threshold Noiseless Trend Programs Versions 1 and 2 (TNT1 Vs TNT2)

J Garcia Feijoo¹, M Jerez Fidalgo¹, M Gonzalez de la Rosa², M Gonzalez Hernandez², J Garcia Sanchez¹

¹ Universidad Complutense. Madrid. Spain

² Hospital Universitario de Canarias. University of La Laguna. Canary Islands. Spain

Purpose: To compare glaucoma progression program TNT versions 1 and 2 (TNT1 Vs TNT2).

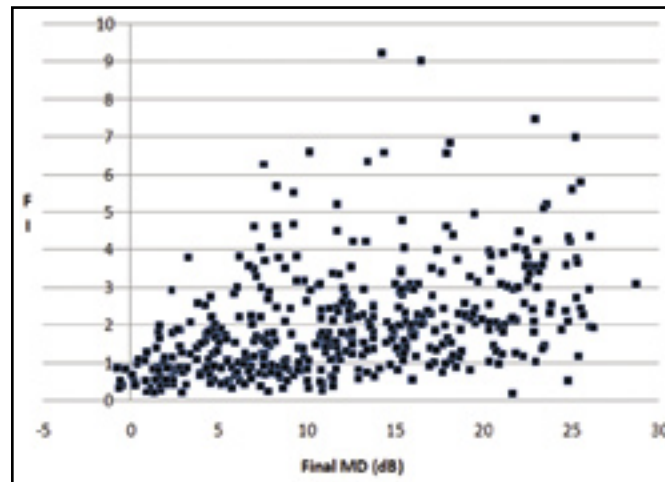
Methods: 1,916 eyes (1,016 patients). Mean number of TOP-G1 exams = 8.9, (sd = 3.7). 2 previous examinations ruled out. Mean follow-up = 4.7 years (sd = 1.4). TNT1 defines progression as $(N1 \times 5) + N2 - N3 > 9$ where N1 is the number of points that worsen with $p < 0.01$, N2 with $p < 0.05$ and N3 those that improve. TNT2 indicates progression as any point exceeding percentile 1.5% on a curve of "p" values due to chance. Also TNT1 and TNT2 analyzing changes in the defect curve.

Results: Both TNT versions showed progression in the same 356 cases; TNT1 in 70 additional cases and TNT2 in another 35. The cases only diagnosed by TNT1 had very low slopes of MD and sLV, and also very low focality indexes (FI) (Table 1). TNT1 and TNT2 showed very good agreement ($\kappa = 0.84$). FI was much lower in patients with initial glaucomas than in those with advanced glaucoma (Fig 1).

Conclusions: The criterion of TNT2 is stricter than that of TNT1 and reduces the diagnoses of diffuse progression with slight increase of sLV. However, progression with low focality is not only typical of cataracts.² In early stage glaucoma, focal progression is unusual. Cataracts must be ruled out using non-perimetric methods.

| | SLOPE MD | SLOPE sLV | MD FINAL | FI |
|-----------|-----------|-----------|------------|-----------|
| TNT1&TNT2 | 1.5 (1.4) | 0.5 (0.7) | 12.6 (6.8) | 2.2 (1.5) |
| ONLY TNT1 | 0.9 (1.6) | 0.2 (0.5) | 7.3 (5.5) | 1.1 (0.7) |
| ONLY TNT2 | 1.1 (0.9) | 0.4 (0.6) | 15.8 (8.1) | 2.1 (1.3) |

Table 1



References

1. Gonzalez de la Rosa M et al. Europ J Ophthalmol 2009;19:416-424
2. Diaz Aleman VT et al. Br J Ophthalmol. 2009;93:322-328.

3-08 Effect on HRT Topographic Change Analysis Parameter Estimates when Combining HRT-I and HRT-II Examinations in Longitudinal Series

C Bowd¹, M Balasubramanian¹, RN Weinreb¹, LM Zangwill¹

¹ Hamilton Glaucoma Center, Department of Ophthalmology, University of California San Diego, La Jolla, CA.

Purpose: To evaluate the compatibility of HRT-I and HRT-II examinations used in the same longitudinal series for Topographic Change Analysis (TCA) and to determine if parabolic error correction (PEC) to the topographies improves compatibility.

Methods: 66 eyes from the UCSD Diagnostic Innovations in Glaucoma Study (DIGS) with baseline HRT-I exam and HRT-II exams obtained on the same day and ≥ 3 HRT-II follow-up exams were included. Two TCA analyses, HRT-I exam at baseline (HRT-I mixed series) and HRT-II exam at baseline (HRT-II only series) were compared. Agreement between the HRT-I mixed and HRT-II only series were estimated using Bland-Altman plots. Agreement was assessed: 1) using the current HRT software settings (PEC applied only to HRT-II only series), and 2) using modified HRT settings (PEC also applied to HRT-I mixed series).

Results: With current HRT software settings, the HRT-I mixed series significantly overestimated change locations (i.e. red-pixels) compared to the HRT-II only series as indicated by statistically significant proportional biases in the Bland-Altman analysis. For example, size of the largest red pixel cluster within the optic disc (CSIZE) was 106.5 (95% CI = 74.4, 138.6) superpixels for HRT-I mixed series and 32.8 (19.8, 45.7) superpixels for HRT-II only series. By applying PEC to HRT-I mixed series there were no statistically significant biases in the TCA parameter estimates compared to the HRT-II only series [e.g., CSIZE was 25.6 (15.7, 35.5) superpixels when PEC was applied to HRT-I mixed series].

Conclusions: In some eyes, HRT-I and HRT-II baseline exams are not interchangeable in TCA analysis without parabolic correction. HRT-I mixed series detected more changes characteristic of glaucoma when there were only minimal changes in the HRT-II only series. Our results suggest that, with parabolic error correction, HRT-I exams can be included in a longitudinal series containing HRT-II exams.

Support: Heidelberg Engineering GmbH, Heidelberg, Germany (MB), NIH/NEI grant EY011008 (LZ), grants for participants' glaucoma medications from Alcon, Allergan, Pfizer, and Santen



4-01 Utility of Fully Automated Kinetic Perimetry (Program K) in detecting and evaluating Visual Fields with Superior Segmental Optic Hypoplasia (SSOH)

T Kayazawa¹, S Takada¹, S Hashimoto¹, C Matsumoto¹, F Tanabe¹, H Nomoto¹, E Arimura², S Okuyama¹, Y Shimomura¹

¹ Department of Ophthalmology, Kinki University School of Medicine, Osaka-Sayama, Japan

² Department of Ophthalmology, Kinki University School of Medicine, Sakai Hospital, Sakai, Japan

Purpose: When assessing a visual field (VF) with superior segmental optic hypoplasia (SSOH), static perimetry may have difficulties to precisely describe the VF characteristics of SSOH; and the results of Goldmann perimetry (GP) can vary among examiners. In this study, we evaluated the clinical usefulness of fully automated kinetic perimetry (Program K) by comparing its results to those obtained by static perimetry and GP in patients with SSOH.

Methods: Nine patients (average age, 47.1 ± 16.0 yrs) confirmed with SSOH were included in this study. Static perimetry using HFA (programs 24-2 or 30-2, and 60-4) and Octopus101 (program G2), and kinetic perimetry using GP and Octopus101 Program K were performed on all the subjects. VF loss was assessed using the following stimulus characteristics: luminance levels of V/4e, I/4e, and I/3e; and target speeds of 3 and/or 5 degrees/sec depending on the patient's VF pattern. Fundus photography, HRT, OCT, and GDx were also performed for quantitative evaluation of SSOH.

Results: Our results indicated that the shape and size of the isopters depicted by Program K were comparable to those obtained by GP on the same eye. In addition, Program K could also detect the VF changes in SSOH. The average examination duration of Program K was 9.14 ± 1.05 minutes.

Conclusions: Fully automated kinetic perimetry using Program K is a useful clinical method that can easily inspect and measure the peripheral VF especially.

4-02 Effects of False-Positive and False-Negative Responses and FOS Curve on Fully Automated Kinetic Perimetry (Program K) in Virtual Patients

S Hashimoto¹, C Matsumoto¹, S Okuyama¹, S Takada¹, E Arimura², F Tanabe¹, J Paetzold³, U Schiefer³, Y Shimomura¹

¹ Department of Ophthalmology, Kinki University School of Medicine, Osaka Sayama, Japan

² Department of Ophthalmology, Kinki University School of Medicine, Sakai Hospital, Osaka Sakai, Japan

³ Department of Pathophysiology of Vision and Neuro-ophthalmology, University Eye Hospital, Tübingen, Germany

Purpose: To evaluate the effects of false-positive (FP) and false-negative (FN) rates, and the frequency of seeing (FOS) curve on fully automated kinetic perimetry (Program K) in virtual patients.

Subjects and Methods: Goldmann manual kinetic perimetry (MKP) was performed on 100 eyes of 100 patients (average age, 57.1 ± 16.4 yrs; 63 eyes with glaucoma, 24 eyes with neuro-ophthalmological diseases, and 13 eyes with retinitis pigmentosa). The obtained isopters were digitized in K-Train (an Octopus kinetic perimetry training software developed by Tübingen University) to be used for 100 virtual patients. Program K was then performed on the 100 virtual patients using target sizes of V/4e, III/4e, I/4e, I/3e, I/2e, and I/1e at a speed of 3 degrees/sec to assess the visual field loss. With K-Train, the virtual patients' FP/FN ratios and FOS curves were adjustable. We evaluated the effects of these parameters on Program K algorithm by comparing the isopter areas, the number of vectors, and the test durations.

Results: If the FP and FN ratios were both less than 20%, the isopters obtained by Program K were comparable to those by Goldmann MKP. If the FP and FN ratios increased to 20% and over and the number of vectors and test durations also increased significantly, spikes-shaped isopters were observed in some of the Program K results. If the FOS parameter in K-Train was less than 0.9, the isopters from Program K were also comparable to those by Goldmann MKP.

Conclusion: Program K algorithm could reduce spikes-shaped isopters if the FP and FN ratios were less than 20%. To further improve the algorithm for fully automated kinetic perimetry, K-Train and computer-simulated virtual patients can provide useful information.

4-03 The Intrasubject Intrasession Variability of Isopter's Position and the Fatigue Effect during Semi-Automated Kinetic Perimetry in Patients with Advanced Visual Field Loss

K Nowomiejska^{1,2}, J Paetzold¹, R Vonthein³, Z Zagorski², T Zarnowski², U Schiefer¹

¹ University Eye Hospital, Dept. of Pathophysiology of Vision and Neuro-Ophthalmology, Tuebingen, Germany

² Department of Ophthalmology, Medical University, Lublin, Poland

³ Department of Medical Biometry, University of Tuebingen, Germany

Purpose: To assess the intrasubject intrasession variability of the III4e isopter position and the fatigue effect during semi-automated kinetic perimetry (SKP) in patients with advanced visual field loss.

Material and methods: Fifty-nine patients suffering from advanced visual field loss: retinal nerve fiber layer (RNFL) defect due to advanced glaucoma (22), concentric constriction of the visual field due to retinitis pigmentosa (19) and hemianopia due to neurological disorders (18) were examined with SKP, implemented in the Octopus 101 instrument (HAAG-STREIT Inc., Koeniz, Switzerland). One eye of each patient was examined with three stimuli in a standard manner; subsequently four repeated presentations of the III4e stimulus along identical vectors were performed. The variability of the isopter position was assessed by calculating the scatter of the kinetic threshold location at each vector location in degrees during repeated examination. The fatigue effect was calculated by measuring the difference in square degrees between the isopter area, obtained by single and repeated presentation of the III4e stimulus.

Results: The mean scatter of the kinetic threshold was 2.05 degrees in the glaucoma group, 1.38 degrees in the retinitis pigmentosa group and 1.73 degrees in the hemianopia group of patients, respectively. For the repeated presentation of the III4e stimulus, the isopter area of the repeated examination was significantly smaller than for the normal examination only within the group of glaucoma patients and accounted to 7.2%.

Conclusion: The variability of the isopter position was mostly pronounced among patients with advanced glaucoma. Repeated presentations along identical vectors within SKP session resulted in a delayed stimulus perception (fatigue) - and thus in a smaller isopter area - only in patients with advanced glaucoma.

4-04 Reproducibility of Semi-Automated Kinetic Visual Field Examinations (SKP)

E Krapp¹, T Röck¹, L Naycheva¹, J Dietzsch¹, F Gekeler¹, B Wilhelm¹, U Schiefer¹

¹ Centre for Ophthalmology, Institute for Ophthalmic Research, University of Tübingen, Germany

² STZ eyetrial at the Centre for Ophthalmology, University of Tübingen, Germany

Purpose: To assess the reproducibility within short time intervals of visual field (VF) results obtained with semiautomated kinetic perimetry (SKP) with respect to isopter area and scotoma area.

Methods: 42 patients (19 male, 23 female, aged 20.2 to 83.0 years) with advanced VF loss, caused by retinitis pigmentosa (9), advanced glaucoma (22), Stargardt's disease (4), unilateral anterior ischaemic optic neuropathy (AION) (3) or other diagnoses (4) were examined with SKP (Octopus perimeter 101 and 900). The visual acuity ranged from 1/50 (at 1m) to 20/16. One eye of each patient was examined, either the affected eye or the eye with the worse visual acuity. The two kinetic VFs of each patient were conducted with a time interval between 1 and 17 days (22 patients) and 92 days (median) in 20 glaucoma patients. Stimuli were presented along 24 meridians, 5.4 (mean) stimuli for the blind spot. Isopter areas (V4e, III4e, I4e, I2e), scotoma areas (III4e) and blind spot scotoma areas (I4e) and their ratios, median and 95% reference interval (RI) were assessed.

Results: The reproducibility proved to be high with ratios of isopter areas and scotoma areas being close to 1.

| Stimulus | Velocity [°/s] | No of isopters | Isopter area ₂ / Isopter area ₁ | |
|----------|----------------|----------------|---|-------------|
| | | | median | 95% RI |
| V4e | 4 | 6 | 1.05 | 0.75 – 1.13 |
| III4e | 3 | 37 | 1.01 | 0.86 – 1.23 |
| I4e | 3 | 20 | 1.05 | 0.83 – 1.16 |
| I2e | 3 | 13 | 1.01 | 0.58 – 2.06 |

| Stimulus | Velocity [°/s] | No of isopters | Scotoma area ₂ / Scotoma area ₁ | |
|----------------|----------------|----------------|---|-------------|
| | | | median | 95% RI |
| III4e | 3 | 9 | 0.97 | 0.79 – 1.15 |
| Blind spot I4e | 2 | 15 | 0.87 | 0.25 – 1.56 |

Conclusions: SKP, using constant angular velocities and individual reaction time correction is characterised by a high reproducibility of isopter areas for the stimuli V4e, III4e and I4e and for the scotoma area tested with III4e. Reproducibility of the isopter areas with the darker small stimuli I2e and the small Blind spot area is poorer.

Support: Okuvision GmbH

References

Nevalainen J, Paetzold J, Krapp E, et al. (2008) The use of semi-automated kinetic perimetry (SKP) to monitor advanced glaucomatous visual field loss (2008) Graefes Arch Clin Exp Ophthalmol. 246:1331-9

Vonthein R, Rauscher S, Paetzold J et al. (2007) The normal age-corrected and reaction time-corrected isopter derived by semiautomated kinetic perimetry. Ophthalmology. 2007 Jun;114(6):1065-72



4-05 Evaluating Pupil Light Reflexes with Three Color Stimuli of Different of Sizes and Intensities under the Same Energy at Each Eccentricity of the Visual Field

K Tanzawa, F Maeda, G Takizawa, Y Kiyokawa, Y Hashimoto, T Yoneda, M Oka, K Kani, A Tabuchi

Kawasaki University of Medical Welfare, Kurashiki, Okayama, Japan

Purpose: We investigated the characteristics of pupil light reflexes (PLR) caused by three color stimuli of white (W), red (R), and blue (B) which of the same energy but were of different sizes and intensities within 15° of the visual field.

Methods: The subjects were three normal adults (25.3 ± 4.5 years). The stimuli were generated by pupil perimeter and the pupil diameter was recorded by an infrared camera. There were three stimulus conditions of the same energy with the colors of W, R (612 nm), and B (437 nm). There were four kinds of sizes and intensities with area of visual angles 0.5° × 125 cd/m² (STI 1), 1° × 31 cd/m² (STI 2), 2° × 8 cd/m² (STI 3) and 4° × 2 cd/m² (STI 4) under the same energy. The stimulus duration time was 400 msec, the background intensity was 0.7 cd/m² and the stimulus locations were on the superior meridians of 45° at eccentricities of 0°, 5° and 15°. The diameter of the pupil was measured for the evaluation of the light reflexes, and the pupil contraction ratio: PCR= {pupil diameter of pre-stimuli – pupil diameter of post-stimuli} / pupil diameter of pre-stimuli} × 100 was calculated.

Results: The PCR with each stimulus at eccentricities of 0°, 5° and 15° are shown in Table1. The PCRs with B were higher than those with W and R stimuli at each eccentricity. The decision coefficients of PCR at eccentricities of 0°, 5° and 15° are shown in teable2. The PCR was in proportion to the stimulation size only at the eccentricity of 15° of the visual field with W, R and B under the same energy stimulation.

Conclusions: PLR with W, R and B stimulation under the same energy depends more on the stimulation size than on the stimulation intensity at an eccentricity of 15° of the visual field. In addition, these characteristics are not dependent on the color difference between W, R and B.

Table 1.

Table 2.

| Average of PCR (%) | | | | | | The decision coefficients | | |
|--------------------|--------------|-------|-------|-------|-------|---------------------------|--------------|-----------------------------|
| Color | Eccentricity | STI 1 | STI 2 | STI 3 | STI 4 | Color | Eccentricity | of PCR at each eccentricity |
| White | 0° | 2.0 | 3.2 | 4.4 | 2.3 | White | 0° | R ² = 0.0006 |
| White | 5° | 1.3 | 2.7 | 1.8 | 3.3 | Red | 0° | R ² = 0.8725 |
| White | 15° | 0.9 | 1.7 | 1.9 | 2.3 | Blue | 0° | R ² = 0.1199 |
| Red | 0° | 4.0 | 3.0 | 4.8 | 6.9 | White | 5° | R ² = 0.0452 |
| Red | 5° | 2.2 | 1.7 | 2.7 | 2.2 | Red | 5° | R ² = 0.5287 |
| Red | 15° | 1.5 | 1.0 | 1.8 | 3.2 | Blue | 5° | R ² = 0.3033 |
| Blue | 0° | 4.5 | 7.6 | 6.0 | 6.7 | White | 15° | R ² = 0.7778 |
| Blue | 5° | 2.9 | 3.1 | 1.8 | 4.2 | Red | 15° | R ² = 0.8787 |
| Blue | 15° | 1.7 | 2.2 | 2.7 | 3.6 | Blue | 15° | R ² = 0.9796 |

STI 1: area of visual angle 0.5° × 125 cd/m²

STI 2: area of visual angle 1.0° × 31 cd/m²

STI 3: area of visual angle 2.0° × 8 cd/m²

STI 4: area of visual angle 4.0° × 2 cd/m²

4-06 Identifying the State of Vigilance during Perimetry with Pupil Dynamics

Y Wang¹, R Gautam¹, S Toor¹, DB Henson^{1,2}

¹ University of Manchester, Manchester, UK

² Manchester Royal Eye Hospital, Manchester, UK

Purpose: To investigate patient vigilance, using pupil dynamics, during standard automated perimetry and the relationship between vigilance and variability in threshold sensitivity.

Methods: 39 patients with suspicious/diagnosed glaucoma performed a 24-2 full threshold perimetric task twice with one eye while the pupil diameter (PD) was recorded at a sampling rate of 60 Hz (HSVET, CRS, UK). Dynamic changes of PD, amplitude of the pupillary fatigue waves (PFW) and Pupillary fatigue index (PFI) were analysed with both subjective grading (2 independent graders) and objective methods (PD, PFW and PFI gradients), to detect the extent (None:0, Mild:1, Moderate:2, High:3,

Advanced:4) and onset of vigilance loss. Test-retest differences of the pupil parameters and responsetimes (RT) were correlated to the between test variability in threshold sensitivity.

Results: Good inter-observer agreement was obtained for the graders (extent k=0.6534; onset k=0.6073). On average over 79% patients were graded with mild to advanced vigilance loss in both tests. Mean extent for all patients was 1.8 (±1.1, Test1) and 2.1 (±1.0, Test2) with a significant increase in second test (t=-0.654, p=0.001). The mean onset of pupillary changes was 2.6 (±1.6) and 2.5 (±1.4) minutes with no significant difference between tests (t=0.446, p=0.658). In the objective analysis, most of the patients (31/39) showed a negative gradient of PD and positive gradient of PFW amplitude and PFI during both tests, indicating an increasing loss of vigilance with time. No significant test-retest difference was observed for the gradients of all pupil parameters. A significant decrease of threshold sensitivity was observed between the first and second test. The test-retest threshold sensitivity variability correlated negatively with the inter-test difference for the subjective grades (r²=0.1837) and median PFI (r²=0.1076). RT varied among the patients and no significant relationship was observed between the RT difference and test-retest variability.

Conclusions: Most patients demonstrate pupillary signs of vigilance loss during perimetry and the pupillary changes of repeated test showed some correlation with the variability of threshold sensitivity.



4-07 Luminance-Balanced Multifocal Objective Perimetry

T Maddess, M Kolic, RW Essex, AC James

ARC Centre of Excellence in Vision Science, and Department of Ophthalmology of The Canberra Hospital, Australian National University, Canberra, Australia

Purpose: To compare examine the effects of luminance balancing of multifocal stimuli using a prototype of the TrueField Analyzer. Luminance balanced stimuli present dimmer stimuli to more sensitive parts of the pupillary visual field. It was hypothesized that balancing the luminances across the field would improve sensitivity and specificity for glaucoma.

Method: There were two experiments containing: 21 normal and 21 glaucoma subjects; and 33 normal and 25 glaucoma subjects; who were age and sex matched. All subjects were examined with Matrix and HFA perimetry, and Stratus OCT. The dichoptic multifocal stimuli extended to 30 deg eccentricity and presented 44 regions/eye. All stimuli were yellow and the background was at 10 cd/m². Multifocal responses were extracted from infrared recordings of pupil diameter at 30 frames/s. Data containing blinks and loses of fixation were removed. The first experiment compared luminance balanced and unbalanced stimuli presented at mean intervals (MI) between stimuli at each field location of either 1 or 4 s. On each presentation the stimulus duration was 33 ms. The second experiment compared 4 balanced stimuli which differed in maximum luminance and MIs of 1 or 4 s. Subjects repeated their tests within 4 weeks, generating 928 fields. The duration of each of the 8 stimulus types was 4 min presented in eight 30 s segments.

Results: Experiment 1: balancing the stimuli improved area under receiver operator characteristic plots (AUC) for combined moderate and severe fields from 0.84 to 0.95 for both MIs. Experiment 2: The best performing stimulus method had an MI of 4s and maximum luminance of 150 cd/m². AUC for moderate fields was 0.84 ± 0.06 , and for severe fields 1.00 ± 0.00 . Although the test duration was 2 min/eye the test-retest variability was comparable to other perimeters.

Conclusions: Diagnostic accuracy was improved by balanced luminance stimuli. Increasing test time to 3 min/eye are predicted to improve signal to noise ratios and reproducibility.

4-08 Multifocal Pupillographic Objective Perimetry in Glaucoma using Blue Stimuli

CF Carle¹, AC James¹, M Kolic¹, RW Essex^{2,3}, TL Maddess¹

¹ ARC Centre of Excellence in Vision Science, Australian National University, Canberra, Australia

² ANU Medical School, Australian National University, Canberra, Australia

³ The Canberra Hospital, Canberra, Australia

Purpose: To investigate the diagnostic potential of blue multifocal pupillographic objective perimetry (mfPOP) stimuli in glaucoma. Blue stimuli could have advantages in mfPOP by targeting the intrinsic response of melanopsin retinal ganglion cells¹.

Methods: 25 normal (aged 59.6 ± 7.1 y) and 19 glaucoma subjects (64.1 ± 9.8 y) were tested using two mfPOP variants. All subjects were examined using HFA achromatic and Matrix 24-2 perimetry, Stratus OCT, slit-lamp and tonometry. Stimulus characteristics are shown below

| Stimulus colour | Max. stimulus luminance | Stimulus duration | resentations sreion | acround colour | acround luminance | Reions eye | Eccen tricity | Recordin duration |
|-----------------|-------------------------|-------------------|---------------------|----------------|----------------------|------------|----------------|-------------------|
| lue | 75 cd/m ² | 750 ms | 1/32 s | blue | 10 cd/m ² | 44 | $\pm 30^\circ$ | 8 min |
| ello | 150 cd/m ² | 33 ms | 1/4 s | yellow | 10 cd/m ² | 44 | $\pm 30^\circ$ | 4 min |

Pupillary response characteristics and diagnostic accuracy were quantified using multivariate linear modelling and receiver operating characteristic (ROC) analysis.

Results: Mean (-5.68dB, t(4398) = -9.0, $p < 0.0001$), a response pattern that was not observed with the pupillary contraction amplitudes of glaucoma subjects were significantly smaller in both stimulus protocols (Blue: -1.01dB, t(7739) = -10.4, $p < 0.0001$; Yellow: -1.04dB, t(7739) = -10.1, $p < 0.0001$). In normal subjects, blue stimulation of the central 9° produced much smaller contraction amplitudes than in more eccentric locations longer wavelength stimuli. ROC analysis indicated that the overall diagnostic accuracy of the two protocols was similar with best AUCs of 71.1% ($\pm 5.5\%$ SE) and 70.7% ($\pm 5.9\%$ SE) for blue and yellow respectively. Both protocols detected patients with severe defects with 100% accuracy and produced similar results to each other for moderate defects (Blue: 79.2% ($\pm 7.2\%$ SE); Yellow: 78.6% ($\pm 9.9\%$ SE)). Inclusion of differing numbers of worst-performing regions affected the accuracy of each protocol; yellow being better with just a small number of regions, blue however, requiring the inclusion of nearly all regions.

Conclusions: Blue and yellow mfPOP stimuli produced similar diagnostic accuracies. The results however, indicate that blue stimulation may be hampered in its ability to detect scotomas, relying instead on total deviations for its accuracy. This, combined with the small contraction amplitudes obtained to stimulation of the parafoveal retina, limit the potential of blue stimuli in the diagnosis of glaucoma.

References

1. Gamlin PD, McDougal DH, Pokorny J, Smith VC, Yau KW, Dacey DM. Vision Res 2007;47:946-954.



5-01 Correlation between SLP with and without ECC and HD-OCT in Normal and Glaucomatous Eyes

J Benitez-del Castillo¹, A Martinez², T Regi¹, I Mota¹

¹ Hospital General S.A.S. de Jerez, Jerez, SPAIN

² Science Research & Sports, Santiago de Compostela, La Coruña, SPAIN

Purpose: To examine association between scanning laser polarimetry (SLP) using enhanced (ECC) and variable corneal compensation (VCC) with High Definition optical coherence tomography (HD-OCT).

Methods: A cross-sectional study of 86 normal and glaucomatous eyes who underwent complete examination, automated perimetry, SLP-ECC, SLP-VCC and HD-OCT. SLP parameters are recalculated in 90 degrees segments (quadrants) in the calculation circle to be compared. Differences between main parameters of retinal nerve fiber layer thickness are observed (average thickness, superior, inferior, temporal and nasal quadrants) and Pearson's correlation coefficients are calculated. Bland & Altman plots are used to evaluate agreement between methods.

Results: HD-OCT parameters of RNFL thickness (average thickness 81,04 microns, SD18,8) are significantly higher than SLP-VCC parameters (average thickness 48,77 microns, SD 9,3) ($p < 0,0001$) and SLP-ECC parameters (average thickness 45,63 microns, SD 9,2) ($p < 0,0001$). Correlation coefficients between HD-OCT and SLP are: average VCC thickness $r = 0,67$ ($p < 0,0001$), superior VCC quadrant $r = 0,76$ ($p < 0,0001$), inferior VCC quadrant $r = 0,7$ ($p < 0,0001$), temporal VCC quadrant $r = 0,09$ ($p = 0,389$), nasal VCC quadrant $r = 0,45$ ($p < 0,0001$), average ECC thickness $r = 0,81$ ($p < 0,0001$), superior ECC quadrant $r = 0,83$ ($p < 0,0001$), inferior ECC quadrant $r = 0,75$ ($p < 0,0001$), temporal ECC quadrant $r = 0,34$ ($p = 0,0017$), nasal ECC quadrant $r = 0,47$ ($p < 0,0001$). There is not statistically significant difference in OCT-SLP correlation coefficients between VCC and ECC except for RNFL average thickness ($p < 0,04$). Bland & Altman plots show a significant association between mean values of average RNFL thickness measured with SLP-VCC and HD-OCT and the difference of average RNFL thickness measured with the same methods ($r = -0,71$; $p < 0,0001$) and a significant association between mean values of average RNFL thickness measured with SLP-ECC and HD-OCT and the difference of average RNFL thickness measured with the same methods ($r = -0,77$; $p < 0,0001$).

Conclusion: HD-OCT parameters of RNFL thickness are significantly higher than SLP-VCC and SLP-ECC parameters. HD-OCT and SLP methods are well correlated but the difference plots show a lack of agreement that changes as a proportion of the mean.

Support: None

References:

1. Bagga H, Greenfield DS, Feuer W, Knighton RW. Scanning laser polarimetry with variable corneal compensation and optical coherence tomography in normal and glaucomatous eyes. *Am J Ophthalmol.* 2003;135:521–529.
2. Sehi M, Ume S, Greenfield DS, and Advanced Imaging in Glaucoma Study Group. Scanning Laser Polarimetry with Enhanced Corneal Compensation and Optical Coherence Tomography in Normal and Glaucomatous Eyes. *Invest Ophthalmol Vis Sci.* 2007;48:2099–2104

5-02 SD OCT Measurements of Cross-Section Area of the RNFL for the Assessment of Optic Neuropathy

RS Harwerth, NB Patel, XD Luo

College of Optometry, University of Houston, Houston, Texas, USA

Purpose: The retinal nerve fiber layer (RNFL) measurements that have been used to model structure-function relationships in glaucoma were based on a translation of optical coherence tomography (OCT) thickness to a RNFL area to estimate the number of retinal ganglion cell axons underlying perimetric visual sensitivity (Prog Ret Eye Res, in press). However, it is not clear whether RNFL thickness or area provides the more accurate assessment if additional factors, such as axial length and distance of the scan from the optic nerve head (ONH) margin, are also included.

Methods: Spectralis HRA+OCT raster and radial scans of the ONHs of macaque monkeys were analyzed. The choroid/optic nerve junction was marked manually to outline the ONH margin and a best-fit ellipse was determined. With conversion of pixels to microns (μm) from each subject's axial length, RNFL cross section scans were extracted in 50 m increments for distances of 300 to 600 m from the ONH. The areas of blood vessels were removed from the RNFL measure.

Results: Preliminary data on 23 normal monkeys demonstrated a systematic decrease in the average RNFL thickness from $151 \pm 10.5 \mu\text{m}$ at a distance of $300 \mu\text{m}$ to $114 \pm 6.3 \mu\text{m}$ at $600 \mu\text{m}$ ($p < 0.05$). In distinction, the cross section area of the RNFL did not vary with distance ($0.85 \pm 0.06 \text{ mm}^2$ at $300 \mu\text{m}$ compared to $0.86 \pm 0.05 \text{ mm}^2$ at $600 \mu\text{m}$). Blood vessels accounted for 9.6% of total RNFL thickness or area, but varied with retinal location.

Conclusions: With appropriate transverse scaling and elliptical ONH shape, the cross-sectional area of the RNFL is independent of retinal eccentricity, to approximately 6 deg from the ONH center, indicating that axonal composition changes little over this range. The results suggest that RNFL cross-section area can provide an accurate assessment of the axonal losses from optic neuropathies, which can be evaluated further in experimental and/or clinical glaucoma.

Support: NIH/NEI grants R01 EY01139 and P30 EY07751.



5-03 Reproducibility of Topcon 3D OCT-1000 Measurements of Retinal Nerve Fiber Layer in Healthy Subjects

AA Shpak, SN Ogorodnikova, AB Guekht

The S. Fyodorov Eye Microsurgery Complex – Federal State Institution, Moscow, Russian Federation

Purpose: Reproducibility of measurements is one of the most important characteristics of diagnostic equipment. There are several kinds of equipment for spectral-domain optical coherence tomography (SD-OCT) on the market. Not all of them have their reproducibility examined by independent observers. The purpose of the present study was to evaluate the intrasession and interobserver reproducibility of retinal nerve fiber layer (RNFL) measurements with Topcon 3D OCT-1000 in healthy subjects.

Methods: Twenty-five healthy volunteers (mean age 51.5 ± 11.4 , range 22-71 years; 2 men, 23 women) were examined with the 3D OCT-1000 (Topcon, Tokyo, Japan), software version 3.20E. Acquisition was performed in "Glaucoma Mode". One randomly selected eye of a subject was studied in one session by two operators, each taking two measurements of RNFL. 3D OCT-1000 shows the RNFL thickness in quadrants, so it was necessary to calculate the average RNFL thickness as a mean of RNFL in 4 quadrants. Intrasession and interobserver reproducibility were evaluated by Bland-Altman analysis (1996). Interobserver reproducibility was calculated using the first measurement of each operator.

Results: Average RNFL thickness was normal in all cases: 102.54 ± 10.95 (mean \pm SD), range 89.5-116.25 μm . For both operators the within-subject SD was similar: 1.45 and 1.63 μm . Interobserver within-subject SD was 1.97 μm . It gives the corresponding values of repeatability (the maximal difference between two measurements for the same subject in 95% of cases) as 4.2; 4.7 and 5.7 μm . According to our previous research those values are approximately 25% lower than similar values for Stratus OCT 3000 (Carl Zeiss Meditec, Dublin, CA).

Conclusions: Method of SD-OCT using Topcon 3D OCT-1000 shows good intrasession and interobserver reproducibility of RNFL measurements.

5-04 GDx Staging System: a New Method for Retinal Nerve Fiber Layer Damage Classification

P Brusini, C Tosoni, ML Salvetat, L Parisi, M Zeppieri

Department of Ophthalmology, Santa Maria della Misericordia Hospital, Udine, Italy

Purpose: To provide a reliable and easy-to-use method for classifying retinal nerve fiber layer (RNFL) damage utilizing the parameters obtained by the scanning laser polarimeter with a variable corneal compensator (GDx VCC).

Methods: The GDx Staging System is a new method that uses the superior and inferior RNFL thickness values plotted on an x-y diagram to classify GDx VCC results. RNFL defects are classified into 6 stages of increasing severity and 3 classes of defect localization (superior, inferior or diffuse defect). The diagram was created based on 378 GDx VCC tests from 98 healthy controls and from 280 patients affected by either ocular hypertension (OHT) or chronic open-angle glaucoma (POAG). Sensitivity and specificity of the method was assessed in a different cohort that included 161 patients with, and 34 normal subjects. The correlations of this staging method were assessed with both a clinical classification of the GDx VCC results and with a visual field defect classification based on the Glaucoma Staging System (GSS) 2.

Results: Sensitivity and specificity of the GDx Staging System ranged respectively between 87.8% and 97.2% and between 81.5% and 91.2%. Correlations with the clinical classification and the GSS 2 results were statistically significant (Spearman correlation coefficient 0.92 & 0.57; $p < 0.0001$).

Conclusions: The GDx Staging System is an easy and quick method for interpreting GDx VCC results. It can be clinically useful especially for non expert ophthalmologists.



5-05 Extracting more Information from Optic Disc Topography using Shape Analysis

H Zhu¹, DP Crabb¹, PH Artes²

¹ Department of Optometry and Visual Science, City University London, London, UK

² Ophthalmology and Visual Sciences, Dalhousie University, Halifax, NS, Canada

Purpose: To develop an analysis to extract shape features from optic disc topography acquired with the Heidelberg Retina Tomograph (HRT).

Methods: HRT topographies of 164 healthy, 252 glaucomatous eyes¹ and 666 glaucoma suspect eyes were investigated. Instead of using the area and volume parameters of the HRT, the topography images were processed with a shape analysis model (non-linear latent variable Gaussian process) to extract multivariate shape features. A feature map derived from this model placed each optic disc in a multivariate space. For comparison, discs were also classified with the Moorfields Regression Analysis (MRA, criterion of ≥ 1 sector borderline or outside normal limits). For eyes with false-positive (FP) and false-negative (FN) MRA classifications, two multivariate Gaussian distributions in the feature map were fitted and were considered as the Least Specific Region (LSpeR) and the Least Sensitive Region (LSenR), respectively.

Results: The shape model required no diagnostic information or manual input and yielded objective shape features of optic disc topography. The three most important features appeared to relate to disc size, cup depth and disc tilt respectively, but more than 100 features were extracted from the disc topography. The MRA classifications contained 47 FNs (19%) and 51 FPs (31%). Forty-eight (including 45 out of 47 FNs) and 55 (including 50 out of 51 FPs) discs were bounded within the LSenR and LSpeR respectively.

Conclusion: The shape feature map identified previously unused information about individual optic disc topography. The map delineated regions where the diagnostic performance of the MRA was unreliable and false-positive and false-negative errors would be expected. The subjects with topography shape features in these regions should be referred to alternative diagnostic techniques, while eyes mapped to other areas of the feature map can be classified with greater certainty. The clinical utility of the technique needs to be proven in other datasets.

References:

1. Coops A, Henson DB, Kwartz AJ, Artes PH. Automated Analysis of Heidelberg Retina Tomograph Optic Disc Images by Glaucoma Probability Score. *Invest Ophthalmol Vis Sci* 2006;47:5348-5355.

5-06 Comparing fMRI-based Visual Field Representation with Perimetry: Can fMRI Provide Objective Measures of Visual Field Enlargement?

RA Schuchard¹, C Glielmi²

¹ VA Rehabilitation R&D Service, Atlanta, USA

² Siemens Medical Solutions, Chicago IL, USA

Purpose: Visual field parameters are accepted efficacy outcome measures. BOLD fMRI retinotopic parameters indicate the amount of visual field that is processed by the visual cortex. However, the application of arterial spin labeling to measure cerebral blood flow (CBF) and estimation of cerebral metabolic rate of oxygen (CMRO₂) provide more longitudinal consistency than BOLD. This study explores these methods in subjects with visual field loss to determine the feasibility of fMRI objective measures.

Methods: Five participants with RP were evaluated before and after monocular retinal prosthesis implantation with BOLD scanning sessions consisting of rings at five eccentricities and checkerboards at five resolutions. Ring eccentricities were customized to cover regions both inside and outside the functioning visual fields. Central visual field was determined with SLO macular perimetry. Each scan consisted of a pseudo-random order of ring eccentricity or checkerboard resolution. Two of these subjects returned for CBF acquisition 9 months after implantation with rings at two eccentricities and checkerboards at two resolutions.

Results: Central visual fields significantly improved in the five subjects implanted eyes ($p < 0.05$). However, variability associated with fellow eye stimuli between scanning session days and months apart suggests that actual treatment effects in the implanted eye are indistinguishable due to inherent BOLD variability. The scans employing hypercapnic calibration demonstrate significant ($p < 0.05$) bilateral CBF activation in the occipital lobe. This activation pattern demonstrates sufficient sensitivity and specificity in CBF acquisition for the visual field loss population.

Conclusions: For the purposes of tracking and evaluating dynamic neuronal activity resulting from treatment of disease progression, BOLD can be prone to variability confounds unrelated to actual pathophysiology (specifically visual stimuli in this study). Therefore, the present findings demonstrate a significant potential problem in using BOLD for functional neuroimaging studies with repeated measures. Inclusion of CBF in treatment protocols will provide more comprehensive analysis of hemodynamics and more objective measures for longitudinal fMRI studies with repeated measures.

Support: Dept of Veterans Affairs Rehabilitation R&D Service



6-01 Corneal Structure and Function Measures as Markers of Diabetic Peripheral Neuropathy

GP Sampson¹, K Edwards¹, N Pritchard¹, N Efron¹

¹ Institute of Health and Biomedical Innovation, Queensland University of Technology, Brisbane, Australia

Purpose: Diabetic peripheral neuropathy (DPN) affects up to 54% of people with diabetes and is a major risk factor for lower limb amputation. Current assessment of DPN involves either invasive or painful procedures such as skin biopsy or nerve conduction assessment, or simple clinical metrics that assess temperature and vibration sensitivity such as the Neuropathy Deficiency Score (NDS). Recent evidence suggests that structural assessment of the corneal sub-basal nerve plexus and a putatively associated functional response (corneal sensitivity) are potentially useful early, non-invasive markers of DPN.

Methods: The Heidelberg Retinal Tomograph (Rostock Cornea Module) was used to capture images (400-700x magnification) of the central sub-basal nerve plexus. Newly developed tracking and postcapture image processing techniques were employed to create an extensive corneal nerve montage in a volunteer with type 2 diabetes (T2DM) and established DPN, and in a healthy control individual. Non-Contact Corneal Aesthesiometry (NCCA), which assesses corneal sensitivity to a controlled air-puff, was performed on 81 people with T2DM, 53 of whom had established neuropathy (NDS > 2/10).

Results: An area under the Receiver Operating Characteristic (ROC) curve of 0.73 (peak profile 72% sensitivity, 70% specificity) was found for NCCA as a predictor of individuals in the T2DM cohort who have DPN. Qualitative analysis of the two sub-basal nerve montages showed consistent comparative reduction of nerve fibre density across the entire map in the individual with DPN.

Conclusion: A novel mapping technique for creating composite montage maps of the sub-basal corneal nerve plexus has demonstrated a qualitative structural difference in nerve fibre density between an individual with DPN and a healthy volunteer. Quantitative analysis techniques are currently being developed. Assessment of corneal sensitivity demonstrated that NCCA has good sensitivity and specificity for detecting the presence of DPN in a cohort with T2DM. Corneal structural and functional parameters show promise as potential non-invasive markers of DPN.

6-02 The Extent of Presenting Visual Field Loss in Patients with Glaucoma

KC Limbachia¹, C Fenerty^{1,2}, DB Henson^{1,2}

¹ University of Manchester, Manchester, UK

² Manchester Royal Eye Hospital, Manchester, UK

Purpose: To establish the extent of presenting visual field loss in patients with glaucoma and relate it to socioeconomic status and age.

Methods: This is a retrospective cohort study of 331 patients referred to Manchester Royal Eye Hospital in 2004/05 with suspect glaucoma. Hospital records were reviewed to establish the extent of visual field loss (Humphrey Visual Field Analyzer MD, PSD and Brusini Glaucoma Staging System (GSS)) at presentation and its relationship to socioeconomic status and patient age. Socioeconomic status was derived from the ACORN index.

Results: 77 patients had a confirmed diagnosis of glaucoma with visual field data. 58 and 19% of the patients were found to have significant field loss (GSS>3) in their worst and best eyes respectively. There was a weak but not significant relationship with socioeconomic status. For patients with early to intermediate loss (MD>12dB) there was a positive relationship with age but for more advanced loss this relationship no longer held, patients with advanced loss at presentation were often younger than those with less advanced loss.

Conclusions: Healthcare avoidance leads to a significant number of patients with glaucoma having advanced visual field loss at first presentation and socioeconomic status, while related to the extent of loss at presentation, is a poor predictor of that loss. Age is also a poor predictor of the extent of loss at presentation.



6-03 Progression Rate of Central 10 Degree mean Deviation in Eyes with Retinitis Pigmentosa

H Iijima

University of Yamanashi, Chuoshi, Yamanashi, Japan

Purpose: We have already demonstrated that linear regression analysis of mean deviation (MD) in Humphrey central 10-2 program could evaluate the progression rate of the disease in eyes with retinitis pigmentosa (RP).

The purpose of the present study is to investigate the variability of progression of central field loss in those who have been tested with Humphrey perimetry for more than 10 years.

Methods: Humphrey 10-2 data were retrospectively reviewed in 41 patients (age ranging from 12 to 67 years, 19 male and 22 female) with RP, who had been followed up with every year testing in University of Yamanashi Hospital. Only data from right eyes were investigated.

Results: Linear regression analysis revealed statistically significant progression of mean deviation (MD) in 29 (71%) out of 41 patients. The regression coefficient ranged between -0.07 and -1.96 dB/year and distributed mainly between -0.25 and -0.5 dB/year. About 30 % of the subjects did not show significant progression of MD during the follow-up period longer than 10 years. The fact was also applied to the subset of the patients whose MD are between -10 dB and -25dB.

Conclusions: The progression rate of central field loss, which could be estimated by yearly testings of Humphrey perimetry, is variable among eyes with RP. There may be a subgroup of patients whose progression of the disease is too slow to be detected in the follow-up period longer than 10 years.

Reference:

Hirakawa H, Iijima H, et al.: Progression of defects in the central 10-degree visual field of patients with retinitis pigmentosa and choroideremia. Am J Ophthalmol 127:436-442,1999

6-04 Logistic Regression Analysis for Glaucoma Diagnosis using Frequency-Doubling Perimetry

MI Fuertes¹, A Ferreras¹, JM Larrosa¹, V Polo¹, LE Pablo¹

¹ Department of Ophthalmology, Miguel Servet University Hospital, Instituto Aragonés de Ciencias de la Salud, Zaragoza, Spain

Purpose: To calculate a linear discriminant function (LDF) for frequency-doubling perimeter (FDT) to increase its diagnostic accuracy to discriminate between healthy and glaucomatous eyes.

Methods: Sixty two normal subjects and 72 glaucoma patients were prospective and consecutively selected. Only one eye per participant was randomly selected. Glaucomatous eyes had intraocular pressure higher than 21 mmHg and abnormal standard automated perimetry results. All of them underwent a full ophthalmic evaluation and a full threshold test with the FDT (Welch Allyn/Humphrey Zeiss, Dublin, California, USA). The contrast sensitivity measures for detection of the frequency-doubled stimulus were obtained for the 17 target locations (C-20-5 strategy). The 17 tested points were numerated from nasal-superior position to temporal-inferior position. Left eye data were converted to a right eye format, in such a way that position 1 corresponded to the nasal-superior location, position 4 to the temporal-superior location, position 13 to the nasal-inferior location and position 16 to the temporal-inferior location. Position 17 corresponded to central location (fixation point). The LDF was calculated according to the stepwise logistic regression results of the threshold values at the 17 points obtained with the FDT. Receiver operating characteristic (ROC) curves were plotted to evaluate the diagnostic accuracy of the LDF and the FDT parameters.

Results: Based on the results of the stepwise binary logistic regression analysis, the function proposed was: $LDF = 4.807 + (0.213 \times \text{FDT central location}) - (0.184 \times \text{FDT location } n^\circ 9) - (0.202 \times \text{FDT location } n^\circ 5)$. The greatest areas under the ROC curve were found for our LDF (0.822), the location $n^\circ 5$ (0.763) and the location $n^\circ 1$ (0.737). There were not significant differences between them. The best sensitivity-specificity balance was observed for the LDF (62.5%-90.3%).

Conclusions: Compared to the FDT-provided measures, the proposed LDF exhibited the best diagnostic ability to discriminate between healthy and glaucoma patients.



6-05 Within-Individual Between-Visit Performance with the Pulsar Perimeter

M Zulauf¹, CA Castelberg², J Wild²

¹ Department of Ophthalmology, University of Basel, Basel Switzerland

² Cardiff School of Optometry and Vision Sciences, Cardiff University, Cardiff, United Kingdom

Purpose: Currently, a commercial version of the Pulsar Perimetry is being developed by Haag-Streit. Pulsar perimetry employs a 5° diameter circular waveform stimulus, which is isoluminant to the background of 100 asb.

Methods: 25 normal individuals naïve to perimetry, and 26 with ocular hypertension 14 [OHT] and 27 with open angle glaucoma [OAG]), with previous experience in both standard automated perimetry and short-wavelength automated perimetry, underwent perimetry in each eye on five occasions each separated by one week. At each visit, all individuals were examined with Program T30W and the TOP strategy of the Pulsar Perimeter and with Program 24-2 and the SITA Standard strategy of the Humphrey Field Analyzer.

Results: No statistically significant difference was found between the five visits for the index MD. For the normal individuals, the group mean MD in the right and left eyes at Visit 1 was 0.64dB (SD 1.18) and 0.53dB (SD 1.01), respectively, and at Visit 5 1.17dB (SD 1.02) and 0.82dB (SD 1.00), respectively. The corresponding values for Pulsar perimetry were at Visit 1 -0.08dB (SD 1.80) and -0.43 dB (SD 1.52), respectively, and at Visit 5 -0.3dB (SD 1.90) and -0.61dB (SD 1.32), respectively. The within-individual difference in the MD between Visits 1 and 5, expressed as the range of the limits of agreement (defined as the mean of the differences 1 ± 1.96 SD), for the SITA Standard algorithm was 2.68dB and 3.05dB for the right and left eyes, respectively, and for Pulsar perimetry, 5.07dB and 3.24dB, respectively. The limits of agreement were wider for those with OHT and widest for those with OAG.

Conclusions: No statistically significant learning effect was present with Pulsar Perimetry presumably due to the considerably larger within-individual between-visit differences compared to SAP.

6-06 Threshold Responses in Glaucomatous Eyes in Areas of Visual Field Judged Normal with Rarebit Perimetry

DA Hackett¹, AJ Anderson¹, P Brusini²

¹ Department of Optometry and Vision Sciences, the University of Melbourne, Melbourne, Australia

² Department of Ophthalmology, Santa Maria della Misericordia Hospital, Udine, Italy

Purpose: Rarebit Perimetry (RBP) samples the visual field with repeated small, nominally suprathreshold (150cd/m²) stimuli. It is claimed¹ to detect low degrees of neural damage in disease by detecting small scotomata left by neural element drop-out, with the percentage of targets detected (the Mean Hit Rate, or MHR) indicating the proportion of healthy neural elements remaining in the visual system. Here we used a customised version of the RBP test within areas of normal MHR (i.e. normal suprathreshold responses) in glaucomatous eyes to determine if threshold responses were similarly normal.

Methods: 16 observers with primary open angle glaucoma and 16 age-matched normal controls were tested with a customised RBP test that presented targets on average 30 times over each of 8 mid-peripheral (~10-15°) regions. The test was repeated for 13 stimulus luminances (10-150cd/m², in 0.14 log unit intervals), and a fourparameter (threshold, slope, false negative and false positive proportions) cumulative Gaussian psychometric function fitted to the response rate data from a normal region in a glaucomatous eye (MHR>80%) or in the corresponding region in an age-matched normal control. Parameters were compared between groups with paired t-tests.

Results: There was no difference in false negative (0.05 [glaucoma] vs 0.03 [normal], $p=0.4$) or false positive (0.01 vs 0.02, $p=0.4$) proportions between groups. Observers with glaucoma showed significantly elevated thresholds (1.33 vs 1.06 log(cd/m²), $p=0.004$) and significantly shallower slopes (s.d. of cumulative Gaussian = 0.25 vs 0.20 log(cd/m²), $p=0.03$). The magnitude of the changes in threshold and slope were not significantly different when converted to z-scores ($p=0.07$).

Conclusions: Threshold performance is significantly compromised in areas of normal suprathreshold responses in glaucomatous eyes. Our results suggest that visual dysfunction can precede the neural drop-out measured by Rarebit perimetry.

Reference:

1. Frisén (2002) Vision Res 42:1931-1939



7-01 A Comparison of Detection Rates using Total Deviation Probability Plots for SAP Sizes III and V, Motion Perimetry and Matrix

CK Doyle, CF Brito, KR Sherman, CA Johnson, M Wall

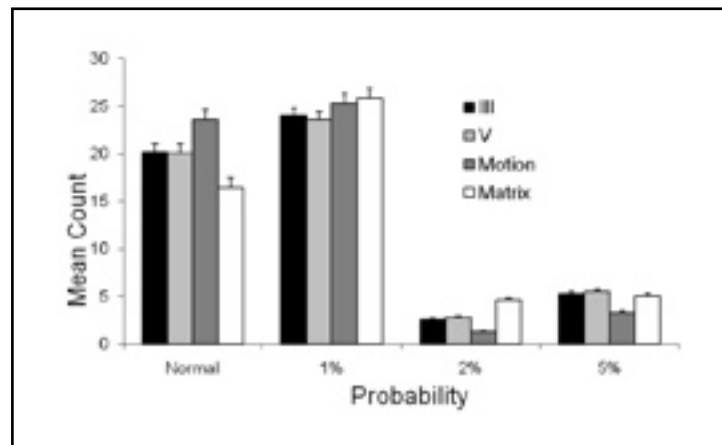
Veterans Administration Hospital, Iowa City, IA; Ophthalmology, University of Iowa, Iowa City, IA; Psychology, Eastern Illinois University, Charleston, IL

Purpose: To develop databases from a common set of normal participants for probability plots for Humphrey size III, size V, Motion Perimetry and Matrix Perimetry; to compare the normal and abnormal probability plot results of the 4 perimetric tests.

Methods: We computed empiric probability plots from data collected from testing 60 common normal participants (ages 40 – 78) with the four perimetry types above. We then analyzed the probability plots of 120 Glaucoma patients (ages 38 – 81, mean deviation -6.67 ± 4.4). We counted the number of test locations without and with loss at <1%, <2%, and <5% levels and compared the number of normal and abnormal test locations from our normative databases using the four tests (Figure). We used two-way repeated measures ANOVA to compare the counts of normal and abnormal test locations among the tests.

Results: The graph shows the differences in the number of normal and abnormal test locations flagged by the four tests' probability plots (average of two visits). For the number of normal test locations, sizes III and V were not significantly different from each other. But both III and V were significantly different from Motion and Matrix (all at $p < .001$); Matrix had significantly fewer normal test locations than the other tests ($p < .001$).

Conclusion: While clinically significant differences among the tests were small (of the order of 2-3 abnormal test locations per visual field exam), Matrix testing produced significantly more abnormal test locations.



Support: VA Merit Review Conflict of interest: None

7-02 Demonstrating a Rapid Testing Strategy for the Moorfields Motion Displacement Test for Glaucoma Case Detection

C Bergin¹, GM Verdon-Roe², W Ferrini³, DP Crabb¹, E Sharkawi³, DF Garway-Heath²

¹ Department of Optometry and Visual Science, City University London, UK

² NIHR Biomedical Research Centre for Ophthalmology, Moorfields Eye Hospital NHS Foundation Trust and UCL Institute of Ophthalmology, London, UK

³ Hôpital Ophtalmique Jules-Gonin Université de Lausanne

Purpose: To demonstrate the application of a fast testing procedure for the Moorfields Motion Displacement Test (MDT) for use as a case finding and screening tool in glaucoma.

Methods: The Moorfields MDT is a multi location perimetry test with 32 white line stimuli presented on a grey background on a standard laptop computer [1]. Each stimulus is displaced between computer frames to give the illusion of "apparent motion"; the threshold is recorded as the smallest discernible displacement. A new testing procedure, based on supra-threshold principles, but adapted using known spatial relationship between test points (Strouthidis et al, IOVS 2006; 47:5356-5362), was developed (Enhanced Spatial Testing Algorithm: ESTA). The testing procedure generates a probability of true damage (PTD) at each test location. Participants self referred to a glaucoma detection event on World Glaucoma Day in Hôpital Ophtalmique Jules-Gonin, Lausanne performed the MDT (with ESTA strategy) in both eyes, and then underwent an examination by a general ophthalmologist including measurement of intra-ocular pressure with Goldmann tonometry, slit lamp optic disc assessment and gonioscopy. Any suspect cases were invited for a follow-up examination, where they underwent full phenotyping by a glaucoma specialist (ES) including imaging and threshold perimetry. At phenotyping, subjects were classified as "healthy", "glaucoma suspect" (ocular hypertension or angle closure or suspicious disc), or "glaucomatous". "Healthy" participants were those that passed the initial or phenotyping examination. Classification by the MDT on the initial visit was retrospectively examined in all participants.

Results: Of 110 subjects attending the initial event, 69 were suspects and attended further testing. Twenty-one percent of the 110 participants had a self reported family history of glaucoma and 81% were older than 55 years. At phenotyping, subject classification was 8 "glaucoma", 24 "glaucoma suspect" and 37 "healthy". With specificity fixed at 95% the MDT, using the PTD score from the rapid ESTA strategy, identified 7 of the 8 glaucomatous cases and 10 of the 24 "glaucoma suspect" cases. The mean test time for the MDT running the ESTA procedure in one eye was 103 seconds (range: 74-191 seconds).

Conclusion: The ESTA procedure enables the Moorfields MDT to act as a quickly administered case-finding perimetry test for glaucoma. Test validation is currently being conducted through a multi-centre collaboration, which will compare the Moorfields MDT with other standard perimetry tests.

[1] www.moorfieldsmdt.co.uk Developers: C. Bergin¹, D.P. Crabb¹, F.W. Fitzke², D.F. Garway-Heath², G.M. Verdon-Roe², A.C. Viswanathan², M.C. Westcott³ [1]City University London; 2 NIHR Biomedical Research Centre for Ophthalmology, Moorfields Eye Hospital NHS Foundation Trust and UCL Institute of Ophthalmology, London; 3 St Bartholomew's Hospital, London]

7-03 The Effects of Optical Correction on Motion Displacement Thresholds in Glaucoma

R Moosavi¹, GM Verdon-Roe², MC Westcott³, AC Viswanathan¹, FW Fitzke², DF Garway-Heath²

¹ Glaucoma Research Unit, Moorfields Eye Hospital NHS Foundation Trust, London, UK

² NIHR Biomedical Research Centre for Ophthalmology, Moorfields Eye Hospital NHS Foundation Trust and UCL Institute of Ophthalmology, London, UK

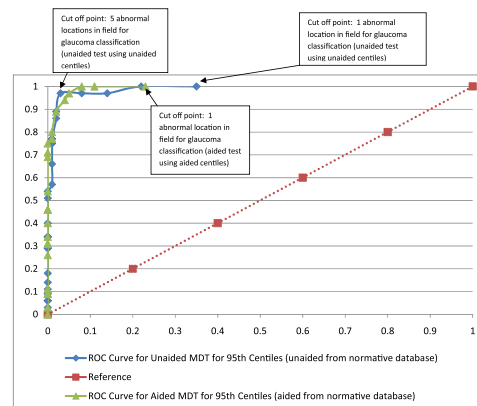
³ St Bartholomew's Hospital, London, UK

Purpose: Motion displacement hyperacuity thresholds have previously been shown to be resistant to the effects of refractive blur in normal subjects. This study explores the hypothesis that discrimination between glaucomatous and normal subjects is similar with and without refractive correction.

Methods: The Moorfields Motion Displacement test (MDT) has 32 line stimuli, each scaled with eccentricity (with the exception of the 4 central locations at 3 degrees eccentricity, which are scaled to be resistant to near refractive blur) presented on a 20-inch monitor at a test distance of 30 cm.[1] One eye of each of 35 glaucomatous subjects was tested. There were 21 POAG, 10 NTG and 4 PDS subjects, mean age 67 (range 47 to 82) years; mean near refractive correction: +2.00 (range -2.25 to +5.50) DS. All had abnormal HRT (by Moorfields regression analysis) and a reproducible Humphrey SITA defect [mean -5.36 (-8.80 to -0.59) db]. MDT thresholds were measured for a baseline test with near refractive correction, followed by two repeat tests with and without near correction (in a randomized order). Receiver operator characteristic curves were created for corrected and uncorrected refractive states for a range of cut-off values (number of abnormal locations to define glaucoma), using two respective sets of 95th centile limits derived from 120 healthy subjects.

Results: There is no significant difference in the ability to discriminate glaucomatous from healthy eyes for the tests with and without refractive correction (see figure).

Conclusions: Although specificity may be overestimated because it is estimated using the same healthy subjects from which the reference limits were derived, the comparison between corrected and uncorrected refractive states is valid. Testing patients without refractive correction has little impact on the ability of the MDT to discriminate between healthy and glaucomatous eyes.



[1] www.moorfieldsmdt.co.uk Developers: C. Bergin¹, D.P. Crabb¹, F.W. Fitzke², D.F. Garway-Heath², G.M. Verdon-Roe², A.C. Viswanathan⁴, M.C. Westcott³ [1 City University London; 2 NIHR Biomedical Research Centre for Ophthalmology, Moorfields Eye Hospital NHS Foundation Trust and UCL Institute of Ophthalmology, London; 3 St Bartholomew's Hospital, London; 4 Glaucoma Research Unit, Moorfields Eye Hospital, London]

Author Disclosure Block: R. Moosavi, Pfizer; G.M. Verdon-Roe, Pfizer; MDT Inventor; M.C. Westcott; MDT Inventor; A.C. Viswanathan, MDT Inventor; F.W. Fitzke, MDT Inventor; D.F. Garway-Heath, Carl Zeiss Meditec; Heidelberg Engineering; Pfizer; MDT Inventor

7-04 Defect Curve Fluctuation in Standard and Pulsar Perimetries

M Gonzalez de la Rosa, T Diaz Aleman, J Rodriguez Martin, R Rodriguez de la Vega, M Gonzalez Hernandez

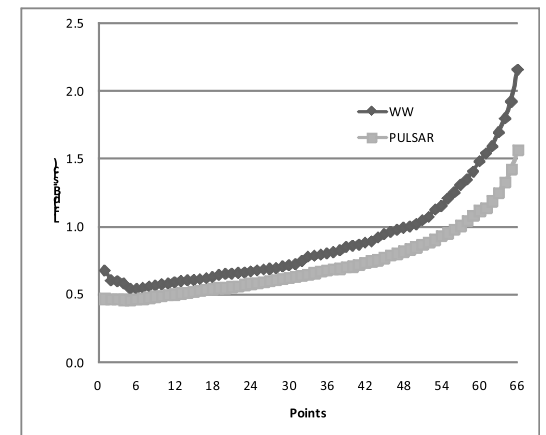
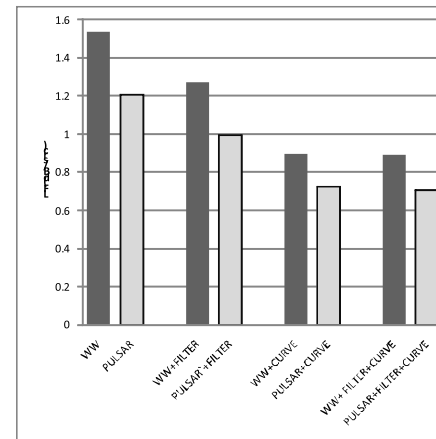
Hospital Universitario de Canarias. University of La Laguna. Canary Islands. Spain

Purpose: To calculate long-term fluctuation (LF) of defect curves, with and without threshold filtering.

Methods: We performed a longitudinal study of 191 eyes with early stage or suspected glaucoma (Mean Defect MD = 0.8 dB, sd = 1.9), without absolute scotomas, examined until completing a mean 11.0 examinations (sd = 5.3) using standard automatic perimetry (SAP, Octopus 311, TOP-32) and Pulsar (Program T30W). To reduce the influence of the learning effect and of progression on LF measurement, we calculated threshold standard deviation for each pair of consecutive examinations, and finally the average value of a total 1,916 pairs of examinations performed (126,456 pairs of thresholds). The calculation was made on the original threshold values, after applying a stabilizing filter as described previously,¹ and after calculating the defect curves.

Results: The values of LF are shown in Figure 1 and defect curve fluctuation (without filtering) in Figure 2. The values of Pulsar LF were significantly lower than those obtained using SAP ($p < 0.001$), both on individual analysis and for all points of the defect curve. On the right side of the curve, where more profound defects are located, Pulsar presented 25% less fluctuation.

Conclusions: Pulsar presented less fluctuation than SAP. Filtering is useful to stabilize thresholds and measure local changes, but has little



Support: In part by FEDER funding and FIS. Instituto Carlos III. Spain

References

1. Gonzalez de la Rosa M et al. Graefes' Arch Clin Exp Ophthalmol. 245:1303-9. 2007.

7-05 The Variability of the SITA Standard, SITA Fast and SITA SWAP Algorithms

CA Castelberg¹, M Zulau², JM Wild¹

¹ Cardiff School of Optometry and Vision Sciences, Cardiff University, Cardiff, United Kingdom

² Department of Ophthalmology, University of Basel, Basel Switzerland

Purpose: To examine, in normal individuals naïve to perimetry, in individuals with ocular hypertension (OHT) who were experienced in Standard Automated Perimetry (SAP), and in individuals with open angle glaucoma (OAG) also experienced in SAP, the between-individual within-visit between-algorithm variability for the SITA Standard, the SITA Fast and the SITA SWAP algorithms.

Methods: 79 individuals (29 normal, 25 with OHT and 25 with OAG) attended for perimetry on five occasions, each separated by one week. At each visit, divided into two sessions, both eyes were examined using HFA Program 24-2 and each of the three algorithms. At one session, SITA Standard was undertaken; at the other SITA SWAP and SITA Fast were undertaken. The order of session and of the algorithm within the session were randomized within individuals and varied over each of the five visits. The right eye was always examined first. The between-individual, within-visit, between-algorithm variability was analysed for Visit 5 in terms of the between-algorithm differences in the: Mean Deviation (MD) and Pattern Standard Deviation (PSD) indices; sensitivity for each stimulus location across all individuals; magnitudes of the Total Deviation (TD) and of the Pattern Deviation (PD) probability values; between-individual variability of the normal individuals in terms of the Coefficient of Variation (CoV).

Results: The between-algorithm difference in MD was narrowest for the two SAP algorithms. The underestimation by the SITA SWAP algorithm of the sensitivity derived by each SAP algorithm was approximately by 5dB at all levels of sensitivity for all groups. The SITA SWAP algorithm overestimated, in terms of the TD probability level, the extent of apparent abnormality in the height of the visual field relative to both SAP algorithms in normal individuals and in individuals with OHT by, on average, 2 fold. The CoV of the between-subject normal variability was twofold larger for SITA SWAP than for either SAP algorithm which indicates wider confidence limits for SITA SWAP.

Conclusions: The residual between-individual within-visit between-algorithm variability for SITA SWAP represents a considerable disadvantage in interpreting perimetric outcomes relative to either SAP algorithm.

7-06 Comparison of the Visual Field Testing Results of FDT, Flicker Perimetry and SWAP between Patients with NTG and POAG

H Nomoto, C Matsumoto, S Takada, S Okuyama, S Hashimoto, E Arimura, Y Shimomura

Kinki university school of medicine, Department of Ophthalmology, Osaka, Japan

Purpose: FDT and SWAP reportedly can detect the early glaucomatous visual field loss in patients with IOP-dependent POAG and ocular hypertension. However, their detectability of the early glaucomatous visual field loss in patients with NTG is still unknown. The aim of this study was to compare the visual field testing results of FDT, flicker perimetry and SWAP between patients with NTG (IOP < 21mmHg) and POAG (IOP > 21mmHg).

Subjects and Methods: Subjects were fifty-four eyes of 54 patients with NTG and 45 eyes of 45 patients with POAG. Both groups were divided to glaucoma suspects (GS), early, moderate and advanced groups (MD and NFLT matched). All subjects underwent HFA, FDT Matrix, flicker perimetry (4-zone 38S), and SITA-SWAP. Retinal nerve fiber layer thickness (NFLT) was also measured by Cirrus OCT. The number of abnormal points (NAP) in HFA, FDT, flicker and SWAP was used to evaluate the visual field and its correlation with NFLT was examined.

Results: In patients of all groups, average NFLT significantly correlated with NAP in HFA, FDT, flicker and SWAP. Particularly in the results of HFA, FDT, flicker and SWAP for early glaucoma and GS, significant correlations were found between inferior average NFLT and NAP in the upper hemifield. However, NTG and POAG did not show any significant differences in the testing results, or correlation between inferior average NFLT and NAP.

Conclusion: There is no difference in the detectability of the early glaucomatous visual field loss by FDT, flicker and SWAP between patients with NTG and POAG.



7-07 The Comparative Performance of Standard Automated Perimetry and Critical Flicker Frequency Perimetry in Individuals with Cataract

K Luraas, JM Wild

Cardiff School of Optometry and Vision Sciences, Cardiff University, Cardiff, United Kingdom

Purpose: Evidence suggests that the Critical Flicker Frequency threshold may be immune to the effects of optical degradation. Consequently, Critical Flicker Frequency perimetry (CFFP) may be more beneficial than standard automated perimetry (SAP) in patients with both cataract and glaucoma in that any diffuse defect arising from the glaucomatous process may be more readily identifiable with CFFP compared to SAP. The purpose of the study was to compare the outcome of CFFP with that of SAP.

Methods: Twenty-two individuals with bilateral cataract (classified using LOCS III), who were naïve to both SAP and CFFP, underwent both SAP and CFFP, at each of four weekly visits using the Octopus 311 and Program G1 and the TOP strategy. The right eye was always examined before that of the left eye and the perimetry was undertaken in an identical manner at each visit. The results over the four weeks for the eye with the severest cataract were principally analysed in terms of the Mean Defect (MD) and the proportionate change from Visit 1 to Visit 4.

Results: Seven individuals had anterior cortical cataract (ACC grade 1 to 4) in the more severely affected eye, 5 posterior subcapsular cataract (PSC grade 1 to 4), 8 nuclear cataract (NC grade 1 to 4) and one each with either ACC and NC or ACC and PSC, combined. The group mean and SD of the MD for SAP at Visit 1 was 3.1 dB (SD 3.9) and for CFFP 3.2 Hz (SD 5.6). The corresponding values at Visit 4 were 1.4 dB (SD 3.1) and 1.8 Hz (SD 5.0). The proportionate improvement from Visit 1 to Visit 4 was 55 % for SAP and 44 % for CFFP. The group mean number of locations at Visit 4 exhibiting abnormality by Comparison (height) probability analysis at $p \leq 0.02$ was 5.4 (SD 12.1) for SAP and 4.1 (SD 7.5) for CFFP.

Conclusion: An improvement in sensitivity was present for both types of perimetry. Within the constraints of the different normative data bases for each type of perimetry, CFFP offers no advantage for the visual field investigation of individuals with cataract.

7-08 Intermittent Visual Loss during Eye Movements

A Bruckmann¹, M Schmalzing², U Schiefer¹

¹ Research Institute for Ophthalmology, University of Tuebingen, Germany

² Department of Internal Medicine, University of Tuebingen, Germany

Purpose: To identify the etiology of painless intermittent visual loss during eye movement in a patient with bilateral optic disk swelling.

Method: Evaluation of the patient's history and symptoms as well as basic neuro-ophthalmologic exam, including ocular motility testing and visual field assessment with semi-automated kinetic perimetry and threshold-oriented slightly supraliminal static perimetry (Octopus 101 perimeter, HAAG-STREIT Inc. Koeniz, Switzerland).

Results: The patient reported about attacks of intermittent visual loss during eye movements, persisting from seconds to 30 min, occurring 10-20 times a day without any signs of dizziness, nausea or faint. The symptoms had started 9 months before the initial visit and were interpreted as typical obscurations. Visual acuity was R 20/20 and L 20/80. A RAPD of 1.5 log units was present in the left eye. Ocular motility was not restricted. Funduscopy revealed pronounced chronic papilledema, optic atrophy (L>R) and absent venous pulsations. The visual field (R) showed a preserved central island; the left eye could not be examined sufficiently, due to persistent obscurations. The following MRI scan showed thickening and enhancement of both optic nerve sheaths. Cerebral spinal fluid (CSF) pressure was borderline (22 cm H₂O). Differential blood count, immunophenotyping of peripheral blood, bone marrow aspirate, CSF and bone marrow biopsy revealed a marginal zone lymphoma. Glucocorticoid therapy and chemotherapy reduced the papilledema and the obscurations.

Discussion: The symptoms were initially misinterpreted by the referring physicians as "amaurosis fugax" (transient visual loss) and as orthostatic problems, respectively. The neuro-ophthalmologic symptoms were then assigned to a "benign intracranial hypertension". However, further examinations revealed a non-Hodgkin lymphoma. Unfortunately, the comparatively long duration of the papilledema resulted in a considerable optic neuropathy with advanced irreversible visual impairment of the left eye.

Conclusion: The constellation "advanced chronic bilateral papilledema" with the chief complaint of severe obscurations in both eyes requires immediate neuro-ophthalmologic diagnostics including testing of visual function, ocular motility, neuro-imaging and spinal tap with assessment of CSF pressure and composition.



7-09 Quantification of Perimetric Results – a Volumetric Approach

U Schiefer¹, S Frick¹, J Nevalainen^{1,2}, J Grobbel¹, E Krapp¹, R Weleber³, J Dietzsch¹

¹ Department / Research Institute for Ophthalmology, University of Tuebingen, Germany

² University Eye Hospital Oulu, Finland

³ Casey Eye Institute, Oregon Health & Science University, Portland, OR, USA

Purpose: The quantification of perimetric results is of major importance for the rating of the degree of visual field loss and for evaluating its change over time in any kind of visual pathway lesion. The purpose of this study was to develop a volumetric approach that can be utilized for the quantitative analysis of visual field loss with relation to an age-corrected normative hill of vision.

Methods: Eighty-one normal subjects, aged from 10 to 79 years were enrolled in this study, which was performed on the new Octopus 900 perimeter (HAAG-STREIT Inc., Koeniz, Switzerland). Eighty-six static stimuli (Goldmann size III = 26°) up to a maximal eccentricity of 80 degrees, with a condensation towards the visual field centre, were presented on a homogeneous background (luminance level 10 cd/m²). A fast thresholding algorithm (GATE: initial step size of 4 dB and at least one reversal) was used. The volumetric analysis was based on a smooth mathematical model and a triangulation routine that was related to the 86 test locations.

Results: The model fit was satisfactory ($R^2 = 0.72$). The visual field volumes for the examined normal cohort ranged from 255,219 dB x square degrees at the age of 10 years to 198,651 dB x square degrees at the age of 80 years. The volume of the hill of vision reached its maximum of 255,989 dB x square degrees at the age of 17.3 years and declined continuously thereafter.

Conclusions: The volumetric approach is almost independent of the test point arrangement. It allows for a quantification and follow-up of visual field results with relation to an age-corrected (80 degree) hill of vision. The volumetric approach can be related to the entire visual field (TLV = „total loss volume“) or to selected sub-regions of the visual field (RLV = „regional loss volume“).

7-10 Reduction of Learning Effects in Studies of Multiple Perimetric Tests in Glaucoma Patients

KS Sherman, CK Doyle, CA Johnson, CF Brito, M Wall

Department of Ophthalmology, University of Iowa, Iowa City, IA; Veterans Administration Hospital, Iowa City, IA; Psychology, Eastern Illinois University, Charleston, IL

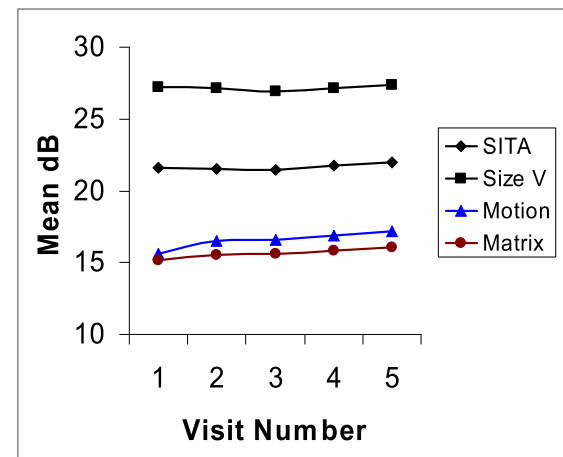
Purpose: To examine how learning effects (performance improvements due to repeated testing) vary in glaucoma patients across four perimetry tests: size III SITA (Size III) and size V full threshold methods of the Humphrey Field Analyzer, as well as Motion and Matrix perimetry.

Methods: About once a week for five weeks glaucoma patients (N=30) were given four perimetric tests: (1) SITA standard Size III, (2) Full-threshold Size V, (3) Motion, and (4) Matrix perimetry. Participants had previous experience with perimetric testing. Each participant first received a SITA test (used for study eligibility) followed by the remaining three tests, administered in random order. On some occasions, tests had to be administered on multiple days. The average number of days between visits was 10. Mean sensitivities in dB were computed across all test locations for each subject, for each test. A 4x5 (test type, visit number) repeated measures ANOVA was performed on the averaged sensitivities.

Results: Significant learning effects between visits 1 and 5 were observed for Motion (1.53 dB improvement) and Matrix (.91 dB improvement) tests but not for Size III or Size V ($p < .001$; Figure). The average learning effect between visits was only .09 dB for Size III SITA and .04 dB for Size V; whereas, for Motion, the average learning effect was .38 dB and .23 for Matrix. Additionally, the largest learning effects in Motion perimetry and Matrix were observed between visits 1 and 2: .86 dB improvement for Motion and .42 for Matrix.

Conclusion: Learning effects may be minimal in glaucoma patients when they are administered multiple perimetric tests. There may be a transfer of learning effects among similar perimetric tests.

Figure:



Commercial Relationship: None.
Support: VA Merit Review



8-01 Automatically Identified Patterns of Glaucomatous Visual Field Loss in SITA Fields from Independent Component Analysis

M Goldbaum¹, PA Sample¹, G Jang¹, T-P Jung², C Bowd¹, LM Zangwill¹, J Liebmann³, CA Girkin⁴, RN Weinreb¹

¹ Hamilton Glaucoma Center

² Institute for Neural Computation, University of California, San Diego, La Jolla, CA, USA

³ New York Eye and Ear Infirmary, New York, NY, USA

⁴ University of Alabama, Birmingham, AL, USA

Purpose: To determine if patterns uncovered with variational Bayesian independent component analysis mixture model (VIM) applied to a large set of normal and glaucomatous fields obtained with SITA are distinct, recognizable, and useful for modeling the severity of field loss.

Methods: SITA fields were obtained with the Humphrey Visual Field Analyzer on 1,146 eyes with normal fields and 939 glaucoma eyes with abnormal fields from the Diagnostic Innovations in Glaucoma Study (DIGS) and the African Descent and Glaucoma Evaluation Study (ADAGES). VIM modifies independent component analysis to develop a set of axes in each cluster. The model with the best separation of normal and glaucomatous fields was chosen from 360 models to create maximally independent axes. Grayscale displays of fields generated by VIM on each axis were evaluated for distinctness. Displays of SITA fields associated with each axis were evaluated for consistency.

Results: The best VIM model had 3 clusters. Cluster 1: two axes (1,193 fields) was mostly normal fields (1,089, 95% specificity). Cluster 2: 2 axes (569) contained mildly abnormal fields (513). Cluster 3: (323) held mostly moderately to severely abnormal fields (322) along 5 axes. Sensitivity for clusters 2 plus 3 was 88.9%. Two masked experts agreed the generated field patterns on each axis differed from those on other axes. The SITA fields associated with an axis resembled each other and the generated patterns. Pattern severity increased in the positive direction of each axis by expansion or deepening of defect.

Conclusions: VIM separated SITA fields into distinct yet recognizable patterns associated with glaucoma and ordered each pattern by defect severity. The axis and pattern properties make VIM a good method for developing the Progression of Patterns (POP) machine learning algorithm (see Sample companion abstract).

Support: NIH/NEI grants: EY08208 (PAS), EY11008 (LZ), EY14267 (PAS, JL, CG), EY13959 (CAG), EY 13928 (MG), Pfizer (CB), Eyesight Foundation (CAG), David and Marilyn Dunn Fund (MG), Grants for participants' glaucoma medications from Alcon, Allergan, Pfizer, and Santen.

8-02 Comparison of Local Differential Luminance Sensitivity (DLS) between Oculus Easyfield Perimeter and Humphrey Field Analyzer 740 (HFA II) in Normal Subjects of Varying Ages

Z Gagyi-Palffy, R Kirchhübel

Oculus Optikgeräte GmbH, Wetzlar, Germany

Purpose: Purpose of this study was to obtain new age-corrected normal values of differential luminance sensitivity for the Oculus Easyfield Perimeter, and to compare these to similar values obtained with the Humphrey Field Analyzer 740 (HFA II). Additionally, the duration of threshold examinations were compared. For completeness, nasal-temporal and superior-inferior asymmetries in the central visual field were analyzed based on the collected dataset.

Methods: 67 ophthalmologically healthy eyes (36 OD, 31 OS), evenly distributed over decades (a single eye per person) were examined with both perimeters using the 30-2 rectangular grid and 4-2 dB bracketing strategy for threshold estimation. The resulting data for both instruments were extracted and subjected to statistical analysis. Various biometric models were developed in order to accommodate the observed asymmetries.

Results: Mean sensitivities (MS) measured on the two different instruments provided by linear regression a correlation coefficient of 0.865, corresponding to $R^2 = 0.748$. Best linear fit of data was obtained with 64 data points out of 67 (95.5%) being located inside the 95% prediction limits.

Conclusions: Local differential luminance sensitivity values obtained with Easyfield and those obtained with HFA II match within statistical errors for all individual grid points. We found that the difference of the mean sensitivity values recorded by the two devices is compatible with zero ($\chi^2=2.955$); the absolute value of the difference is not higher than 1.026 dB with 95% confidence level.

References:

1. Lorch, L. et al. (2001) Klin. Monatsbl. Augenheilk. 218: 782-794
2. Schwabe, R. et al. (2001) in: Wall, M., Mills, R.P. (Eds.) Perimetry Update 2000/2001. Kugler Publications, The Hague/The Netherlands pp. 71-79
3. Wohlrab, T.-M. et al (2002) Ophthalmologica 216: 96-100



8-03 Exploratory Eye Movements – a Compensatory Option for Patients with Homonymous Visual Field Defects?

E Papageorgiou^{1,2}, G Hardieß³, H A Mallot³, U Schiefer¹

¹ Centre for Ophthalmology & Institute for Ophthalmic Research, University of Tübingen, Germany

² Department of Ophthalmology, General Hospital of Larissa, Greece

³ Lab of Cognitive Neuroscience, University of Tübingen, Germany

Purpose: Aim of this study was to assess the impact of homonymous visual field defects (HVFDs) on collision avoidance in a virtual reality scenario under additional consideration of the visual exploration (use of eye and head movements).

Methods: Overall performance in the task was quantitatively assessed as the number of collisions in a virtual intersection at two difficulty levels. HVFDs (assessed by binocular semi-automated kinetic perimetry within the 90° visual field, stimulus III4e; OCTOPUS_101, HAAG-STREIT Inc., Koeniz, Switzerland) as well as exploratory movements (assessed with eye and head tracking) were superimposed on the trajectories of the virtual vehicles on a temporal or spatial scale. The following parameters were visualized and analyzed: (i) if at all, and if yes, (ii) in which time-point/in which distance from the intersection, (iii) for how long regarding distance and time, a potentially collision-relevant vehicle was explored, and (iv) if exploration of collision-relevant vehicles resulted in a modification of driving behavior (in terms of speed adjustment). Additionally, the effect of the area of sparing within the affected hemifield (A-SPAR in degrees²) on performance was investigated

Results: 30 patients (10 female, 20 male, age range: 19-71 years) with HVFDs due to unilateral vascular brain lesions (time span after brain lesion at least 6 months) were examined. The control group included 30 group-age-matched subjects with normal visual fields. Although the mean number of collisions was higher for patients, 26 out of 30 patients were within the 95% reference range of the normal-sighted subjects regarding performance (number of collisions) in the passage of the intersection. Lower A-SPAR was associated with worse performance, however individual variation was remarkable. Patients with better performance exhibited substantially different gaze characteristics compared to those with worse performance. The gaze strategy of patients with better performance was characterized by longer scanpaths, more gaze shifts and longer saccadic amplitudes.

Conclusion: Location and extent of HVFDs per se – as expressed by A-SPAR – seem to be inadequate in predicting the successful passage of an intersection under virtual reality conditions. A subgroup of patients with HVFDs compensates for the visual impairment by using exploratory eye and head movements.

Support: European Union: PERACT – Marie Curie Early Stage Training MEST-CT-2004-504321

Acknowledgements: Prof. Dr. K. Dietz, Department for Medical Biometry, University of Tübingen, Germany

8-04 Visual Acuity Loss of Unknown Origin in a Patient with Suspected Low Tension Glaucoma

C Heine, U Schiefer

Department/ Institute for Ophthalmic Research, University of Tuebingen, Germany

Purpose: Routine neuroimaging in patients with low tension glaucoma (LTG) is a contentious issue since it is expensive and compressive optic neuropathy is rarely found. The purpose of this case report is to identify typical neuro-ophthalmological signs in which neuroimaging is mandatory.

Methods: Visual acuity, funduscopy, suprathreshold automated static perimetry (Octopus 101, Haag-Streit Inc., Köniz, Switzerland) and OCT (Stratus OCT, Carl Zeiss Meditec AG, Jena, Germany) were performed.

Results: A 76 year old male patient was presented with LTG. Visual acuity (VA) was 20/25 on the right and 20/100 on the left eye. The optic discs showed a cup disc ratio (CDR) of 0.8 and a subtle pallor on the right eye and a CDR of 0.6-0.7 on the left. In the perimetry a small paracentral scotoma on the left and no defect on the fellow eye were seen. Intraocular pressure was between 10 and 13 mmHg under therapy with dispraclonidine on both eyes. OCT was performed in order to rule out any macular pathology and showed normal results. A MRI was recommended but not performed.

At the patient's next visit, seven month later, a drop of VA to 20/200 on the left eye and a massive visual field alteration, attributable to an anterior junction syndrome was seen. The MRI showed an extensive pituitary adenoma. Due to the tumor's configuration and size, stereotactic fractionated radiation was performed. Unfortunately VA und visual field defects did not improve after therapy.

Conclusion: The constellation of VA loss and optic disc pallor that is not located in the area of rim loss is not compatible with glaucomatous optic neuropathy but rather suspicious of optic neuropathy of other origin. An immediate MRI should be performed to rule out a compressive or other lesion involving the anterior visual pathway. Severity of visual field defects increase with tumor volume. Anterior junction syndrome is the second most frequent visual field defect that can be found in patients with chiasmal lesions.



8-05 Predictability of Future Perimetric Change in Glaucoma using a Linear-Scaled Global Index

SK Gardiner¹, S Demirel¹, CA Johnson², WH Swanson³

¹ Devers Eye Institute, Portland, OR, USA

² University of Iowa, Iowa City, IA, USA

³ Indiana University, Bloomington, IN, USA

Purpose: To determine whether a global index summarizing the visual field based on a recent glaucoma structure-function model by Hood et al^A is more predictable than Mean Deviation (MD), as defined by the ability of the initial value of the index to predict subsequent change. This model relates loss of retinal ganglion cells (RGCs) to perimetric sensitivity on a linear, rather than logarithmic (decibel) scale.

Methods: At each location in the field, the Total Deviation was transformed onto a linear scale, as an estimate of the amount of loss of RGCs, using the structure-function model of Hood et al. The mean of these pointwise values was used as a global estimate of loss (after transforming back onto a decibel scale). 50 subjects with early or suspected glaucoma who exhibited glaucomatous optic neuropathy at baseline performed annual visual field tests over seven years. These visual fields were summarized using MD and the new global index. The initial value for each index was used to predict the subject's rate of change over the subsequent years (tests 2-7 in the series).

Results: The non-parametric correlation between initial value and subsequent rate of change was 0.343 for MD and 0.570 for the new index; this difference was significant with $p=0.031$. Using linear regression to account for effects of baseline IOP, treatment status and age, the subsequent rate of change in MD could be predicted from its baseline value (adjusted $R^2=14\%$). A better fit was obtained using the new index (adjusted $R^2=27\%$); this difference was significant with $p=0.014$.

Conclusions: The linear-based global index was significantly more predictable than MD. Global indices based on models relating perimetric sensitivity to RGC count may improve the ability to identify those subjects at highest risk of more rapid future functional progression.

Support: NIH/NEI grants: R01 EY03424, R01 EY019674

Reference:

^A Hood DC, Kardon RH. Prog Retin Eye Res. 2007;26:688-710

8-06 Properties of the Statpac Visual Field Index (VFI)

PH Artes, L Heckler, BC Chauhan

Ophthalmic Sciences, Dalhousie University, Halifax, NS, Canada

Purpose: To compare the statistical properties of the visual field index (VFI) to those of Mean Deviation (MD), in patients with glaucoma followed over time

Methods: Mean Deviation and VFI were calculated for visual fields from 109 patients followed for 10 years (median, 22 tests). Variability, rates of change, their statistical significance, and evidence for non-linear linearity in progression were compared between the two indices.

Results: The relationship between the MD and VFI ($r=0.83$, $p<0.001$) appeared linear, except with MDs better than -5.0 dB where 7/132 eyes (5.3%) had a VFI of 100% (ceiling effect). The predicted VFIs for fields with MD values of 0 dB, -10 dB, and -15 dB were 100%, 87%, and 81%, respectively. Rates of change of the two indices were moderately closely related ($r=0.75$, $p<0.001$), and statistically significant trends over time ($p<0.05$) occurred in the same number of eyes (87/204, 43%). Of the 104 eyes with significant trend on either VFI or MD, 70 eyes showed trends in both indices ($\kappa=0.66$). In terms of variability over time, the VFI was even more dependent on damage (Spearman r , -0.67) than the MD ($r = -0.56$), and there was no evidence that change over time was more linear with the VFI than the MD (Durbin-Watson statistics).

Conclusions: The VFI provides a simple and understandable metric of visual field damage. However, it does not appear to have any real advantages over the MD for estimating a patient's rate of change over time. The reliance of the VFI on pattern deviation probability maps causes a ceiling effect which may reduce its sensitivity to change in eyes with early damage

References

Bengtsson B and Heijl A, A Visual Field Index for Calculation of Glaucoma Rate of Progression, American Journal of Ophthalmology, 2008, 145, 343-353



9-01 Grey Scale Map of Perimetric Progression using Multiple Defect Curves

M Gonzalez Hernandez, M Sanchez Mendez, J Aguilar Estevez, J Muiños-Gomez, M Gonzalez de la Rosa

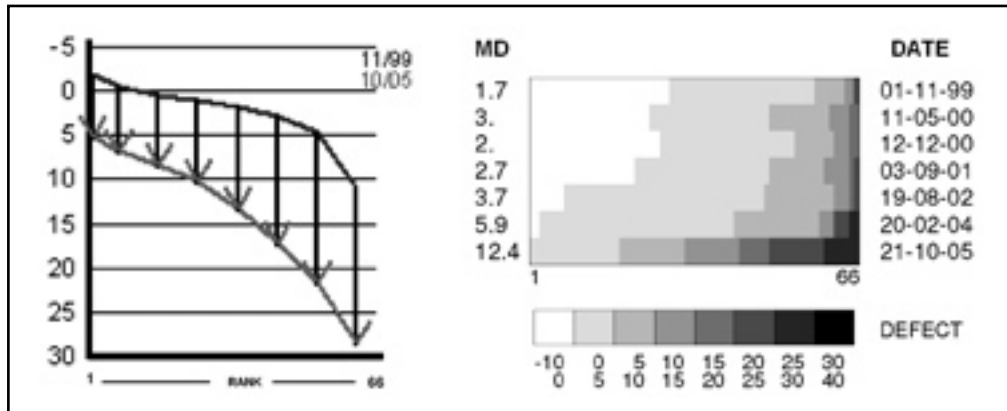
Hospital Universitario de Canarias. University of la Laguna. Canary Islands. Spain

Purpose: To show a new graph that represents perimetric progression in the form of a grey scale map.

Methods: At the Portland congress, we proposed analyzing the defect curve by sectors in order to interpret visual field progression (Program Threshold Noiseless Trend, TNT).¹ Subsequently, we verified that the stability of the curve allows early diagnosis of progression² and easy interpretation of the degree of focality, thus proving to be more efficient than the GPA program or the opinion of experts.³ The representation that we proposed using vectors allows one to easily visualize the statistical significance of changes (Fig. 1) but it only reflects the initial and final situations of the curve.

Results: A cumulative representation of defect curves in the form of a grey scale map allows an overall view of defect evolution (Fig. 2). The graph is complemented with numerical data on MD change. In the example below, the MD slope is 1.98 dB/year ($p < 0.002$) and the focality index is high ($FI = 4.34$), corresponding to curves (initial and final) that are not parallel.

Conclusions: The two modes of representing progression of the visual field are complementary; taken together they allow improved interpretation of the amplitude, focality and sequence of change.



References
 1.- Gonzalez de la Rosa M et al. *Europ J Ophthalmol* 2009;19:416-424
 2.- Gonzalez de la Rosa M. *Br. J. Ophthalmol.* 2008;92;1564-1565
 3.- Diaz-Aleman VT et al. *Br J Ophthalmol.* 2009;93:322-328.

9-02 A Continuous Probability Scale for Size III, Size V, Motion and Matrix Perimetry

CA Johnson, M Wall, CK Doyle, CF Brito, KR Sherman, K Woodward

Ophthalmology, University of Iowa, Iowa City, IA
 Veterans Administration Hospital, Iowa City, IA
 Psychology, Eastern Illinois University, Charleston, IL

Purpose: To apply a continuous probability scale to Size III, Size V, Motion and Humphrey Matrix Frequency Doubling Technology Perimetry and compare their results in glaucoma patients.

Method: Age adjusted empiric continuous probability plots were determined for each test procedure based upon data obtained from both eyes of the same 60 normal control subjects (ages 40-78), using test patterns similar to a 24-2 stimulus configuration. These evaluations were then applied to eyes from 120 glaucoma patients with varying degrees of damage (Size III MD = -6.67 ave, 4.4 s.d.).

Results: At the 1%, 2% and 5% probability levels, normal and abnormal values were similar for Size III and V, but both Size III and V were different from Motion and Matrix while Matrix had the fewest normal locations. The table below presents the increase in percentage of abnormal points at the 10, 15 and 20% levels for the four tests in comparison to the expected normal increases. The size III results were slightly below expected normal values, while Size V, Motion and Matrix yielded higher than expected increases in abnormal values at the 10, 15 and 20% levels.

| Percentile | Normal Expected Increase of Abnormal Points from the 5% Level (%) | Size III | Size V | Motion | Matrix |
|------------|---|----------|--------|--------|--------|
| 10 % | 5 % | 2 % | 22 % | 17 % | 9 % |
| 15 % | 10 % | 6 % | 37 % | 29 % | 16 % |
| 20 % | 15 % | 17 % | 49 % | 40 % | 21 % |

Conclusions: Size V, Motion and Matrix Perimetry reveal a greater proportion of points below the 20, 15 and 10 % normal levels in glaucoma patients than size III. This suggests a better clinical combination of higher sensitivity and lower variability. Continuous probability scales may be useful in detecting early glaucomatous visual field losses and progressive visual field changes.

Support: VA Merit Review Conflict of interest: None



9-03 autoSCOPE - an Algorithm for Automated Regional Condensation of Stimulus Density for Polar and Rectangular Perimetric Grids

J Dietzsch¹, J Pascual², E Krapp¹, D Fischer¹, PA Sample², U Schiefer¹

¹ Centre for Ophthalmology, Institute for Ophthalmic Research, University of Tübingen, Germany

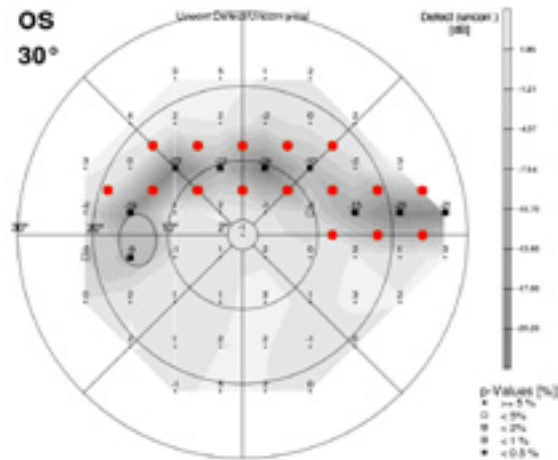
² Hamilton Glaucoma Center, Department of Ophthalmology, University of California, San Diego, CA, USA

Purpose: The introduction of an algorithm for automated, standardized test point condensation in regions of interest – i.e. the (peri-)scotoma area – which is applicable to polar and rectangular stimulus arrangements.

Methods: A reference grid with maximum test point density was specified in order to maintain inter-subject comparability of stimulus locations (rectangular: 3° x 3° grid, 136 locations; polar: 30-NO grid, 192 locations). The initial input for the condensation algorithm is a visual field calculated as the local median of the differential luminance sensitivity (DLS) values for each test location of three baseline examinations. These baseline examinations are carried out with grids of regular density (rectangular: 24-2 grid, 55 locations; polar: 30-A, 83 locations). The algorithm operates on a triangulation mesh and consists of several iterative filtering and weighting steps to identify potential locations that are attributable to regions of interest. The maximum of added test locations was restricted to 33% of the number of test locations at baseline in order to avoid an exhaustive examination duration.

Results: For a first evaluation the condensation results of a set of eight representative visual field cases from our glaucoma patient database were reviewed by four experienced examiners. In seven of eight cases the local condensation was rated as “good” to “sufficient”. The figure shows an example of condensation. The 16 added test locations are marked with red filled circles.

Conclusions: The autoSCOPE algorithm is a promising step towards a fully automated, standardized local test point condensation in regions of interest.



9-04 Modeling the Hill of Vision in Health and Disease

R Weleber¹, P Francis¹, E Chegarnov¹, J Paetzold², J Dietzsch², U Schiefer², C Johnson³

¹ Casey Eye Institute, Oregon Health & Science University, Portland, Oregon, USA

² Department / Research Institute for Ophthalmology, University of Tuebingen, Germany

³ Department of Ophthalmology, Univ of Iowa, Iowa City, USA

Purpose: To model the “Hill of Vision” (HOV) and develop metrics for quantification of field defects.

Methods: We measured thresholds to 80° eccentricity using the Octopus 101 perimeter, a fast thresholding strategy (GATE), with radially-oriented, centrally-condensed grids of 102 to 187 test loci. Seven normal subjects were tested with two or more grids with both Goldmann size III (26´) and size V (103´) stimuli on a 10 cd/m² background. The HOV was modeled using the sensitivity values and a flexible spline. The volume was quantified using the decibel-steradian (dB-sr). We compared the volume of the total HOV, central 30° volume, and central 30° Mean Sensitivity (MS in dB) among the grids and between the two stimuli.

Results: Larger grids sampled more of the HOV. After adjustments for this truncating effect, no significant differences existed among the grids for total HOV volume, central 30° volume, and MS. Sensitivity was 1 to 5 dB greater centrally and 7 to 13 dB greater peripherally with size 103´ than 26´. Using size 26´, mean volume (dB-sr ± 1SD; n=32 eyes) was 78.0±4.8 for the total HOV and 23.0±0.7 for the central 30°. Using size 103´, mean volume (n=33 eyes) was 104.9±6.5 for total HOV and 27.4 ±0.6 for the central 30°. The central 30° MS (dB) was 23.5 ±0.91 with size 26´ and 29.7±1.3 with size 103´. The time for full-field static testing varied from 13 to 23 minutes and was shorter with greater field loss. Specific regions of the HOV can be measured, e.g., scotomas or delivery sites for gene therapy. Over 500 patients have been studied.

Conclusions: The size V stimulus provides greater dynamic range and avoids floor “effects” with severe field loss. HOV modeling provides sensitive, robust metrics for diagnosis, characterization, staging, and as endpoints for clinical trials.

Support: Hear See Hope, The Grousbeck Family Foundation, Foundation Fighting Blindness



9-05 The Effect of Stimulus Size on Repeatability in Glaucoma using Goldmann Sizes III, V, and VI

M Wall, CK Doyle, KD Zamba, CA Johnson

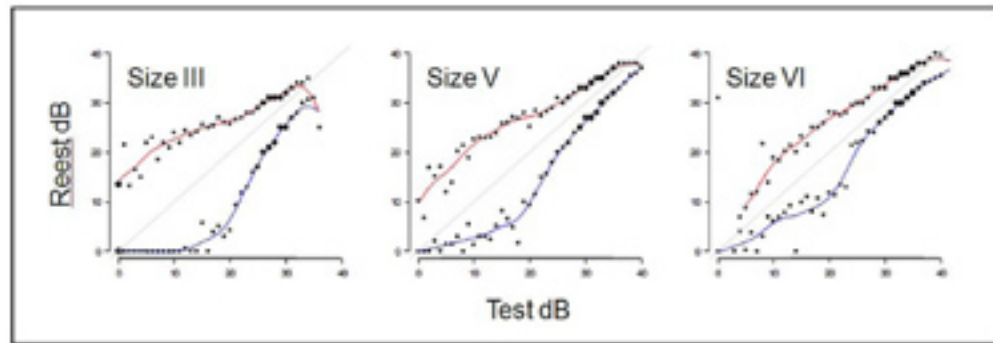
Veterans Administration Hospital and Departments of Ophthalmology, Neurology and Biostatistics, University of Iowa, Iowa City, IA

Purpose: Standard automated perimetry is limited by an exponential rise in variability with decreasing sensitivity and a limited effective dynamic range (EDR). We therefore studied the effect of stimulus size on repeatability and EDR using Goldmann stimulus sizes III, V and VI in glaucoma patients, using a customized Humphrey Field Analyzer modified to produce a size VI stimulus.

Methods: We tested 70 glaucoma patients twice within one month with Humphrey program 24-2 testing using stimulus sizes III (SITA), V and VI; Size III MD was -8.1 ± 4.8 dB and PSD was 9.1 ± 4.36 dB. Point-wise limits of test-retest variability were then established from the empirical 5th and 95th percentiles of the distribution of retest values, stratified by the sensitivity value of the test location at the first test (Fig). The log differences between test and retest values were linearly regressed onto the averages of the two tests to determine the relationship between variability and sensitivity.

Results: The average sensitivities were size III: 21 ± 4.5 dB.; size V sensitivity: 27.6 ± 3.7 dB and size VI: 30.3 ± 3.2 dB. Using floor effect as an index of effective dynamic range, the numbers of 0 dB trials were: size III – 391, size V – 76 and size VI – 21; this indicates a greater dynamic range for the larger stimuli. There was increasing variability associated with lower visual field sensitivity but the rise in variability was less with the larger stimulus sizes, with size VI having the least rise (Fig). After eliminating the values subject to a floor effect, we found the following correlations: with size III, sensitivity explained 25% of the test-retest variability (r^2), while corresponding figures for size V and size VI were 13%, and 9%, respectively.

Conclusion: Large sized conventional perimetric stimuli have a diminished increase in variability with decreasing sensitivity and a greater effective dynamic range. These stimuli show promise for use in moderate to severe glaucoma.



9-06 Introduction of a Portable Campimeter, based on a Laptop/Tablet PC

E Tafaj¹, C Uebber¹, J Dietzsch², U Schiefer², M Bogdan^{3,1}, W Rosenstiel¹

¹ University of Tübingen, Wilhelm-Schickard-Institute of Computer Science, Computer Engineering, Tuebingen, Germany

² Centre for Ophthalmology, Institute for Ophthalmic Research, Tuebingen, Germany

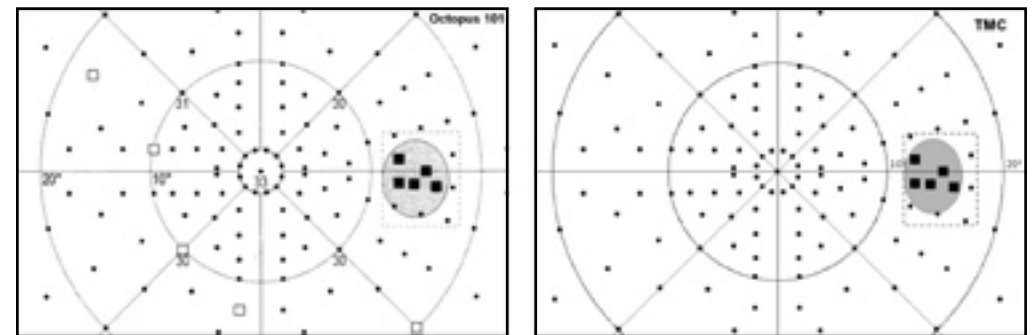
³ University of Leipzig, Institute of Computer Science, Computer Engineering, Leipzig, Germany

Purpose: To present a new and portable campimeter (Tuebingen Mobile Campimeter, TMC) for an automated and fast detection of visual field defects.

Methods: The underlying system architecture allows for portability on different hardware platforms and enables several application scenarios. Running on laptops or tablet-PCs the TMC is well suitable for usage in emergency or intensive care units or for bed-ridden patients. We evaluated the TMC in a pilot study comparing the assessed size and location of the blind spot in nine healthy subjects with the examination results of an Octopus 101 perimeter (O-101, HAAG-STREIT Inc., Koeniz, Switzerland). For both examinations a polar stimulus arrangement with 192 test locations condensed towards the centre (see Figure; grid 30-NO, stimulus size Goldmann III [26']) was used. The examination with the O-101 was performed using a threshold-related, slightly supraliminal strategy (background luminance 10 cd/m²). The TMC examination was carried out on a standard laptop (15" screen size, 2.4GHz) with a stimulus luminance of 270 cd/m². Concordance of location and size of the blind spot was defined as the ratio of intercept areas and union areas, obtained with both instruments.

Results: TMC results were highly concordant with O-101 results for the estimation of the location and size of the blind spot. The concordance in the detected size of the blind spot was 0.89 (1.0 represents the best and 0.0 the worst result). The average examination time was 5 minutes with O-101 and 4 minutes with the TMC.

Conclusions: TMC results are highly concordant with O-101 results regarding location and size of the blind spot. This indicates that the TMC is well applicable for the measurement of visual field defects. Due to its portability the TMC is suitable for use in emergency, intensive care units, for bed-ridden patients and as a screening device.



Optimizing Test Intervals for Clinical Trials

Dr. David Garway-Heath

NIHR Biomedical Research Centre for Ophthalmology, Moorfields Eye Hospital NHS Foundation Trust and UCL Institute of Ophthalmology, City Road, London, England, EC1V 2PD, UNITED KINGDOM

Purpose: Historically, trials assessing the efficacy of new glaucoma treatments have evaluated intra-ocular pressure (IOP)-lowering, a surrogate for the outcome of greatest importance – visual function. Patients progress at widely different rates at all IOP levels, so that IOP is a poor surrogate for visual function outcomes. A better outcome is the effect of treatment on the rate of progression of visual field loss. Most glaucoma progresses at a relatively slow rate. The consequence is that, with conventional study designs, trials need to be very large and/or need to be conducted over an extended period.

Methods: The UK Glaucoma Treatment Study is a randomized, double-masked, placebo-controlled trial of medical therapy in newly diagnosed glaucoma patients utilizing a novel study design. The primary outcome is consistent with previous trials, but the test frequency has been designed to provide greater power to identify treatment differences by analyzing the rate of progression of visual field loss and by combining imaging and visual data. This will permit a direct comparison of the novel trial design with conventional approaches.

Results: The advantages of the novel study design and methods for combining structure and function data are reviewed and the implications for clinical care of patients discussed. Potential solutions to overcome the barriers to the adoption, by regulatory authorities, of structural endpoints as surrogates for glaucomatous progression in clinical trials are proposed.

Conclusions: Novel trial designs, by altering the frequency and interval of visual field testing, analysing rates of progression and incorporating structural imaging may shorten the duration of clinical trials and reduce the number of patients needed.

Acknowledgements: Pfizer, Inc.

Tailoring Progression Analysis to the Individual Patient

Prof. Fritz Dannheim, MD

Dept. of Ophthalmology, Asklepios Hospital Hamburg-Harburg, Hamburg, Germany

In real world glaucoma management, no patient is average and simple statistical analysis often falls short to do justice to the individual. Global MD trends may over- or underestimate changes in crucial areas. If progression is detected, a reduction of the progression rate is desired and needs to be identified. Subtle changes are tempting to be overestimated but might just as well be missed. This complex situation is in contradiction to the short time window available for every single patient. How do new analysis functions like cluster trends, structure function correlation and non-linear trend analysis help the situation? Case studies are presented and discussed using EyeSuite Perimetry, a software solution for Octopus and Humphrey visual fields, and Octopus Field Analysis, a research tool available to interested doctors.

2010.03.25

8:30-9:15

Morning Seminar

CARL ZEISS

Clinical Management using Quantitative Progression Tools

Garway-Heath D¹, Goñi F²

1 NIHR Biomedical Research Centre for Ophthalmology, Moorfields Eye Hospital NHS Foundation Trust and UCL Institute of Ophthalmology, City Road, London, England, UK
2 Barcelona Glaucoma Center, Sant Quirze Valles, Spain

Purpose: The goal of the glaucoma management is to prevent loss of quality of life through impaired vision within a patient's lifetime. The European Glaucoma Society Terminology and Guidelines for Glaucoma state that visual field testing is mandatory for glaucoma follow-up and that quantitative imaging supports progression monitoring. However, perimetry and imaging devices provide enormous quantities of data that are difficult to interpret without software support. This seminar will provide guidance on integrating newly available clinical information from quantitative commercial tools with therapeutic decision making for monitoring changes in glaucoma patients.

Methods: The EGS guidelines for monitoring progression will be considered and software tools for managing and interpreting data from perimetry and imaging devices will be reviewed.

Results: Available software tools identify statistically significant change that need to be interpreted in the clinical context. Statistically significant change needs to be distinguished from clinically significant change and management decisions need to be made accordingly. Measurement variability may mask clinically significant change, so that all patient data need to be considered when evaluating treatment targets.

Conclusions: By quantifying the likelihood of progression across structure and function and identifying high-risk patients, software tools deliver better information for making challenging therapeutic decisions, enabling doctors to change how they manage glaucoma patients, particularly in early to moderate cases.

Acknowledgements: Carl Zeiss Meditec, Inc.

2010.03.26

14:00-14:45

Luncheon Seminar

ALLERGAN

Rates of Visual Field Progression in Clinical Practice

Francisco Javier Goñi and David Garway-Heath

The concept of visual field progression rates in glaucoma has been recently revisited in the literature. The importance to detect not only the functional change but also the speed at which this change occurs, expressed in terms of "continuous" functional loss per time unit (Rate of Progression, RoP) has been stressed. Needs to adequately estimate RoP include a sufficient number of quality visual field tests throughout a sufficient elapsed time. Nevertheless, these requirements frequently clash with limitations in the clinical setting, due to different reasons like patient overload, patient non-adherence, lack of validated protocols, etc.

The aim of this symposium is to present and discuss on how to move from these apparently insurmountable technical obstacles to a more realistic and feasible approach, allowing to implement RoPs in day-to-day clinical practice.



GDxPRO:

The perfect tool dedicated to RNFL assessment.

The new GDxPRO™ takes a leap forward in performance and workflow enhancements.

- Unsurpassed RNFL assessment, ideal where ease of use, affordability and portability are key.
- Uniquely assesses RNFL health by measuring RNFL Integrity, bringing more diagnostic confidence with an analysis that goes beyond thickness.
- Proven to aid in detecting early glaucoma and quantifying RNFL progression.
- Offers multiple performance advancements with ECC™, GPA™ and Automatic Image Alignment.
- Delivers superior workflow with Simple-Touch Pupil Alignment, Live Fundus View, Low Vision Target and connectivity options to office networks and ZEISS FORUM® Eye Care Data Management Solutions.
- Solid investment with affordable high performance validated by hundreds of published studies.

Stop by the Carl Zeiss exhibit at the IPS meeting for a live demonstration of the GDxPRO – unsurpassed value for any size practice.



Wherever you
want to go!

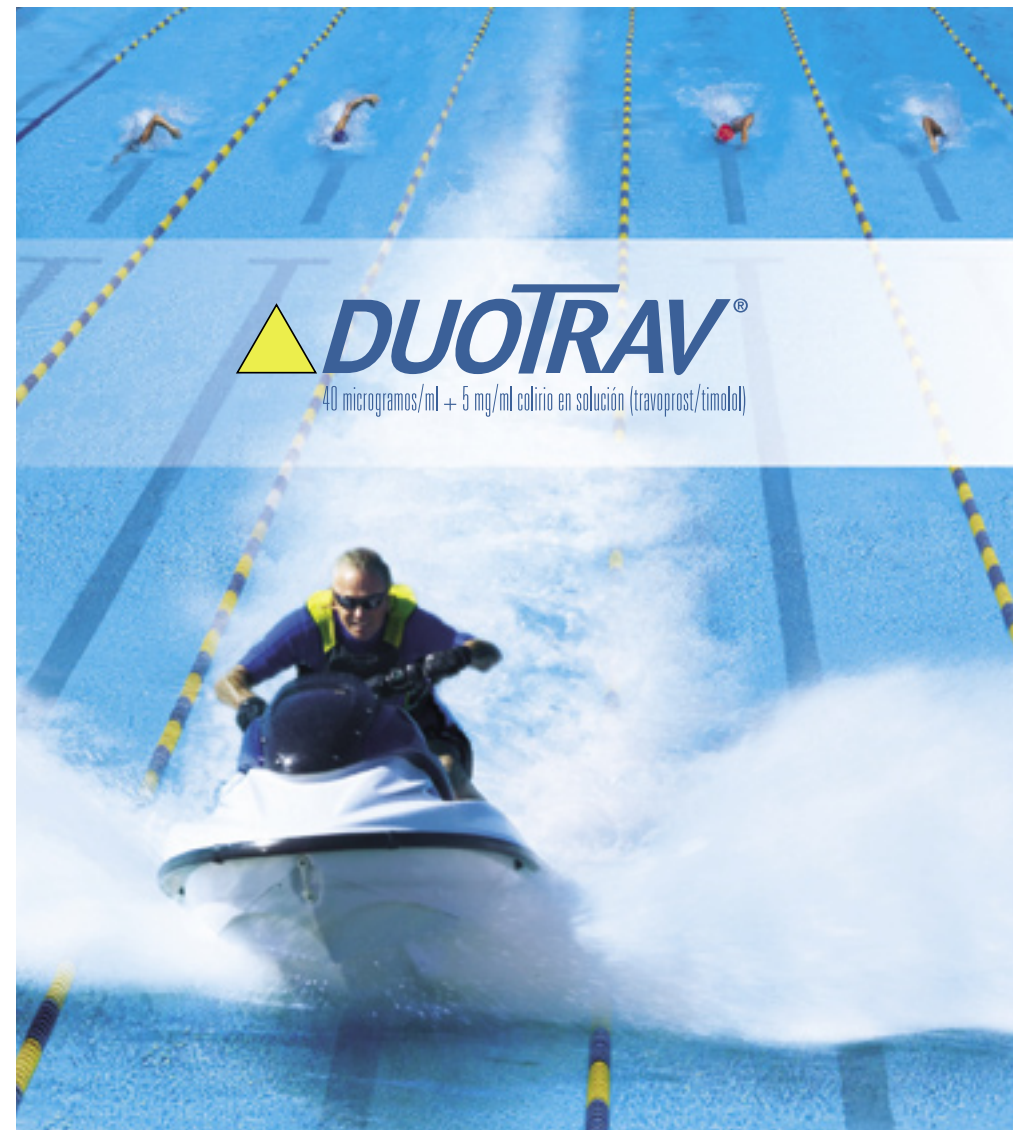
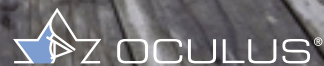


The Oculus Centerfield –
A Real Compact Perimeter

Improve your visual field test results with the Centerfield's exclusive ability to test suspect areas with a more dense test pattern. The results from these additional test point locations will increase your confidence in your final diagnosis.

Please visit our
Booth #10

www.oculus.de



 **DUOTRAV**[®]
40 microgramos/ml + 5 mg/ml colirio en solución (travoprost/timolol)

Alcon[®]



A fondo contra el Glaucoma

Now Available

SAFLUTAN^{®†}

(tafluprost)

The **first**¹ and **only**

Preservative-Free prostaglandin

for the treatment of open-angle glaucoma
and ocular hypertension

Please, before initiating therapy read the full Prescribing Information for SAFLUTAN[®] included in the congress bag.

SAFLUTAN[®] is indicated for the reduction of elevated intraocular pressure in patients with open-angle glaucoma and ocular hypertension.²
As monotherapy in patients:

- Who would benefit from preservative-free eye drops.²
- Insufficiently responsive to first-line therapy.²
- Intolerant or contraindicated to first-line therapy.²

As adjunctive therapy to beta-blockers.²



[†]Registered trademark of Merck Sharp & Dohme Corp., a subsidiary of Merck & Co., Inc., Whitehouse Station, NJ U.S.A.



Merck Sharp & Dohme de España, S.A.
Josefa Valcárcel, 38 · 28027 Madrid



Manufactured by Santen Pharmaceutical Co., Ltd.

REFERENCES:

1. Hamacher T. et al. Efficacy and safety levels of preserved and preservative free tafluprost are equivalent in patients with glaucoma or ocular hypertension: results from a pharmacodynamics analysis. *Acta Ophthalmol* 2008; 86: S242: 14-19. 2. Ficha técnica de SAFLUTAN[®]

07-2010-SFT-2010-E-4861-J (07-2010-SAFI-2009-W-1303902-J) (Creado: febrero 2010)

The perfect couple
for a reliable glaucoma diagnosis!

Heidelberg Retina Tomograph + Heidelberg Edge Perimeter

Structure and Function - Together at last

Comprehensive glaucoma diagnosis combining
HRT with the new multi-functional HEP

HEIDELBERG
ENGINEERING

© 2010 Heidelberg Engineering GmbH. All Rights Reserved. 93.153-001

The advertisement features a photograph of a couple in formal attire walking on a red carpet. The woman is wearing a white dress and high heels, while the man is in a dark suit. The background is dark, and the carpet is a vibrant red. The text is overlaid on the image in white and red. The Heidelberg Engineering logo is at the bottom right.

Most Advanced Progression Analysis.

Octopus EyeSuite Perimetry

NEW

Overview at a Glance

- EyeSuite provides a complete overview of all examinations to analyse changes

Progression Analysis

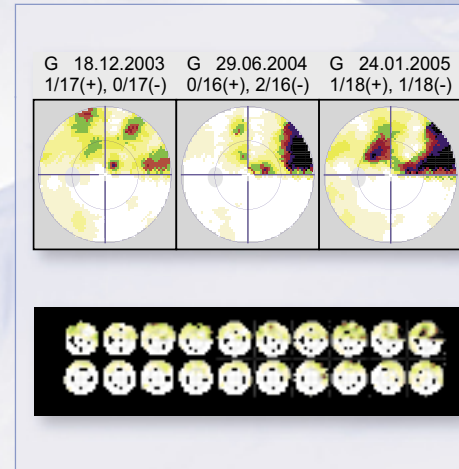
- Calculate the progression rate in dB per year as recommended by the International Glaucoma Societies

Connectivity

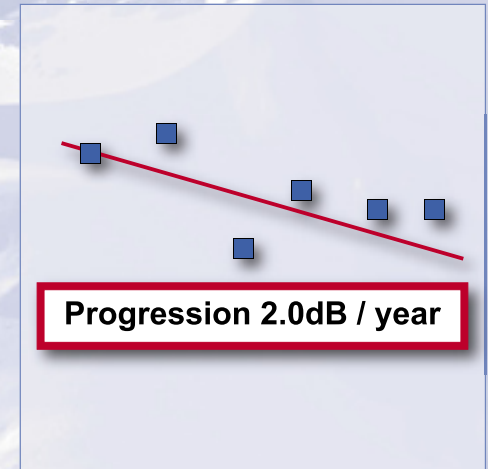
- Import existing visual fields and manage ongoing Octopus and HFA examinations in one solution



Octopus 900®



Overview at a Glance



Progression Analysis

For more information visit our website
www.haag-streit.com

Perimetry

HAAG-STREIT
INTERNATIONAL

Tradition and Innovation

A person is seen from behind, holding up a large, light-colored flag that is billowing in the wind. The scene is set outdoors against a bright, clear sky with a sun flare on the left side. The person is wearing a white t-shirt and dark pants. The overall mood is one of optimism and achievement.

visionary science through partnership

> **We see potential. And invest in it.**

At Pfizer Ophthalmics we're investing in the future of eye health both internally and externally. In pursuit of new therapies for eye disorders we have initiated more than nine strategic partnerships in just five years with biotechnology companies, universities, hospitals, nonprofits, and pioneering ophthalmologists. .

OUR VISION IS CLEAR.

Pfizer Ophthalmics

When monotherapy is not enough



Control under pressure

GANFORT® (bimatoprost 0.03%/timolol 0.5%). Abbreviated Prescribing Information. Presentation: Eye drop solution, one ml contains 0.3mg bimatoprost and 5mg timolol (as maleate). **Indications:** Reduction of intraocular pressure (IOP) in patients with open-angle glaucoma or ocular hypertension who are insufficiently responsive to topical beta-blockers or prostaglandin analogues. **Dosage and Administration:** Please refer to the Summary of Product Characteristics before prescribing. Recommended dose is one drop in the affected eye(s) once daily, administered in the morning (evening dosing may be considered). If more than one topical ophthalmic product is to be used, each should be instilled at least 5 minutes apart. Not recommended in children or adolescents (under the age of 18). Use with caution in renal or hepatic impairment. **Contraindications:** Hypersensitivity to active substances or to any of the excipients. Reactive airway disease including bronchial asthma or a history of bronchial asthma, severe chronic obstructive pulmonary disease. Sinus bradycardia, second or third degree atrioventricular block, overt cardiac failure, cardiogenic shock. **Warnings/Precautions:** Ganfort may be absorbed systemically. The same types of cardiovascular and pulmonary adverse reactions as seen with systemic beta-blockers may occur. Cardiac failure should be adequately controlled before beginning therapy. Patients with a history of severe cardiac disease should be watched for signs of cardiac failure and have their pulse rates checked. Cardiac and respiratory reactions, including death due to bronchospasm in patients with asthma, and, rarely, death in association with cardiac failures have been reported following administration of timolol maleate. Beta-blockers may also mask the signs of hyperthyroidism and cause worsening of Prinzmetal angina, severe peripheral and central circulatory disorders and hypotension. Beta-adrenergic blocking agents should be administered with caution in patients subject to spontaneous hypoglycemia or to diabetic patients (especially those with labile diabetes) as beta-blockers may mask the signs and symptoms of acute hypoglycemia. While taking beta-blockers, patients with a history of atopy or a history of severe anaphylactic reaction to a variety of allergens may be unresponsive to the usual dose of adrenaline used to treat anaphylactic reactions. In patients with a history of mild liver disease or abnormal alanine aminotransferase (ALT), aspartate aminotransferase (AST) and/or bilirubin at baseline, bimatoprost had no adverse reactions on liver function over 24 months. There are no known adverse reactions of ocular timolol on liver function. Before treatment is initiated, patients should be informed of the possibility of eyelash growth, darkening of the eyelid skin and increased iris pigmentation since these have been observed during treatment with bimatoprost and Ganfort. Some of these changes may be permanent, and may lead to differences in appearance between the eyes if only one eye is treated. After discontinuation of Ganfort, pigmentation of irises may be permanent. After 12 months treatment with Ganfort, the incidence of iris pigmentation was 0.2%. After 12 months treatment with bimatoprost eye drops alone, the incidence was 1.5% and did not increase following 3 years treatment. Cystoid macular oedema has been reported with Ganfort. Therefore, Ganfort should be used with caution in patients with known risk factors for macular oedema (e.g. aphakic patients, pseudophakic patients with a torn posterior lens capsule). The preservative in Ganfort, benzalkonium chloride, may cause eye irritation. Contact lenses must be removed prior to application, with at least a 15-minute wait before reinsertion. Benzalkonium chloride is known to discolour soft contact lenses; avoid contact. Benzalkonium chloride has been reported to cause punctate keratopathy and/or toxic ulcerative keratopathy. Therefore monitoring is required with frequent or prolonged use of Ganfort in dry eye patients or where the cornea is compromised. Ganfort has not been studied in patients with inflammatory ocular conditions, neovascular, inflammatory, angle-closure glaucoma, congenital glaucoma or narrow-angle glaucoma. Potential for additive effects resulting in hypotension, and/or marked bradycardia when eye drops containing timolol are administered concomitantly with oral calcium channel blockers, guanethidine, or beta-blocking agents, anti-arrhythmics, digitalis glycosides or parasympathomimetics. The hypertensive reaction to sudden withdrawal of clonidine can be potentiated when taking beta-blockers. There are no adequate data from the use of Ganfort in pregnant women. Do not use during pregnancy unless clearly necessary. Ganfort should not be used by breast-feeding women. Ganfort has negligible influence on ability to drive and use machines. **Adverse Effects:** No adverse drug reactions (ADRs) specific for Ganfort have been observed in clinical studies. The ADRs have been limited to those earlier reported for bimatoprost and timolol and the majority were ocular, mild in severity and none were serious. Based on 12-month clinical data, the most commonly reported ADR was conjunctival hyperaemia (mostly trace to mild and thought to be of a non-inflammatory nature) in approximately 26% of patients and led to discontinuation in 1.5% of patients. The following ADRs were reported during clinical trials with Ganfort. **Eye disorders:** Very common (≥1/10): conjunctival hyperaemia, growth of eyelashes. Common (≥1/100 to <1/10): superficial punctate keratitis, corneal erosion, burning sensation, eye pruritus, stinging sensation in the eye, foreign body sensation, eye dryness, eyelid erythema, eye pain, photophobia, eye discharge, visual disturbance, eyelid pruritus. **Skin and subcutaneous tissue disorders:** Common: blepharal pigmentation. Additional adverse events that have been seen with one of the components and may potentially occur also with Ganfort. Please refer to Summary of Product Characteristics for full information on side effects. **Basic NHS Price:** £13.95 per 3ml bottle. £37.59 for 3x3ml bottle. **Marketing Authorisation Number:** EU / 1 / 06 / 340 / 001-002. **Marketing Authorisation Holder:** Allergan Pharmaceuticals Ireland, Castlebar Road, Westport, Co. Mayo, Ireland. **Legal Category:** POM. **Date of Preparation:** March 2009. Further information is available from: Allergan Ltd, Marlow International, The Parkway, Marlow, Bucks, SL7 1YL.

Adverse events should be reported to your local regulatory authority and Allergan office.

Allergan Ltd, Marlow International, The Parkway, Marlow, Bucks, SL7 1YL
 Tel: +44 (0)1628 494026 Fax: +44 (0)1628 494057
 www.allergan.co.uk
 EU/0507/2009 Date of preparation:
 November 2009.

GANfort
 (bimatoprost/timolol ophthalmic solution) 0.03%/0.5%

Sponsors

Major Sponsors



Allergan



Haag Streit AG



Pfizer



Zeiss

Sponsors



Alcon



Heidelberg Ing



Merck Sharp & Dome



Oculus

Supporting Groups



Cabildo de Tenerife



Universidad de La Laguna



Sociedad Canaria de Oftalmología